ANALYTICAL STUDY ON UPGRADING THE SEISMIC PERFORMANCE OF NOMINALLY DUCTILE RC FRAME STRUCTURES USING DIFFERENT REHABILITATION TECHNIQUES

Hossam El-Sokkary

A Thesis

in

The Department of

Building, Civil and Environmental Engineering

Presented in Partial Fulfillment of the Requirements

for the Degree of Master of Applied Sciences (Civil Engineering) at

CONCORDIA UNIVERSITY

Montréal, Québec, Canada

August 2007

Your file Votre référence
ISBN: 978-0-494-37773-4
Our file Notre référence
ISBN: 978-0-494-37773-4

ABSTRACT

ANALYTICAL STUDY ON UPGRADING THE SEISMIC PERFORMANCE OF NOMINALLY DUCTILE RC FRAME STRUCTURES USING DIFFERENT REHABILITATION TECHNIQUES

Hossam El-Sokkary

There exist many reinforced concrete (RC) buildings that are located in seismically active zones and designed according to older strength-based codes. These buildings are susceptible to abrupt non-ductile strength deterioration once their ultimate strength is reached, which reduces the energy dissipation capacity of those buildings and results in a brittle failure. Therefore, enhancing the seismic performance of such structures is essential and should not be overlooked. Recently, performance-based seismic design methodology is being adopted by several codes, in which seismic performance is described by designating the maximum allowable damage state index for an identified seismic hazard level. Overall lateral deflection, ductility demand, and inter-storey drift are the most commonly used damage state indices.

The objective of this study is to analytically investigate the effectiveness of different rehabilitation patterns in upgrading the seismic performance of existing non-ductile RC frame structures. The study investigates the performance of three RC frames (with different heights) with or without masonry infill when rehabilitated and subjected to three types of ground motion records. The heights of the RC frames represent low, medium and high-rise buildings. The ground motion records represent earthquakes with low, medium and high frequency contents. Three models were considered for the RC frames; bare frame, masonry-infilled frame with soft infill, and masonry-infilled frame with stiff infill. The studied rehabilitation patterns include (1) introducing a RC shear wall, (2) using steel bracing, (3) using diagonal FRP strips (FRP bracings) in case of masonry-infilled frames, and (4) wrapping or partially wrapping the frame members (columns and beams) using FRP confinement.

The seismic performance enhancement of the studied frames is evaluated in terms of the maximum applied peak ground acceleration or velocity resisted by the frames, maximum inter-storey drift ratio, maximum storey shear to weight ratio and energy dissipation capacity.

ACKNOWLEDGEMENTS

I would like to express my sincere gratitude to my supervisor, Dr. Khaled Galal, for his guidance, encouragement and patience during my research. I believe that this research wouldn't have been completed without his continuous support. His efforts in reviewing and correcting this thesis drafts are greatly appreciated.

The financial support of Le fonds Québécois de la recherche sur la nature et les technologies (FQRNT) through a Team research project led by Professor Pierre Léger of École Polytechnique de Montréal, and the Natural Science and Engineering Research Council (NSERC) of Canada are greatly appreciated. Encouraging awards from Concordia University are also acknowledged.

I would like to thank all my professors in Ainshams University, Cairo, Egypt. Their great help and support during my undergraduate study really helped me to continue my studies here in Canada and to achieve what I aimed to. I would like also to thank all my friends here in Montréal for their support for me during my study.

Finally, I dedicate this thesis to my parents, my brother and my sister for their invaluable support during my study. Their presence in my life encouraged me a lot to achieve my goals and to work hard on my research.

TABLE OF CONTENTS

LIST OF FIGURES

LIST OF TABLES

LIST OF SYMBOLS

A_i	Area represented by the spring
A/V	Peak ground acceleration to peak ground velocity ratio
E_i	Material Young's modulus
f_c'	Characteristic strength of concrete
f_t	Concrete tensile strength
f_y	Yield strength of steel
K_0	Initial stiffness of spring
L_0	Clear length of the member
R	Ductility factor defined in NBCC 1995
α	Slope of force-deformation line in compression for linear models
β	Post-yielding parameters.
γ	Unloading stiffness degradation parameter
ε_c	Concrete material strain
ε_{sy}	Steel material yield strain
ζ	Inner loop stiffness reduction
η	Ratio of the plastic zone length to the member clear length
θ	Unloading control parameter
λ	Post-peak residual strength / maximum compressive strength ratio
μ	Ductility factor (ultimate strain / strain at maximum strength)
μ_Δ	Displacement ductility
ν, κ	Skeleton curve parameters for steel model
σ_c	Concrete material compressive strength
σ_{sy}	Steel material yield stress
τ	Tension descending part after tension crack
Φ	Parameter to direct the unloading

CHAPTER 1

INTRODUCTION

1.1 GENERAL

In the recent few decades, the world had suffered from increasing hazards of earthquakes. Some of these earthquakes were of severe intensities which caused the failure of many existing buildings or at least left severe damage behind. Many of the existing reinforced concrete (RC) frame structures designed according to pre-1970 codes were not able to survive such ground motions as they were designed according to strength-based concept which didn't enforce ductility limits and energy dissipation capacity of the structure. The lack of appropriate reinforcement detailing of the frame columns, beams and joints lead to low shear capacity of the beams and columns and hence non-ductile strength deterioration when that shear capacity was reached. Despite the fact that many nominally ductile existing structures did survive previous low to moderate ground motion events, the level of damage attained in these structures deems them vulnerable to collapse in future earthquake events. Therefore, strengthening such structures is essential and can not be neglected.

A large number of pre-1970 designed buildings used masonry infill panels in their construction. Although representing the masonry infill panels can be beneficial or detrimental to the seismic response of the structure, they are not usually considered in the analyses of frame structures. Traditional rehabilitation methods of masonry-infilled RC frames include adding anchored steel mesh with plaster to the panel or by demolishing

the masonry panel and introducing a RC infill. Such methods can be labor intensive, add considerable mass, and cause significant impact on the occupants.

Fibre-reinforced polymer (FRP) composite materials have received an increasing attention in the past decades as a potential method for rehabilitation or strengthening of existing structures due to their tolerable characteristics and ease of application. Fibre composites are used to increase the shear strength of existing RC beams and columns by wrapping or partially wrapping the members. Additional shear strength contribution is introduced by orienting the fibres normal to the axis of the member or to cross potential shear cracks. The wrapping pattern and the number of FRP layers used in the strengthening determine the additional strength and ductility of the members, and hence the ductility of the structure and its overall response when subjected to a specified seismic hazard level. Another way of retrofitting the existing buildings which can be used in case of masonry-infilled frame structures is by using carbon reinforced polymer (CFRP) sheets or strips, in that method FRP sheets or strips can be applied on one side or two sides of the masonry infill, and anchor dowels can be used to anchor the CFRP sheets to the wall and the RC frame. The use of fibre-reinforced polymer (FRP) composites offers also a faster and easier rehabilitation alternative, especially when the evacuation of the entire building during the retrofitting is not possible, in that case FRP will be provide the required strengthening without interrupting the use of the building.

RC structural walls and steel bracing are also effective lateral force resisting systems that have been used widely in the last decades, and they are considered as efficient methods for rehabilitation of existing structures. RC walls can provide the required lateral stiffness and strength for resisting the lateral loads due to wind or

earthquakes, and hence several research studies and experimental work were done to investigate the behaviour of RC structural walls under the lateral loads, and to enable the designers to predict the seismic response of a RC wall in a certain building when subjected to a severe ground motion. Steel bracing system has several advantages which make it another effective alternative to provide additional lateral stiffness and strength to the structure, despite its high initial cost and the continuous maintenance needed. Steel bracings are easy to apply, and they can be applied externally without disturbance of the building occupants. The steel has high strength to weight ratio, so the additional mass added to the structure is less compared with the case of introducing a RC structural wall.

Most of the experimental work done was on models with limited number of stories and bays (usually one or two). The results of such tests can be used to calibrate the analytical models used to simulate the real behaviour of different materials, and conduct an analytical study to investigate the performance of rehabilitated RC structures with realistic dimensions and configurations when subjected to real ground motion records.

Performance-based (PB) seismic engineering is the modern approach to earthquake resistant design. Seismic performance (*performance level*) is described by designating the maximum allowable damage state (*damage parameter*) for an identified seismic hazard (*hazard level*). Performance levels describe the state of a structure after being subjected to a certain hazard level as: Fully operational, Operational, Life safe, Near collapse, or Collapse (FEMA 273/274, 1997 and Vision 2000, 1995). Overall lateral deflection, ductility demand, and inter-storey drift are the most commonly used damage parameters. The five qualitative performance levels are related to corresponding five

quantitative maximum inter-storey drifts (as a damage parameter) to be: <0.2%, <0.5%, <1.5%, <2.5%, and >2.5%, respectively.

The hazard level can be represented by the probability of exceedence of 50%, 10% and 2% in 50 years for low, medium and high intensities of ground motions, respectively. Figure 1.1 shows the typical seismic performance of existing non-ductile structures versus structures designed according to performance-based seismic engineering. From the schematic it can be seen that upgrading the seismic performance of existing non-ductile structures can be achieved by increasing the capacity of the structure with or without reducing its drift. Increasing the capacity with reducing the structure drifts can be achieved by increasing the stiffness of the building, e.g. by using RC walls or FRP bracings. Increasing the capacity without reducing the drifts can be achieved by increasing the ductility capacity of the structural elements of the building without altering their stiffness, e.g. by using FRP confinement.

1.2 OBJECTIVE

The objective of this research is to conduct a comparative study on the effectiveness of different rehabilitation techniques used in upgrading the seismic performance of nominally ductile existing RC frame structures. The study investigates the behaviour of three RC frame structures with different heights –representing existing buildings designed according to pre-1970 strength based codes– when rehabilitated using different rehabilitation schemes and subjected to three types of scaled ground motions records. The heights of RC frames representing low, medium and high-rise buildings. The ground motion records represent earthquakes with low, medium and high frequency contents.

The studied rehabilitation patterns include (1) introducing a RC structural wall, (2) rehabilitating using steel bracing, (3) rehabilitating using FRP bracings, and (4) wrapping or partially wrapping the structural elements using FRP composites. To evaluate the importance of accounting for the masonry infill in the analysis, both bare frames and masonry-infilled frames are considered in the analysis. The study also investigates the effect of infill stiffness on the seismic behaviour of structures. The analyses results and conclusions are drawn by evaluating the seismic performance enhancement in terms of maximum inter-storey drift ratio, maximum peak ground acceleration or velocity, maximum storey shear to weight ratio and maximum energy dissipation of the studied structures.

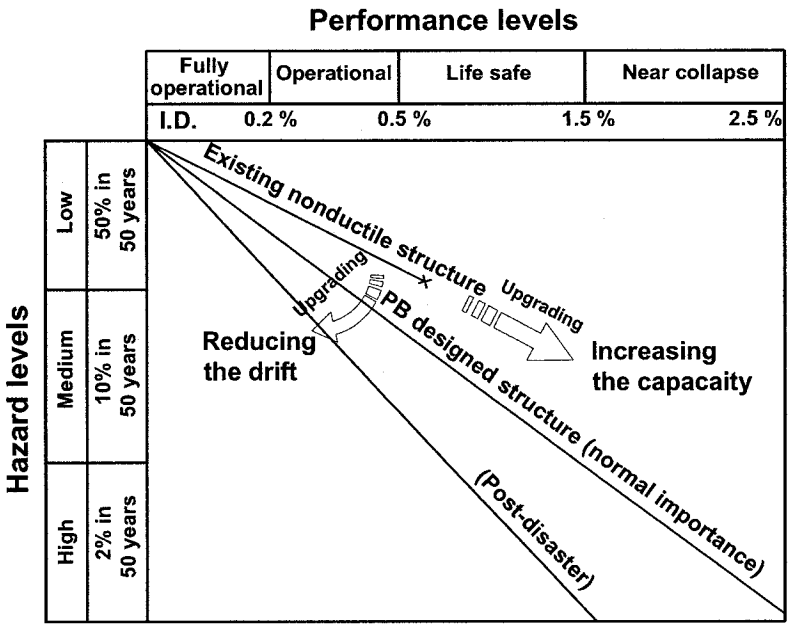

Fig. 1.1. Seismic performance of existing non-ductile structures and possible ways of upgrading.

CHAPTER 2

LITERATURE REVIEW

2.1 INTRODUCTION

The seismic behaviour of multistory frame structures has been studied extensively in the last few decades due to their efficiency as earthquake resisting systems. The multistory framed systems can be categorized as reinforced concrete (RC) frames, masonry-infilled frames, and wall-frame system. The literature survey in this chapter highlights some of the previous experimental and analytical work done on the seismic performance of existing and rehabilitated structures. The survey covers retrofitting and analytical models of different structural systems, namely: RC frame structures, RC structural walls, FRP confined beams and columns, rehabilitated frames using FRP bracings, rehabilitated frames using steel bracing and masonry-infilled frames.

2.2 NONLINEAR MODELS

Several analytical models for the non-linear analysis of reinforced concrete structural components have been proposed. These range from very refined and complex finite element models (Ngo and Scordelis 1967) to simplified macro-models (Chen and Powell 1982, Lai et al. 1984, Powell and Campbell 1994, Petrangeli et al. 1999). Refined analytical models are typically used in predicting the response of small structures or structural subassemblies. The use of refined finite element models in non-linear static, cyclic and dynamic response of reinforced concrete frames is complex, time consuming

and may not be practical. On the other hand, simplified macro-models have been typically used in the dynamic response analysis of large structures.

Inelastic macro-models for beams and columns can be categorized into three main categories, namely: Fibre (Filament) models, Multi-axial Spring models and Yield Surface (Section) models. In the "fibre" type model (Powell and Campbell, 1994), the member cross section is divided into a number of small areas (fibres). Each area is assumed to be uniaxially stressed and to have behaviour governed by the hysteretic stress-strain characteristics of the material it simulates (steel or concrete). Figure 2.1 shows the discretization of a cross section incorporating two different fibre elements.

Lai et al. (1984) considered two inelastic elements at the two ends of an elastic member (Figure 2.2.a). The region undergoing inelastic yielding is modeled by a set of springs representing concrete and reinforcing steel (Figure 2.2.b). A yield surface is not required since the inelastic behaviour is controlled by the stress-strain properties of steel and concrete springs. The model is called a nine-spring model, and each element comprises four effective steel spring elements (A_{s1}, A_{s2}, A_{s3}, and A_{s4}) and five effective concrete spring elements (A_{c1}, A_{c2}, A_{c3}, A_{c4}, and A_{c5}). The hysteretic behaviour of the springs is determined from concrete and steel hysteretic loops.

In the "Section" type models, it is assumed that inelastic behaviour is defined for the cross section as a whole. The force-deformation relationship for the cross section is specified as a function of the cross section dimensions and the hysteretic force-deformation characteristics of the member material. An important advantage of this type

of element is that it is controlled by only a few parameters (yield force, yield displacement, hardening parameter, and unloading parameter) with clear physical meaning. There are two basic approaches used in modeling the inelastic behaviour of a structural element using a "Section" model, namely Distributed Plasticity Approach, and Lumped Plasticity (Plastic Hinge) Approach. Lumped plasticity models are particularly suitable for the analysis of building frames under seismic loads, since plastic behaviour in such structures is usually confined to small regions at the beam and column ends. Figure 2.3 shows some of the existing popular models (modified from Mo, 1994). Table 2.1 shows the main characteristics of these models.

2.3 EXISTING AND RETROFITTED RC FRAME STRUCTURES

RC moment resisting frames are considered as one of the most efficient systems for resisting lateral loads, provided that they obsess sufficient ductility capacity in order to be able to dissipate the earthquake energy efficiently.

Filiatrault *et al.* (1998) tested two 2-storey reinforced concrete frames designed according to the provisions of the National Building Code of Canada (NBCC 1995) and of Canadian concrete standard (CSA 1994), one frame was designed as nominally ductile frame (R=2) and the other one as ductile frame (R=4), and they were subjected to two level of ground motion intensities applied using a shake table. The other part of their study was an analytical model of the two frames using the computer software Ruaumoko (Carr 1996), the frame members were modeled using the bilinear degrading stiffness moment-curvature hysteretic model Q-Hyst as shown in Figure 2.4. The study showed that the ductile frame performed very well during the test and it was able to withstand the

strong ground motion, while the nominally ductile frame had a column-sway mechanism in the first floor which leads to the collapse. The tests imply that increasing the ductility of non-ductile RC frames enhances their seismic performance.

Ghobarah *et al.* (1999) studied a non-ductile and a ductile three-storey reinforced concrete frame buildings, representing building designed according to old design code and NBCC 1995, respectively. The study evaluated the available response-based damage models and developed a new technique for damage evaluation. The frame beams and columns were modeled using inelastic single-component elements, the element use a non-symmetric bilinear curve and take into account the stiffness degradation, pinching and strength deterioration. Figure 2.5 shows the hysteretic behaviour of the nonlinear model used in the analysis. Both nonlinear pushover analysis and dynamic analysis were conducted. The study proposed also a damage model that can be applied for both non-ductile and ductile structures. The analyses were conducted only for low-rise building, and three ground motion records were only considered in the time history analysis, which is not sufficient to generalize the analysis results on the seismic performance of structures when subjected to different earthquake records.

Heidebrecht and Naumoski (1999) studied the seismic performance of six-storey RC ductile frame structures designed according to the NBCC 1995. Nonlinear static pushover and dynamic analyses were done using a McMaster enhanced version of IDARC software. The moment-curvature relationships of the columns and beams were calculated using sectional analysis, and they were modeled using trilinear models to represent the cracking, yielding and post yielding of the element. Stiffness degradation and pinching

behaviour were considered in the hysteretic model. The post-peak degradation was not considered in this study. The study concluded that the pushover analysis underestimated the seismic response of structures compared to nonlinear time history analysis, yet it is beneficial as a measure of the global capacity of structures to sustain inelastic deformations.

Ghobarah *et al.* (2000) studied different strategies used for upgrading the seismic response of existing RC low-rise buildings. A three-storey RC frame structure was selected to be rehabilitated by retrofitting its columns. The rehabilitation schemes included increasing the strength, ductility, stiffness or a combination of these parameters as shown in Figure 2.6. The effectiveness of each strategy on the seismic response of the building was evaluated in terms of drift demands and damage levels. A probabilistic study on the nonlinear dynamic behaviour of the structure were done, nonlinear dynamic analyses using artificial ground motion records were conducted, as well as nonlinear static pushover analyses. The analyses were conducted for both existing and rehabilitated structures using the computer software IDARC2D (Kunnath *et al.* 1992). Four retrofitting strategies were selected for the analysis; the first is by increasing the strength of all columns by 30%, the second is by increasing the ductility of columns by 100%, the third is by increasing the stiffness of columns by 500% and the fourth is by increasing the stiffness by 500% and the strength by 50% at the same time. The study concluded that increasing the column strength (or strength and stiffness together) is the most efficient rehabilitation strategy for reducing the drift of the structure. Increasing the ductility of columns may reduce the damage level due to increased energy dissipation capacity, but the drift demands will be higher which may result in damage of nonstructural elements. It

was concluded also that increasing the columns' stiffness only will result in higher attracted forces without improving the performance of structure. The study didn't cover the applicability of the analysis findings to medium- or high-rise buildings

Marini and Spacone (2006) studied shear failure of existing nonductile RC structural members. The study compared the hysteretic behaviour in two cases; the first case when neglecting the shear capacity of the structural member (i.e. without shear degradation or with infinite shear strength), the second case when considering the shear capacity calculated using Euro Code 2 (EC2) (limited shear strength). Figure 2.7 shows the experimental and analytical hysteretic behaviour of the tested column for the two studied cases. The comparison showed that modeling the column taking the shear capacity into account resulted in a good correlation with the experimental test results. In the experimental test considered in this study (UC San Diego Column R3) (Xiao *et al.* 1993), the column was observed to have nonductile shear failure, which is the usual type of failure for the existing structures designed using strength-based design codes. This ensures the importance of representing shear degradation in the nonlinear analysis of RC structures.

2.4 MODELING OF RC STRUCTURAL WALLS

RC structural walls have been widely used in rehabilitation and strengthening of existing non-ductile frame structures or as an earthquake resisting system for new structures. Hence, many research work is conducted in order to understand the behaviour and modeling of RC walls under lateral load excitations.

Linde (1998) studied the behaviour of structural walls designed according to EC8, the walls' model was made up of inelastic springs connected by rigid beams as shown in Figure 2.8. The model has three vertical nonlinear springs that represent the axial and flexural behaviour, and a horizontal spring to represent the shear behaviour. The hysteretic behaviour of these springs is shown in the figure. From the figure it can be seen that, one wall element was used to model each storey of the wall, except for the first storey where the plastic hinge is expected. This storey was modeled using three elements. The nonlinear analyses were conducted using the finite element software ABAQUS (1996).

Tremblay *et al.* (2001) studied a 12-storey structural RC wall to investigate the importance of P-delta effects on the seismic response of the wall and to evaluate the effect of higher modes of vibration on the behaviour of RC walls. The analytical model of the wall was done using the computer software RUAUMOKO (Carr 1996), the walls were modeled using linear elastic elements with nonlinear springs at their ends. The modified Takeda hysteretic model with degrading stiffness (Figure 2.9) was used to model the inelastic behaviour of the flexural springs. The shear deformations were assumed to be linear in this study. This model is not able to represent the strength degradation due to cyclic loading, and it can not define the properties that control the ductility of RC structural walls.

The same model for the RC wall was used in another study by Panneton *et al.* (2006) to evaluate the impact of new requirements for inclusion in new editions of the

NBCC and CSA-A23.3. The study investigate the behaviour of 8-storey RC wall building designed according to NBCC 1995, the higher mode effects were investigated, and an upper bound on the fundamental period estimate was discussed. The same Takeda hysteretic model was considered in the nonlinear analyses, the shear behaviour was assumed to be linear, and the p-delta effects were taken into account.

Kim and Foutch (2007) proposed a macro-model for RC walls, the model includes a spring element to represent the flexure behaviour and another spring to represent the shear behaviour. The hysteretic models for the flexure and shear springs are shown in Figure 2.10. Four wall test specimens were selected from different US RC wall test programs to verify the analytical model. The modeling parameters of the backbone curves and the hysteretic behaviour were determined for each wall. A parametric study was also done to check the influence of modeling parameters on the response of RC walls under static and dynamic excitation. The analytical model showed a good agreement with the experimental results.

Several experimental tests were conducted to investigate the performance of RC walls when subjected to strong ground motions, e.g. CAMUS experiments that were conducted at the Commissariat á l'Energie Atomique (CEA) facilities in Saclay, France since 1996 (Combescure 2002). In these tests, one-third scaled walls with different steel reinforcement ratios and special configurations were subjected to two types of ground motions records using the Azale shake table (representing far-field and near-fault ground motion records).

Kazak *et al.* (2006) introduced a finite element model of CAMUS walls (Combescure 2002) using nonlinear static and dynamic analysis software ANSYS (2002), and the numerical model was found to be representative especially for the nonlinear static analysis. In that model, the computer program ANSYS was used to model both the wall and the shake table, as it was found that the representation of the boundary conditions of the wall has a significant influence on the results of the analytical model. Yet modeling of structural walls using finite element approach will be impractical if the wall is assembled in a complete structure due to the time efficiency, in that case macro modeling will be a suitable alternative.

Galal (2007) presented an analytical macro-model of CAMUS wall in order to investigate the response of RC walls when subjected to lateral loads, the analyses were conducted using nonlinear static/dynamic structural analysis program CANNY (Li 2006), the analyses included nonlinear static pushover, linear spectral, displacement-based and nonlinear dynamic time history analyses. The analytical model was verified using the experimental results of CAMUS wall. In that model the stiffness of the spring that represents the shake table was calculated in order to have accurate representation of the wall. In this study the RC structural wall was modeled using CANNY panel element. Multi-axial spring model was used to represent the flexural and axial behaviour of the panel element.

Other tests were conducted on six reinforced concrete structural walls on the ETH earthquake simulator at the Institute of Structural Engineering (IBK) of the Swiss Federal Institute of Technology (ETH) in Zurich, Switzerland. The tests were conducted to

investigate and predict the nonlinear behaviour of RC structural walls when subjected to ground motion excitations. Belmouden and Lestuzzi (2007) used the results of ETH tests to develop a simplified macro-model that can predict the inelastic performance of RC walls. The element used in the analysis is composed of multilayer beam element with two fibre connection hinges at the ends as shown in Figure 2.11. The inelastic behaviour of concrete and steel layers was defined, and shear deformations were considered in the model. The model is able to represent the stiffness degradation, strength deterioration, pinching and slippage. Drain 2DX was used to conduct the nonlinear analyses. The analysis results showed a good agreement with the experimental ones. Yet this model can be used to predict the behaviour of a RC structural wall when assembled in a complete structure.

2.5 REHABILITATION USING STEEL BRACINGS

Several studies were conducted to investigate the performance of RC frame structures strengthened using steel bracings. Steel bracings can be used to increase the stiffness and strength of the RC frame structure (e.g. using X-bracing systems) which decrease the ductility level of the frame, or they can provide the ductility required for a ductile design (e.g. using knee-bracing systems). The shape of the bracing cross-section, the slenderness ratio of the bracing member and the connection strength between the RC frame and the bracing member are important parameters that affect the cyclic behaviour of the steel braced RC frame structures.

Jain *et al.* (1980) tested seventeen tube and 8 angle specimens to investigate the influence of mode of buckling, local buckling and cross-section shape on the hysteretic

behaviour of steel bracings. Figure 2.12 shows the hysteretic behaviour of a tube specimen tested under cyclic loading. The study proposed an analytical model for the tubular members based on the experimental tests done (Figure 2.13). The model can represent the reduction in the maximum compressive strength with increasing the number of load cycles as shown in Figures 2.12 and 2.13. It was found that the slenderness ratio of the bracing member is the main parameter that controls the hysteresis behaviour of the member. The same model was used by Abou-Elfath and Ghobarah (2000) to investigate the effect of the distribution of steel X-bracing along the height of RC frame structure.

Galano and Gusella (1998) studied the seismic performance of masonry structures strengthened using X steel bracing. The study considered a single storey structure with masonry infill walls strengthened using two steel x-bracings (located at the end walls) made of tubular sections. Twenty artificial ground motion records were generated and applied to the analytical model. Three different steel x-bracing stiffnesses were used in the analyses to investigate the effect of relative stiffness of steel bracing to that of masonry wall on the seismic performance of the structure. The steel bracing was modeled as a tension/compression strut, and the force-displacement backbone curve of the steel bracing model is shown in Figure 2.14. In this model, a plastic behaviour was assumed after reaching the maximum tensile strength (L_y) or the maximum compressive strength (L_b) which was taken equal to 0.5 L_E, where L_E is the first Euler buckling load. It was found that the relative stiffness of the steel bracing to that of the masonry wall affect the seismic response of the structure significantly.

2.6 REHABILITATION USING FRP-CONFINEMENTS

Fibre-reinforced polymers (FRP) composite materials are considered to have a high potential in strengthening and rehabilitation of existing structures due to their high strength and ease of application. Many FRP rehabilitation schemes are being proposed and used for frame structures' elements. Bakis *et al.* (2002) introduced a concise survey on the applications of FRP composites in civil engineering. The survey included the use of FRP in the highway bridge decks, as internal reinforcement instead of the steel reinforcement, as externally bonded reinforcement, or the use of FRP in strengthening of RC structures. FRP composites can be used by wrapping or partially wrapping the structural elements, such as the columns and beams, to increase their ductility and shear strength capacity. In case of masonry-infilled frames, epoxy-bonded FRP overlays can be applied on the whole surface of the infill or by using diagonal FRP strips (bracing) that are anchored to the infill and frame elements. The survey discussed also the standard and code developments activities done in several countries around the world.

Seible *et al.* (1997) studied the seismic retrofit of RC columns using CFRP jackets. The study presented the possible modes of failure of RC columns; the shear failure and the flexural failure (plastic hinge failure). The study presented the design guidelines for estimating the FRP jacket thickness for both modes of failure. The analytical study was verified using the experimental tests carried out at the Powell Structural Research Laboratories, California. It was found that retrofitting the columns using CFRP jackets increased the ductility capacity of the existing columns significantly. Retrofitting the column using CFRP jackets was compared to the retrofitting using steel jackets. It was

found that although the steel jacketed column showed a higher load capacity than the CFRP jacketed column, both columns had very similar structural performance as shown in Figure 2.15. In all cases, it was found that the CFRP jacketed column had higher deformation capacities than that of steel jacketed column, which is an indication of the efficiency of FRP confinements in upgrading the seismic performance of RC columns. The study highlighted also the importance of increasing the speed of retrofitting, reducing the maintenance, and improving the durability. For these reasons, the CFRP confinements are considered an efficient alternative for rehabilitation of RC columns.

Haroun *et al.* (2002) conducted experimental and analytical studies on fourteen half-scale bridge rectangular and circular RC columns retrofitted using FRP jackets. The specimens were tested under laterally reversed cyclic loading. The results showed that the existing columns failed in a non-ductile manner (shear mode of failure), while the rehabilitated columns failed in flexure mode of failure. It was found that as-build (existing) columns failed at displacement ductility equal to 2 due to bond deterioration of the lap-spliced longitudinal reinforcement. On the contrary, the jacketed columns were able to reach displacement ductility greater than 6.

Sheikh (2002) studied the retrofitting of different structural elements using FRP composites. The study investigated the seismic performance enhancement of beams, slabs, walls and columns when rehabilitated using FRP. The study was based on experimental tests conducted at the University of Toronto on near full-scale specimens. Both the existing elements and the rehabilitated ones were tested and subjected to increasing cyclic loading. It was found that the use of FRP improved the seismic behaviour of the tested

columns significantly, and increased the flexural capacity of the tested wall-slab specimens by approximately 50%. The study concluded also that wrapping the tested beams with one layer of CFRP increased the capacity by 50% and made the beam to fail in a ductile mode of failure (flexural failure) instead of the brittle shear failure.

FRP can be an effective rehabilitation technique when used for strengthening the beam-column joints of an existing RC frame structures, these joint are susceptible to plastic hinge formation at the beam or column ends. Said and Nehdi (2004) studied the effect of FRP on the rehabilitation of beam-column joints of non-ductile RC frames. In this study, a full scale beam-column joint designed according to the CSA requirements were tested under cyclic loading for cases of unrehabilitated and rehabilitated with FRP composites. It was found that the rehabilitation technique using FRP was effective in enhancing the seismic performance of the tested specimen.

Galal *et al.* (2005) studied the performance enhancement of RC columns when strengthened using glass or carbon composite materials, and they evaluated the effect of number of FRP layers on the behaviour of columns. Figure 2.16 shows the lateral load deflection for three specimens, the first one was unstrengthened which represents the existing column, the second one was retrofitted using carbon FRP (CFRP) which represents the moderately ductile column and the third one was retrofitted but with higher amount of CFRP which represents the highly ductile column. From the figure, it can be seen that the existing column and the rehabilitated ones reach the same yield displacement while the displacement ductility and energy dissipation capacity (defined as the area enclosed by the hysteretic loops) increased with the increase of CFRP content.

Galal (2007) proposed a method to predict the backbone lateral force-displacement ductility relationship for non-ductile RC squat columns rehabilitated with FRP confinement. The model considered both the flexure and shear capacity of the column. The model considered that stiffness, yielding displacement and yielding capacity of columns didn't change after rehabilitation, while the ductility of the rehabilitated members increased significantly. The analytical model was verified using the experimental work available in the literature for different rehabilitation schemes using carbon or glass FRP.

Sheikh and Li (2007) proposed a procedure for determining the required number of confining FRP layers required for a column to reach a specific ductility level knowing the axial load on the column and the properties of the FRP. The procedure could be applied for both new and existing square columns. The study was based on the results of several experimental tests that were conducted on square columns confined using FRP composites. The authors concluded that for square FRP-confined column, the ductility level increased with the increase of the number of FRP layers, with the increase of FRP strength, and with the decrease in the axial load carried by the column. The study clarified the main differences between the confinement provided by the traditional lateral steel reinforcement (stirrups or ties), and that provided by the confining FRP. The study proposed also a design equation for calculating the number of FRP layers required to reach a certain ductility level, and proposed a design curve to estimate the number of FRP layers needed for a certain column as function of the axial load level to be moderately ductile or highly ductile as shown in Figure 2.17.

2.7 REHABILITATING MASONRY-INFILLED FRAMES USING FRP BRACINGS

Masonry infill is commonly represented by diagonal compression struts that connect the corners of the enclosing RC frame as was first suggested by Stafford-Smith (1966). Since then, different analytical models were proposed by several researchers for the hysteretic characteristics of the struts based on the results of experimental tests carried out on masonry infilled frames.

Madan *et al.* (1997) proposed an analytical macro-model for the masonry infill panels based on the equivalent compression strut. The hysteretic model of the strut can represent the stiffness and strength degradation of the infill in addition to the pinching behaviour due to opening and closing of masonry gaps. Figure 2.18 shows the hysteretic model used in the analyses. Nonlinear static and dynamic analyses were conducted using the computer program IDARC2D. The analytical model was used to simulate the experimental work done by Mander *et al.* (1993), on the behaviour of masonry-infilled frames. Three storey steel frames with masonry infill were tested under in-plane quasi-static cyclic loading. A bare frame was also tested to be compared with the infilled frames. Another highly reinforced concrete frame was analyzed using the same model when subjected to selected ground motion records to ensure the validity of the model to represent the dynamic behaviour of RC frames. The study showed that the macro-model enabled studying the global behaviour of the infill, without studying the local effects such as the interaction between the frame and the infill. In that case, micro-modeling such as finite element model is efficient. Generally, the macro-modeling was able to evaluate the

nonlinear force-deformation behaviour of the structure under lateral loads efficiently, and it would be useful for representing large structures with several components.

Dolsek and Fajfar (2002) studied analytically the seismic response of a three-storey reinforced concrete frame with masonry infill in the lower two storeys, when subjected to an artificial ground motion generated to have a response spectrum similar to the elastic response spectrum of EC8. The model was tested at ELSA facility in Ispra, Italy. In the numerical model used in this study, the masonry infill panels were modeled as diagonal struts that carry compression force only. The beams and columns were modeled using elastic element with two inelastic rotational springs at the ends. Takeda's hysteretic rule was used to represent the moment-rotation relationship. In this study, no strength degradation was considered in the force-displacement backbone curve of the structural elements. The study proposed a technique for estimating the force-displacement backbone curves for the infill struts using the results of pseudo-dynamic test, and it was found that this analytical model is able to represent the behaviour of masonry-infilled frames under dynamic loads efficiently. The proposed force-displacement backbone curve for the infill panels are shown in Figure 2.19.

Lu (2002) introduced a comparative study of the seismic behaviour of reinforced concrete multi-storey frame structures. Four six-storey frames were tested at the National Technical University of Athens, the structures were designed to have medium ductility according to EC 8. The four frames represent; a regular bare frame, a discontinuous-column frame, a partially masonry-infilled frame, and a RC wall-frame system. The frames were scaled to 1: 5.5 of the original dimensions and subjected to several levels of

the simulated El Centro N-S component. It was found that the masonry infill increased the storey shear strength and stiffness by 60% which indicates better seismic response of the frame. The study indicated that the wall-frame system has a higher control of the displacement and drifts compared to the bare frame. The study recommended an interstorey drift limit of 3% or a top drift limit of 2.5% as possible damage indices that could be used to assess the damage state of the frames.

Özcebe *et al.* (2003) proposed an analytical representation to predict the behaviour of masonry-infilled frames when rehabilitated with FRP bracings. The analytical model was correlated to experimental tests carried out at Middle East Technical University (METU) on a number of two-storey masonry-infilled frame specimens rehabilitated with different patterns of FRP, and subjected to cyclic displacement excitations at the storey levels. The existing frame was tested as well to get the characteristics of the masonry infill. The FRP bracings were modeled as uniaxial tension strut, while the unrehabilitated infill panels were modeled as compression struts. The strut model for the infill is shown in Figure 2.20. The model for the rehabilitated infill panels took into account the effect of CFRP, plaster, infill and the anchorage. The strut model of the composite material is shown in Figure 2.21. Drain 2DX (Prakash *et al.* 1993) nonlinear structural analysis software was used for the static pushover and the dynamic analyses. It was concluded that the analytical model was able to represent the actual behaviour of the existing masonry infill frame and the rehabilitated ones using FRP for both pushover and dynamic analyses.

Humar and Bagchi (2004) studied two 6-storey buildings with RC moment resisting frames designed according to the provisions of NBCC 2005. Both the bare frame and masonry-infilled frame were considered in the analyses. DRAIN-2DX was used for the modal and pushover analyses, and DRAIN-RC was used for the inelastic dynamic analyses. Section analyses were done to get the moment-curvature relationship for the frame members. The infill panels were modeled using equivalent struts that carry compression force only. It was concluded that the presence of masonry infill panels increased the frame strength and stiffness, and they decrease the period of the structure significantly.

Almusallam and Al-Salloum (2007) studied the effectiveness of FRP in strengthening and/or rehabilitation of unreinforced masonry-infilled frames. Two single-storey frames with masonry infill panel were tested. The first specimen which represented the existing structure was tested till failure of masonry infill, and then it was rehabilitated using horizontal FRP sheet strips. The second specimen was strengthened using FRP, and both specimens were tested under lateral cyclic loading up to failure. The results of tests showed that FRP sheets were very efficient in enhancing the seismic performance of the masonry-infilled frames. The use of FRP increased the strength and ductility of the studied frames. It was found that the ductility of the infill walls increased up to 3 times of the original existing wall which indicated a higher energy dissipation capacity of the rehabilitated frames and better seismic response.

Binici *et al.* (2007) proposed other analytical models for the FRP bracings and masonry infill struts based on the experimental tests carried out in METU. The stress-strain relationship of the compression strut and tension strut are shown in Figure 2.22.These models were used in the analysis of an existing RC building with hollow clay tile infills strengthened using FRP bracings. This building is located in the most active seismic zone in Istanbul. After the retrofitting using FRP bracings, it was found that the seismic performance enhancement of the structure was significantly high in terms of the drift and deformation demands.

Table 2.1 Comparison of reinforced concrete hysteretic models (Modified from Mo, 1994).

Model reference	Type	Controlled Parameters			Comparative remarks	
		Stiffness Degradation	Pinching	Strength Deterioration	Overall versatility	Overall complexity
Clough, 1966	S	N	N	N	L	L
Fukada, 1969	S	Y	N	N	L	L
Aoyama, 1971	S	N	Y	Y	M	H
Kustu *et al.*,	S	N	Y	N	M	H
Tani *et al.*, 1973	S	Y	N	N	H	M
Takeda *et al.*, 1970	S	Y	N	N	L	M
Park *et al.*, 1984	C	Y	N	N	H	H
Iwan, 1973	S	N	Y	N	L	M
Takayanagi *et al.*, 1977	S	Y	Y	Y	M	M
Muto *et al.*,	S	Y	N	N	L	L
Atalay *et al.*,	C	Y	Y	N	L	H
Nakata *et al.*,	C	Y	Y	Y	H	H
Blakely, 1973	S	Y	N	Y	L	L
Mo, 1988	S	Y	Y	N	L	L
Abou-Elfath,	S	Y	Y	Y	H	H

Notation: S: Straight line C: Curved line
Y: Yes N: No
L: Low M: Medium H: High

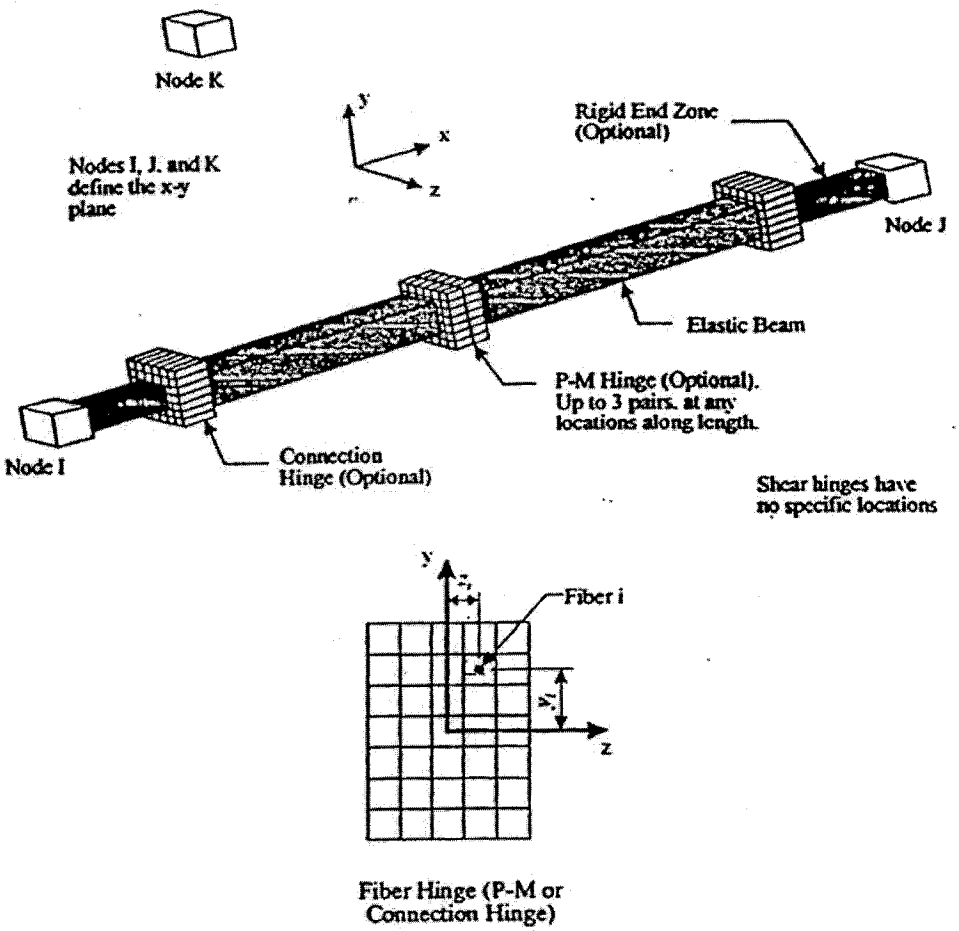

Element No. 08 (Powell and Campbell, 1994)

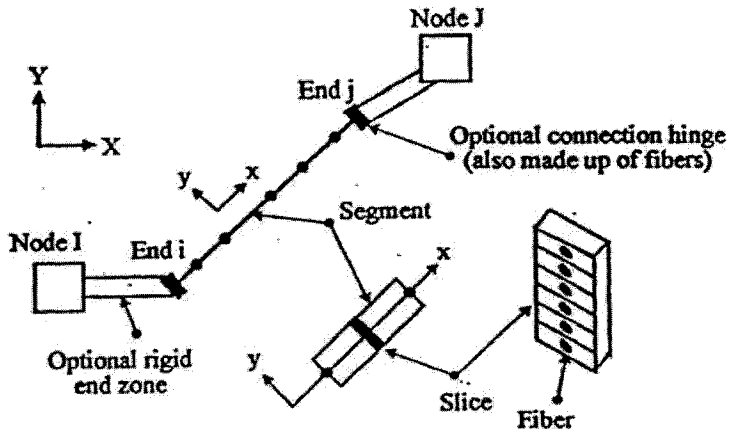

Element No. 15 (Powell and Campbell, 1994)

Fig. 2.1. Fibre models

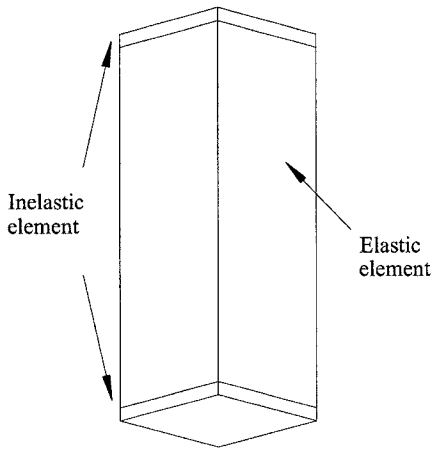

a) Member model

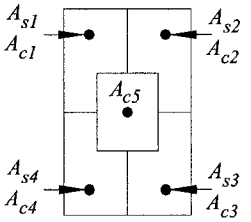

b) Nine-spring model
Lai et al. (1984)

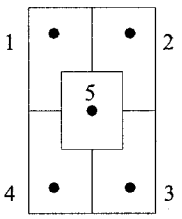

c) Five-spring model
Saiidi et al. (1986)

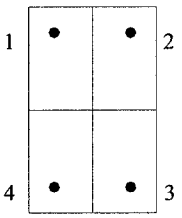

d) Four-spring model
Jiang and Saiidi (1990)

Fig. 2.2. Multi-axial spring models (MS models)

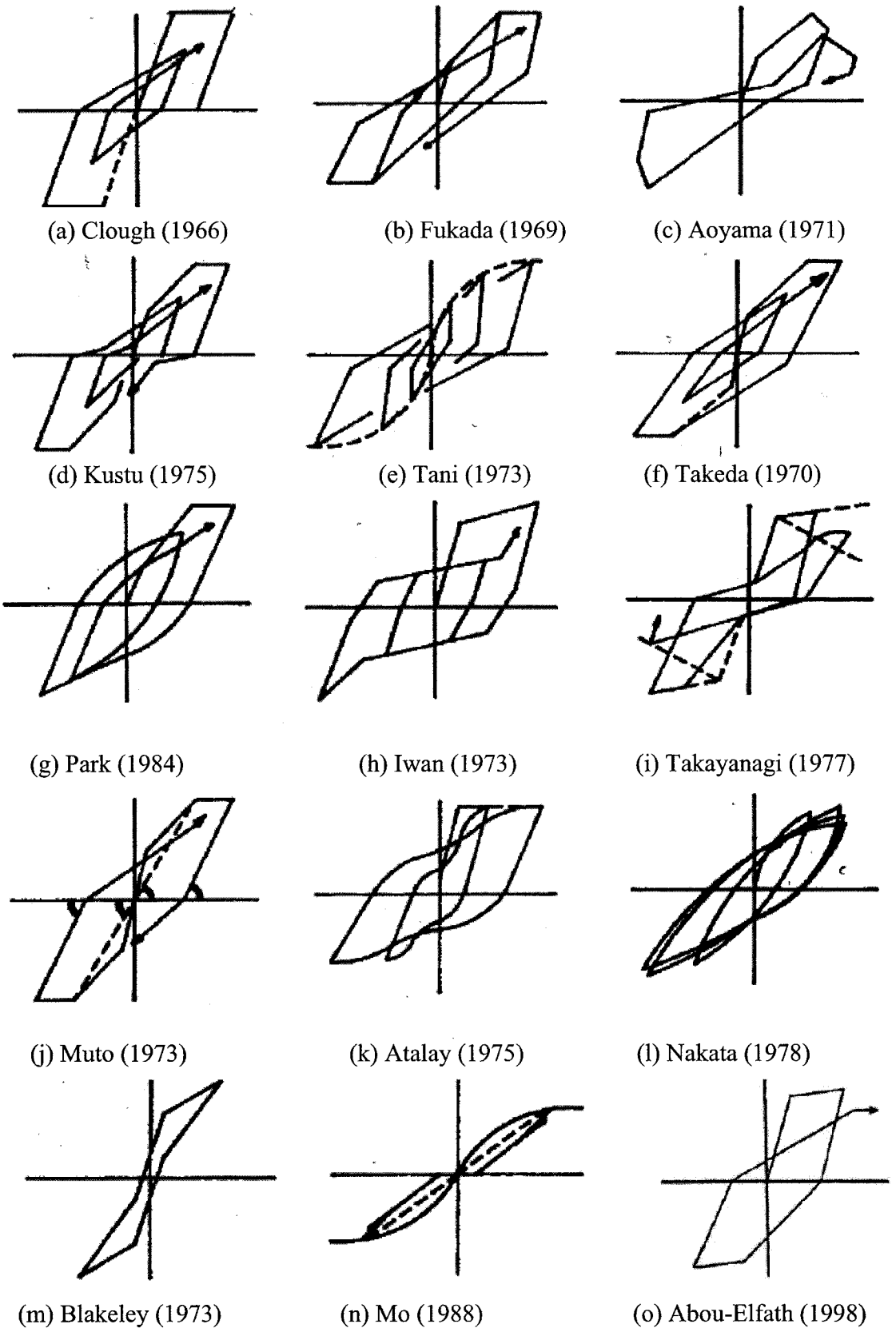

Fig. 2.3. Different models for hysteresis loops (Modified from Mo, 1994).

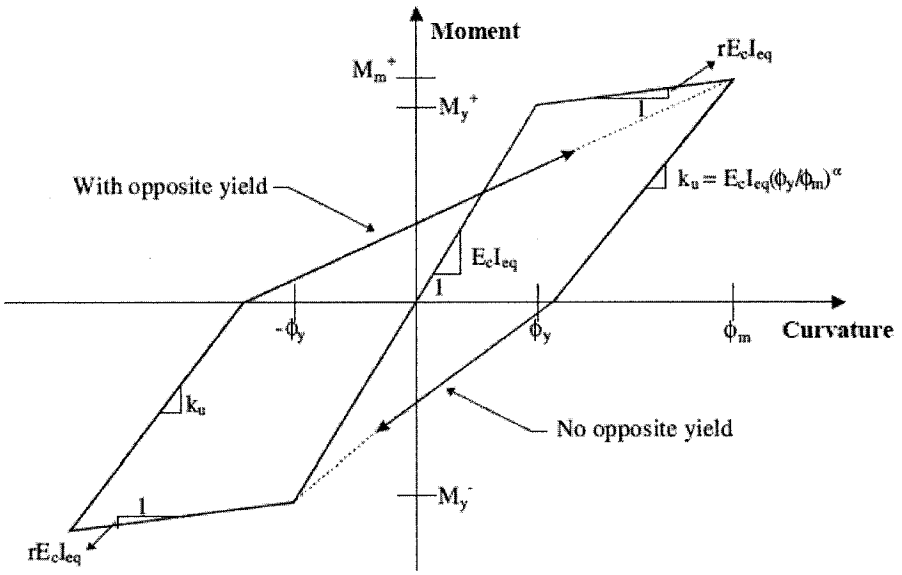

Fig. 2.4. Q-Hyst degrading stiffness moment-curvature hysteretic model. (Filiatrault *et al.* 1998)

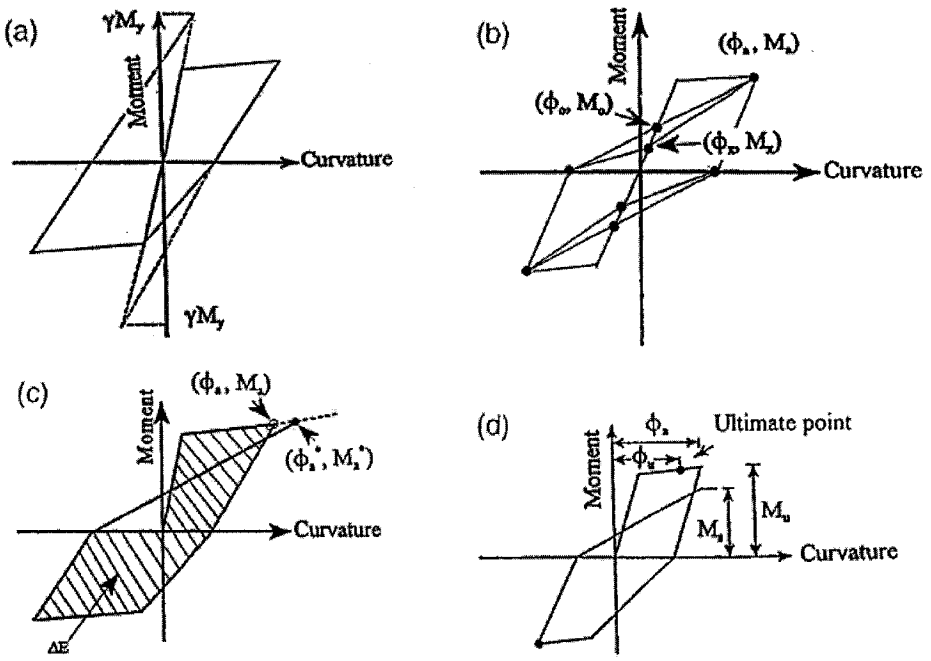

Fig. 2.5. Hysteretic model of the moment-curvature relationship: (a) Stiffness degradation; (b) pinching; (c) strength deterioration; (d) softening. (Ghobarah *et al.* 1999)

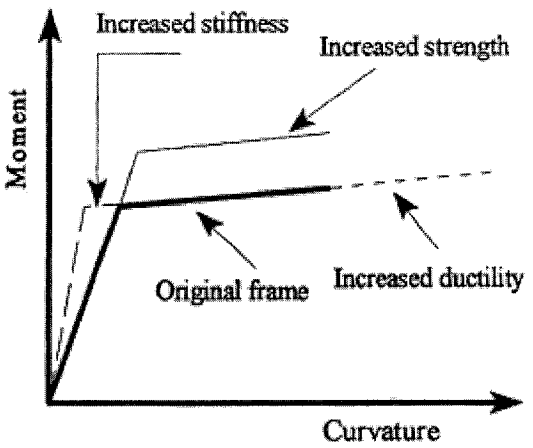

Fig. 2.6. Moment-curvature relationship for different rehabilitation strategies (Ghobarah *et al.* 2000)

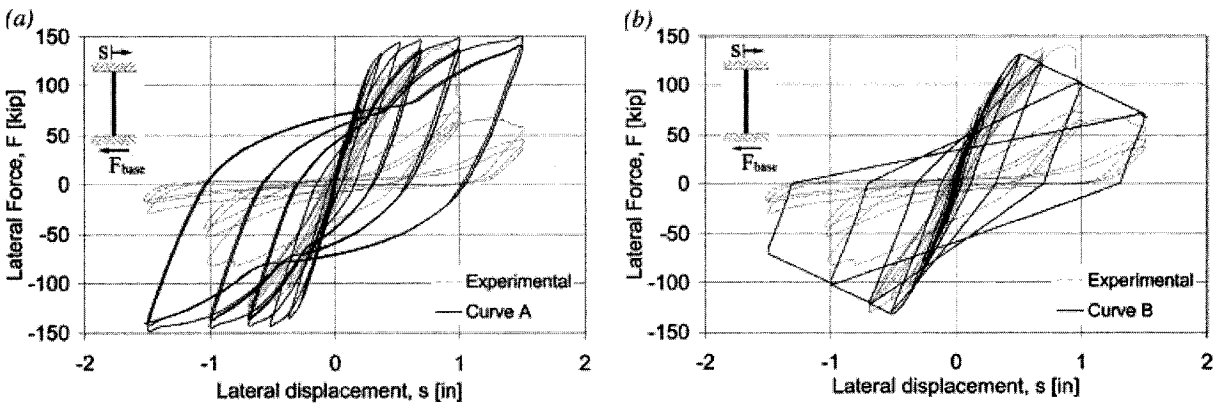

Fig. 2.7. Lateral force versus applied lateral displacement for Column R3: (a) infinite shear strength; and (b) limited shear strength. (Marini and Spacone 2006)

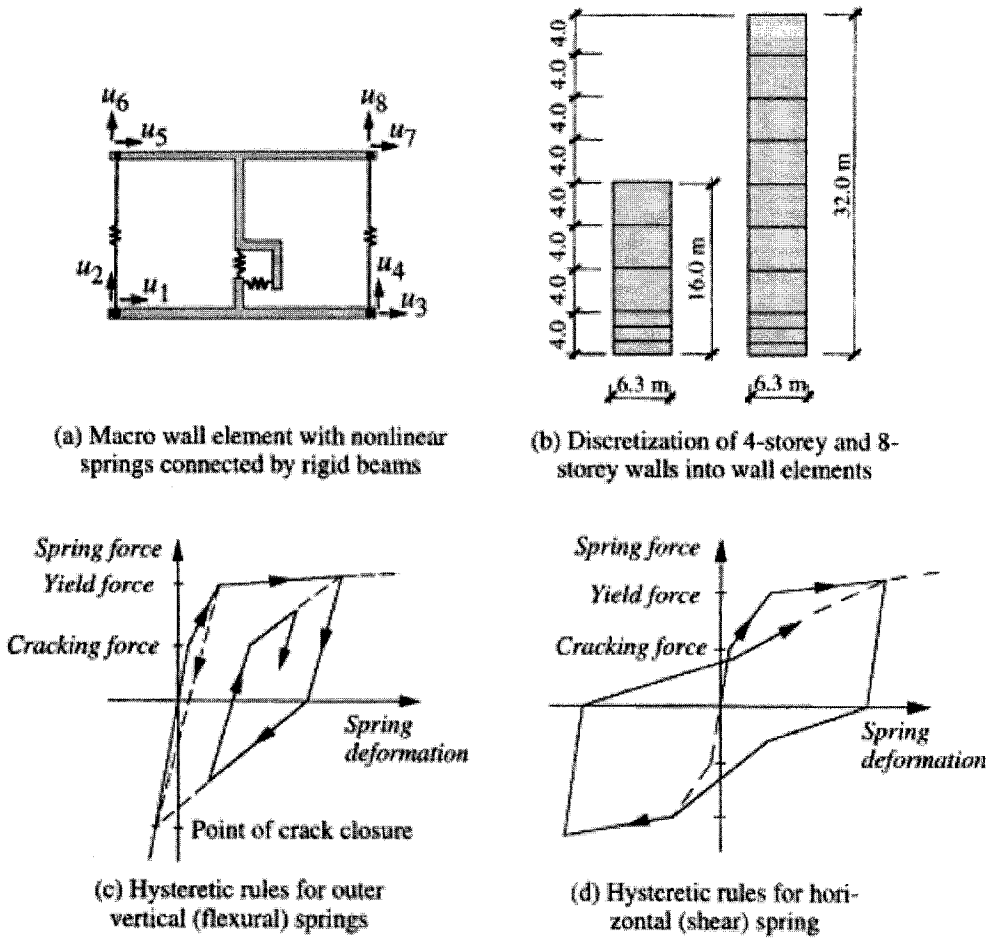

Fig. 2.8. Numerical model used in the nonlinear analysis and the hysteretic rules. (Linde 1998)

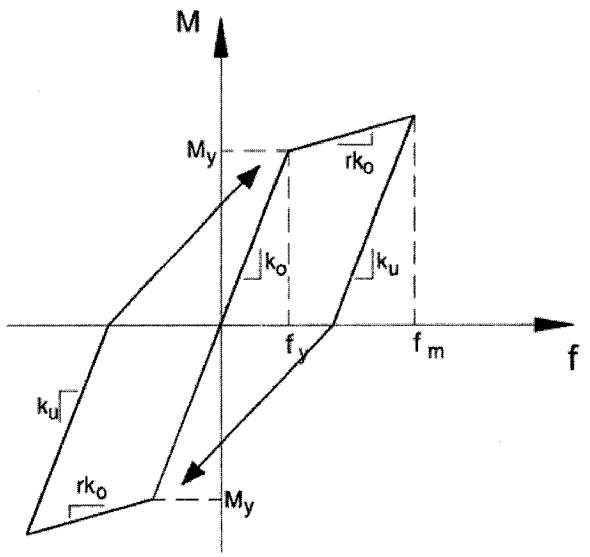

Fig. 2.9. The modified Takeda hysteretic model used in the nonlinear analyses of the RC wall. (Tremblay *et al.* 2001)

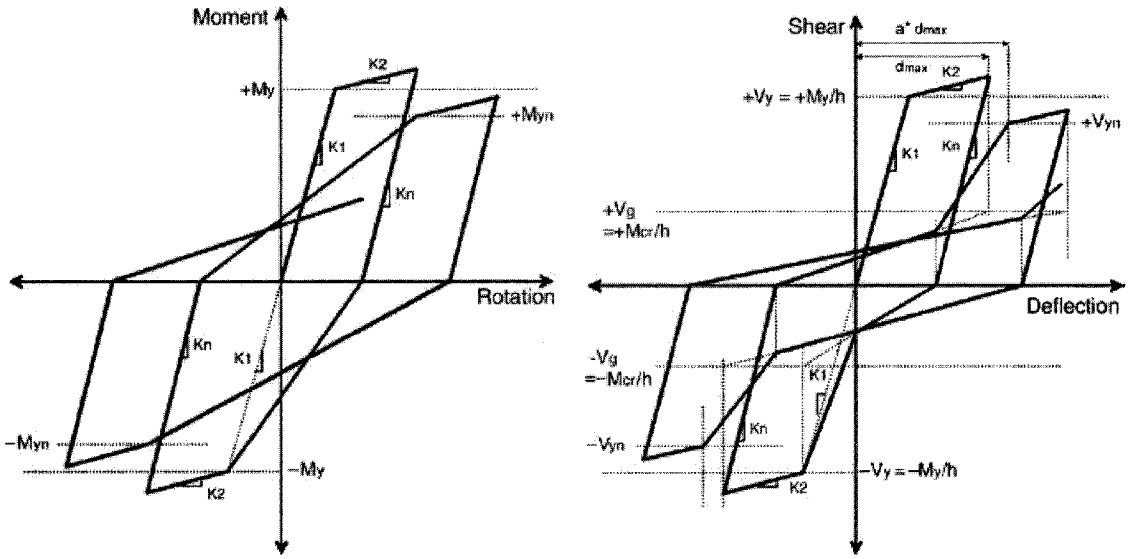

(a) Moment vs. rotation model.

(b) Shear force vs. shear deflection model.

Fig. 2.10. Hysteretic model for the flexure and shear springs. (Kim and Foutch 2007)

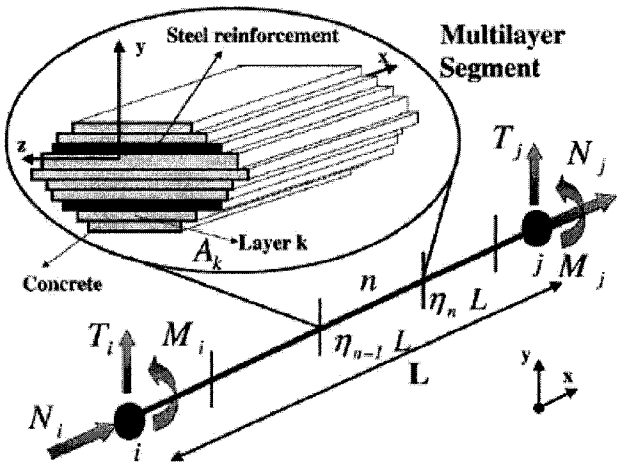

Fig. 2.11. Multilayer beam element (Belmouden and Lestuzzi 2007)

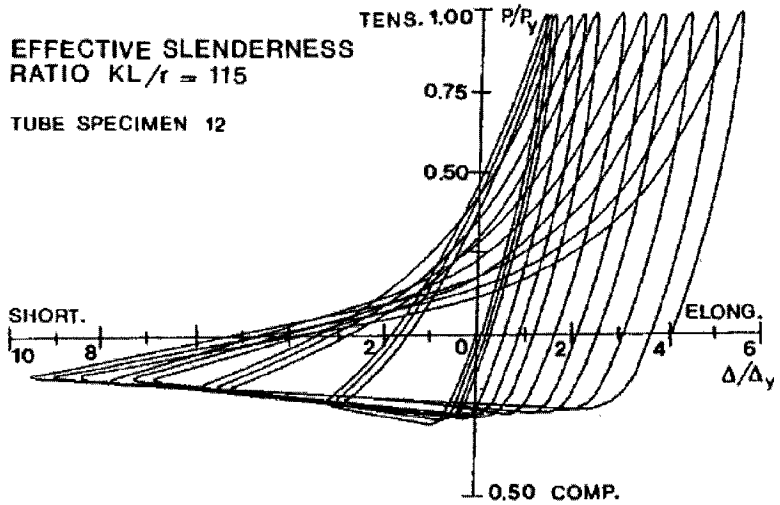

Fig. 2.12. Hysteretic behaviour of tubular steel bracing member (Jain *et al.* 1980).

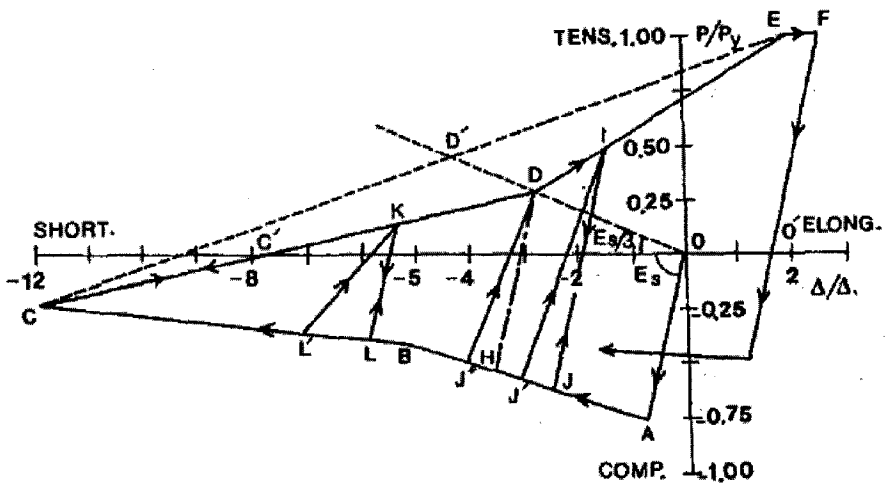

Fig. 2.13. Hysteretic model for tubular steel bracing member proposed by Jain *et al.* (1980)

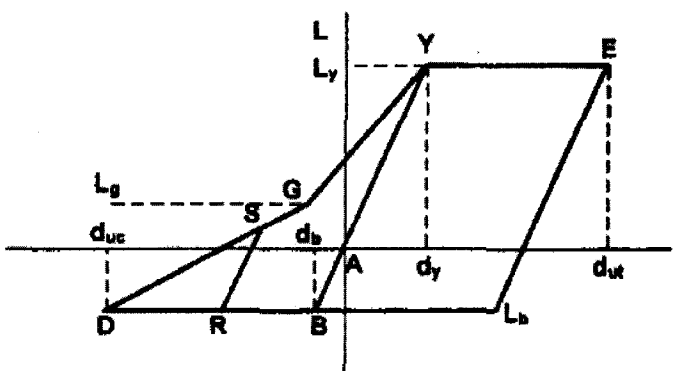

Fig. 2.14. Modeling of cyclic behaviour of pin-ended steel element (Galano and Gussela 1998).

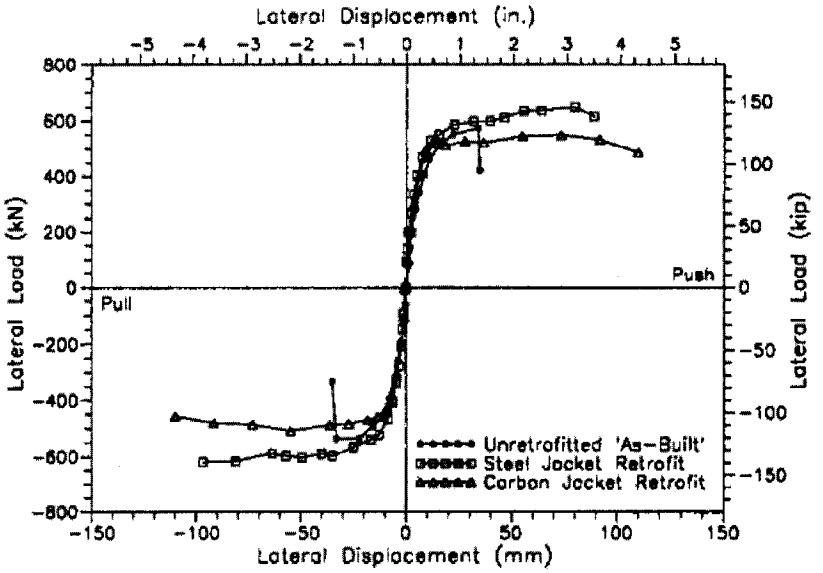

Fig. 2.15. Retrofitting the existing column using CFRP jacketing or steel jacketing. (Seible *et al.* 1997)

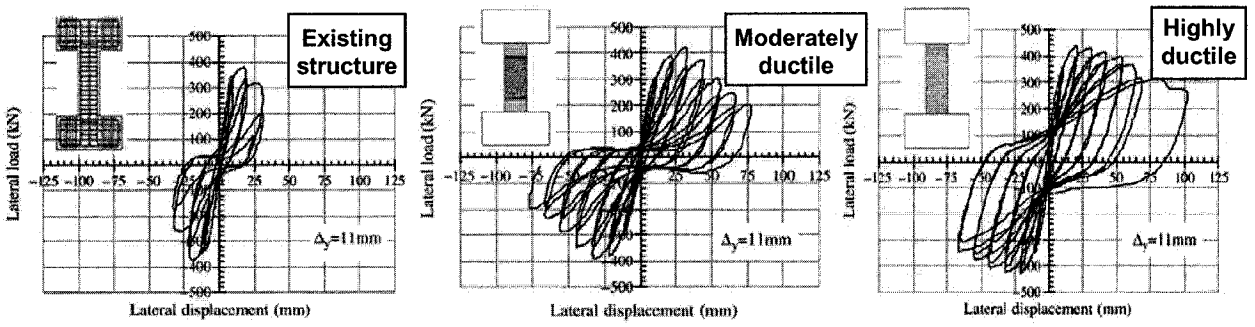

Fig. 2.16. Lateral force displacement relationship for different rehabilitation schemes. (Galal *et al.* 2005).

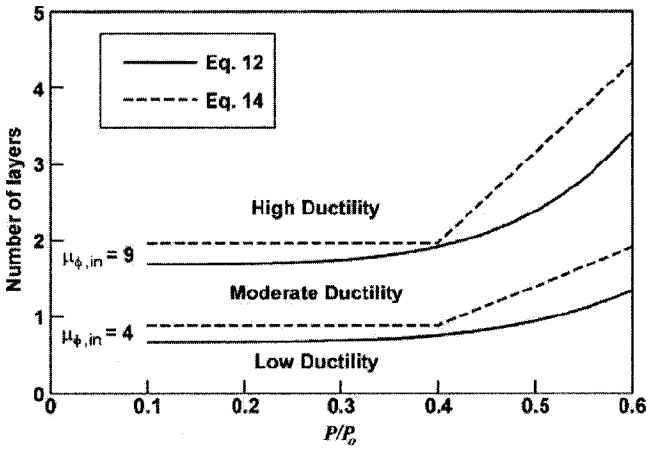

Fig. 2.17. The number of FRP layers needed as a function of the column axial load to reach a certain ductility level (Sheikh and Li 2007)

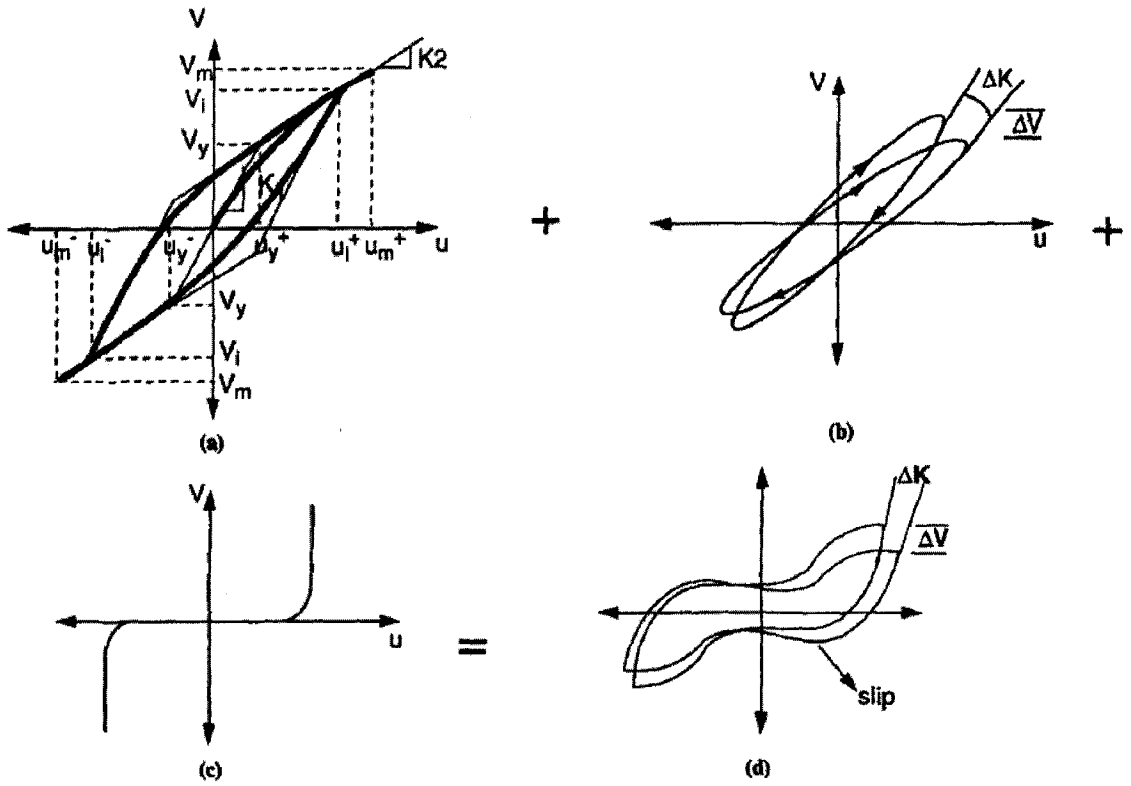

Fig. 2.18. Integrated hysteretic model for degrading pinching elements: (a) Wen-Bouc hysteresis model; (b) Hysteretic model with stiffness and strength degradation; (c) Slip-lock model; (d) Integrated model in IDARC. (Madan *et al.* 1997)

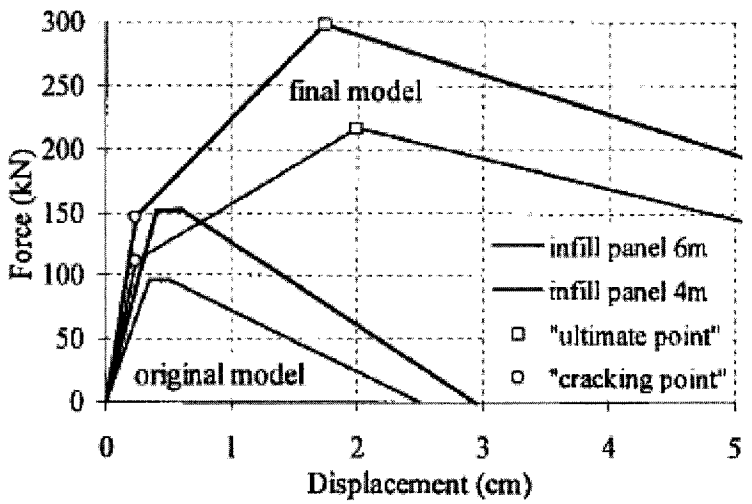

Fig. 2.19. Force-displacement backbone curve for the infill panels. (Dolsek and Fajfar 2002)

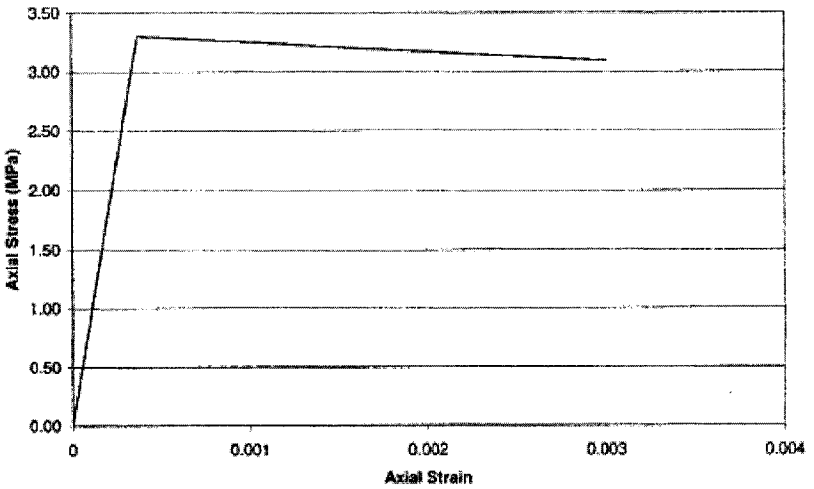

Fig. 2.20. Strut model of the infill. (Özcebe *et al.* 2003)

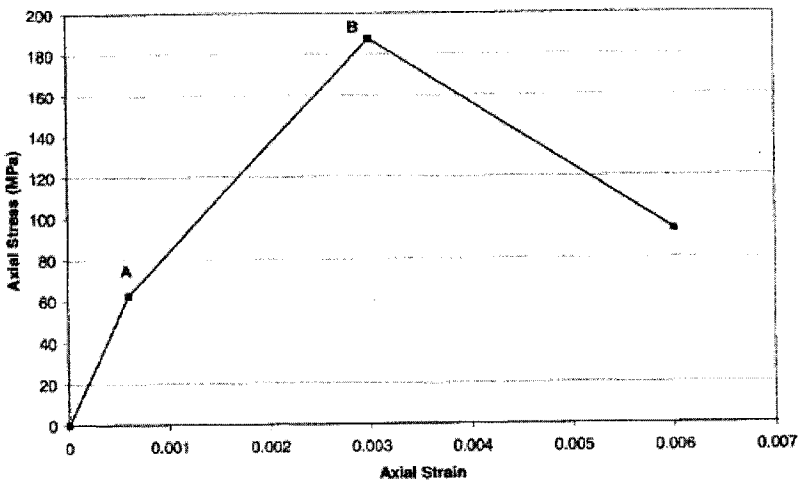

Fig. 2.21. Strut model of the composite material. (Özcebe *et al.* 2003)

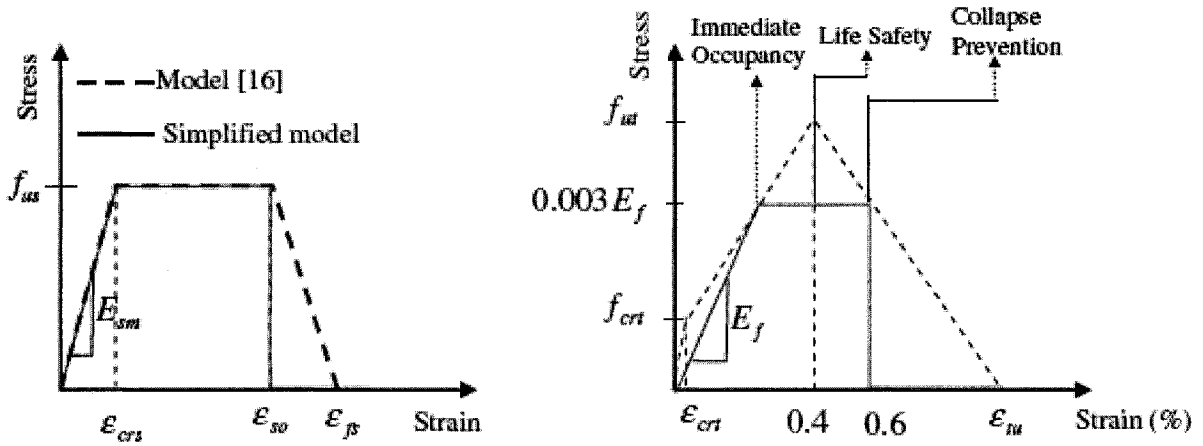

Fig. 2.22. Stress-strain relationship of the infill compression strut and FRP tension strut, respectively. (Binici *et al.* 2007)

CHAPTER 3

MODELING OF STUDIED FRAMES AND DIFFERENT REHABILITATION TECHNIQUES

3.1 INTRODUCTION

Reinforced concrete (RC) frames are considered as one of the most efficient lateral load resisting systems due to their ductility capacity, which increases the energy dissipation capacity of the structure. In order to achieve that required level of ductility, special attention should be considered for the detailing of reinforcement of beams, columns, and joints of the moment resisting frames. Most of the existing buildings that were designed according to pre-1970 design codes don't posses this ductility level. Consequently, this makes them susceptible to the hazard of partial damage or total collapse in the event of strong ground motion.

Pre-1970 design codes adopted a strength-based philosophy, and hence once the ultimate strength of the structure is reached, a non-ductile deterioration follows, which reduces the energy dissipated by the structure and results in a brittle failure. Therefore, structures designed according to old codes need to be strengthened in order to meet the requirements of the newly adopted performance-based design approach. This approach is expected to decrease the probability of brittle failure of the structures, and increase the energy dissipation capacity when subjected to the design ground motions.

This chapter discusses the modeling assumptions and procedures used to investigate the behaviour of the studied frames, including the different models that were used to represent different structural elements, and the properties of each model. The

properties of the selected buildings, ground motion records and the studied rehabilitation techniques are also presented.

3.2 PROPERTIES OF THE SELECTED BUILDINGS

Three building models designed according to pre-1970 strength based code (ACI 1968) are selected for this study. The buildings are of heights five, ten and fifteen storeys that represent low, medium and high-rise buildings, respectively. The three buildings have the same floor plan that consists of three symmetrical bays in both directions, where the bay width is 6 m. The floor height is 3.25 m and the total heights of the three buildings are 16.25, 32.5 and 48.75 m, respectively. The plan and elevations of the three buildings, the concrete dimensions for the beams and columns as well as the steel reinforcement are shown in Figure 3.1.The dimensions of the column sections and the steel reinforcement ratios varied along the height of the frames according to the change of axial load acting on each group of columns, while the beam dimensions and steel reinforcement were assumed to be the same for the entire frame.

3.3 DESIGN PARAMETERS

3.3.1 Material properties

For existing buildings, the compressive strength of concrete was assumed to be f_c' = 25 MPa and the yield strength of steel was set to be f_y = 400 MPa. The modulus of elasticity for concrete was taken 20 GPa and that of steel was taken 200 GPa. The concrete density was assumed to be 24 kN/m^3 and concrete Poisson's ratio υ was taken 0.15.

3.3.2 Design loads

The existing frames were designed according to old design code (ACI 1968). The frames' columns and beams were designed to carry a reinforced concrete slab of 120 mm thick, super imposed dead load of 2 kPa, live load of 2 kPa and equivalent load from interior partitions, mechanical and plumbing loads equal to 2 kPa.

3.4 PROPERTIES OF THE SELECTED GROUND MOTIONS

Tso *et al.* (1992) examined the significance of A/V ratio as a parameter to indicate the dynamic characteristics of earthquakes. Three sets of strong ground motion records were analyzed with low, medium and high A/V ratio. It was found that A/V ratio can be used as a simple indicator for the frequency content of the ground motion. In this study, a set of 9 far-field earthquake records was selected for the analysis (PEER 2006 and Tso *et al.* 1992). The ground motion records represent earthquakes with low, medium and high frequency contents. Acceleration time histories for the selected ground motions with low, medium and high A/V ratio are shown in Figures 3.2 (a), (b) and (c), respectively. The properties of selected ground motions are summarized in Table 3.1. A similar set of ground motion records was used to study the effectiveness of eccentric steel bracings in rehabilitation of low-rise RC frames by Ghobarah and Elfath (2001). Figures 3.3 (a), (b) and (c) show the 5% damped elastic acceleration response spectra for the selected ground motions for low, medium and high A/V ratio, respectively.

3.5 EXISTING STRUCTURES AND DIFFERENT REHABILITATION SCHEMES

In this study, two cases were considered in the analyses, the case of bare frames (i.e. without masonry infill) and the case of masonry-infilled frames. Moreover, in order to investigate the effect of infill stiffness on the seismic response of the frames, two different masonry infill types with different stiffnesses were considered. The infill stiffnesses represent soft and stiff infills. The 5, 10 and 15 storey existing frames were rehabilitated using four different techniques as follows:

3.5.1 Introducing a RC structural wall

The existing frames were strengthened by introducing a RC wall in the middle bay of the frame. The RC wall used is 6 m long, and has a thickness of 100, 150 and 200 mm for the 5, 10 and 15-storey frame, respectively. The thicknesses represent the cases of introducing a RC wall in the middle panel of the exterior frames with thicknesses of 200 mm, 300 mm, and 400 mm for the 5, 10, and 15-storey building, respectively. The steel reinforcement ratio was taken 0.015 for the walls. The wall dimensions and steel reinforcement ratio were assumed to remain constant along the wall height.

3.5.2 Rehabilitated frames using steel bracings

The existing bare and masonry-infilled frames were strengthened by introducing steel X-bracings in the middle bay along the full height of the frame. A tubular cross-section was selected for the X-bracing. The 5, 10 and 15 storey frames were strengthened using HSS 219 x 6.4, HSS 219 x 9.5 and HSS 273 x 11, with cross-sectional area of 4240, 6270, and 9160 mm^2, respectively. The effective slenderness ratio for the pin-ended

diagonal bracing was calculated to be 90, 92, and 74 for the 5, 10, and 15 storey frames, respectively. The maximum tensile strength for the steel material f_y was taken 400 MPa.

3.5.3 Rehabilitated frames using FRP bracings

In this technique, the studied masonry-infilled frames are rehabilitated by applying X-FRP bracings on the three panels of the frame along the full height, in which they are anchored to the infill and to the concrete members. The case of applying the X-FRP bracing to the intermediate panel only was also studied. Figure 3.4 shows the rehabilitation schemes using FRP bracing and the introduction of RC wall.

3.5.4 Rehabilitated frames using FRP-confinements

In this technique, the studied frames are rehabilitated by wrapping the columns laterally with FRP composites, while the beams are wrapped using FRP U-wraps near their ends. The effect of rehabilitating either the columns only or both columns and beams of the existing frames is also investigated.

3.6 NONLINEAR ANALYSES OF THE STUDIED FRAMES

Non-linear static and dynamic analyses were conducted for the 5, 10 and 15 storey frames with different rehabilitation schemes, a computer software for three dimensional nonlinear static and dynamic structural analysis CANNY (Li 2006) was selected for the analyses.

3.6.1 Program description

CANNY program (Li 2006) is able to perform different types of nonlinear analyses, e.g. push over analysis, dynamic analysis, pseudo dynamic analysis, etc. The

program has a library of linear and nonlinear models that can represent different types of backbone curves; linear, bilinear, tri-linear and degradation models. Different hysteretic behaviour can be represented by these models, also stiffness degradation, strength deterioration and pinching behaviour can be represented. The software is able to account for P-Δ effect in the analysis.

3.6.2 Selected models for the analyses

3.6.2.1 Yield surface (section) model (Lumped plasticity):

This model is the simplest model that can represent different structural components (e.g. columns, beams or walls). In this model, the flexural element is modeled as linear elastic line element with two inelastic single-component flexure rotation springs located at the end of the member. The axial and shear deformations can be represented using single axial tension/compression spring and single uniaxial shear spring, respectively. Figure 3.5 shows the section models for the line element. CANNY deterioration model CP4 (Li 2006) is used to model the nonlinear flexure rotation springs, which allows representation of the combined flexural and shear backbone curve with a parameter that controls the displacement ductility capacity after which the post-peak degradation occurs. The hysteretic behaviour of the model CP4 is shown in Figure 3.6. The main input data for this model is the element's force-displacement backbone curve. This model is able to represent the unloading stiffness degradation, the unloading rules are shown in Figure 3.7.

Unloading before yielding:

$$K_{10} = \begin{cases} K_5 & if \ |f'_p| < |f_p| \\ \dfrac{f'_p - f_c}{d'_p - d_c} & if \ |f'_p| \geq |f_p| \end{cases} ; \ K_{11} = \begin{cases} K_4 & if \ |f_p| < |f'_p| \\ \dfrac{f_p - f'_c}{d_p - d'_c} & if \ |f_p| \geq |f'_p| \end{cases} \quad \ldots. (3.1)$$

Unloading after yielding:

$$K_8, K_{10} = \frac{f'_y - f_c}{d'_y - d_c}\left(\frac{d'_y}{d'_m}\right)^{\gamma} \ ; \quad K_9, K_{11} = \frac{f_y - f'_c}{d_y - d'_c}\left(\frac{d_y}{d_m}\right)^{\gamma} \qquad \ldots\ldots\ldots (3.2)$$

$$K_8, K_{10} \geq \frac{f'_m - f_c}{d'_m - d_c} \ ; \quad K_9, K_{11} \geq \frac{f_m - f'_c}{d_m - d'_c} \qquad \ldots\ldots\ldots (3.3)$$

Unloading of interior loop:

$$K'_{10} = \xi'.K_{10} \ ; \ K'_{11} = \xi.K_{11} \qquad \ldots\ldots\ldots (3.4)$$

Where, γ is the unloading stiffness degradation parameter ($\gamma = 0 - 0.7$)

ζ is the inner loop stiffness reduction ($\zeta = 0.5 - 1.0$)

3.6.2.2 Linear elastic models:

These models are able to represent the tension only or compression only force-displacement relationship. The model ET1 is a tension only linear elastic model while EC1 can be compression only if the parameter α is set equal to zero, these models have no cracking or yielding events. Figure 3.8 shows the linear elastic models ET1 and EC1.

3.6.2.3 Multi-axial spring model (MS model):

Multi-axial spring model is able to represent the interaction of flexural and axial (tension or compression) deformations of column or wall element. In this model shear deformations can be represented using a shear spring, in which shear deformations can be

linear or nonlinear according to the hysteretic rule used for that spring. A column or wall element is modeled as linear element with nonlinear multi-axial spring elements at their ends, as shown in Figure 3.9. In this model the spring properties can represent the material (i.e. concrete and steel) stress-strain relationship. The initial stiffness of the spring is based on equivalent plastic zone stiffness which can be calculated by:

$$K_0^{\,i} = \frac{E_i A_i}{\eta L_0} \qquad \textit{(for the } i^{th} \textit{ spring)} \qquad \ldots\ldots\ldots (3.5)$$

$$f_c = \sigma_c A_i, \qquad \textit{(for concrete)} \qquad \ldots\ldots\ldots (3.6)$$

$$f_{sy} = \sigma_{sy} A_i, \quad d_{sy} = \varepsilon_{sy} \eta L_0 \qquad \textit{(for steel)} \qquad \ldots\ldots\ldots (3.7)$$

Where

K_0 is the initial stiffness of spring.

E_i is the material Young's modulus.

A_i is the area represented by the springs.

σ_c, ε_c are the concrete material compressive strength and corresponding strain.

σ_{sy}, ε_{sy} are the steel material yield stress and strain.

η is the ratio of the plastic zone length to the member clear length, and is taken empirically half the depth of the member cross-section .

L_0 is the clear length of the member.

3.6.2.3.1 Concrete spring:

Figure 3.10 shows the bilinear model CS2 that is used to represent the concrete material, this model has compression ascending part in linear elastic curve. After reaching the maximum strength, the step-down rule is applied for the descending branch in

compression side and tension side to solve for negative stiffness. In this rule, the software uses a slight positive stiffness (almost equal to zero) and evaluates the element resistance in negative stiffness, then the unbalanced force which is the difference between the element resistance and the required force for equilibrium is corrected in the next iteration.

The unloading stiffness degradation is calculated as follows:

$$K_5 = \begin{cases} K_{cu}(d_c / d_m)^{\gamma} & if \quad d_m \rangle d_c \\ K_{cu} & if \quad d_m \le d_c \end{cases} \qquad \ldots\ldots\ldots (3.8)$$

$$K_{cu} = \begin{cases} K_c & if \quad \phi = 0 \\ \dfrac{\varphi . f_c + f_m}{\phi . f_c / K_c + d_m} & if \quad d_m \le d_c \\ \dfrac{\varphi . f_c + f_m}{\phi . f_c / K_c + d_c} & if \quad d_m \rangle \; d_c \end{cases} \qquad \ldots\ldots\ldots (3.9)$$

The tensile strength of concrete is considered only if the tensile strength f_t and the parameter τ are specified. $\tau \geq 3.0$ represents the tension descending part after reaching the maximum tensile strength f_t.

The parameters taken for this model in our study are as follow:

- Strain at maximum compressive strength = 0.002 mm/mm
- Ultimate strain / strain at maximum compressive strength ratio μ = 1.75
- Post-peak residual strength / maximum compressive strength ratio λ = 0.2
- Post-peak unloading stiffness parameter γ = 0.2
- Tension descending part after tension crack τ = 3.0

3.6.2.3.2 Steel spring:

Figure 3.11 shows the trilinear/bilinear model SS3 that is used to represent the steel material. This model is able to represent the stiffness degradation of the whole section before yielding that can result from cracking or bond slippage of tension reinforcement. In that model the stiffness is reduced before reaching the yielding point by reducing the yielding point from point P_1 to point P_2 then the curve is connected to point P_3 which is corresponding to spring yield displacement equal to $\kappa\, d_{sy}$, where κ is equal to 1 for bilinear curve.

The unloading stiffness calculation depends on whether both tension and compression steel has yielded or not, if yielding has not occurred then:

$$K_u = \begin{cases} \min of \dfrac{f_m - \varphi f'_{sy}}{d_m - \varphi f'_{sy}/K_s} \; or \; \dfrac{f'_m - \phi f_{sy}}{d'_m - \phi f_{sy}/K_s} & if \;\; \phi \rangle 0 \\ K_s & if \;\; \phi = 0 \end{cases} \quad \ldots\ldots\ldots (3.10)$$

Where ϕ defines the target points A, A' as shown in Figure 3.12. If ϕ is set to zero then no unloading stiffness degradation occurs before yielding. If yielding has occurred in either tension or compression then:

$$K_{uy} = \begin{cases} \min of \dfrac{f'_{sy} - \varphi f_{sy}}{\kappa' d'_{sy} - \varphi f_{sy}/K_s} \; or \; \dfrac{f_{sy} - \varphi f'_{sy}}{\kappa d_{sy} - \varphi f'_{sy}/K_s} & if \;\; \phi \rangle 0 \\ K_s & if \;\; \phi = 0 \end{cases} \quad \ldots\ldots\ldots (3.11)$$

$$K_u = K_{uy}\left(\frac{\kappa d_{sy} - \kappa' d'_{sy}}{d_m - d'_m}\right)^{\gamma}, \text{ where } d_m \geq \kappa . d_{sy}\,,\; d'_m \leq \kappa' . d'_{sy} \quad \ldots\ldots\ldots (3.12)$$

When the compression unloading curve passes the horizontal axis and $F < \theta . f_{sy}$, then the loading toward tension maximum point, M', where θ is the factor defining the unloading end point. The parameters taken for this model in our study is as follow:

Skeleton curve parameters ν and κ are taken = 1.0 (i.e. bilinear curve)

Post-yielding parameter $\beta = 0.01$

Parameter φ to direct the unloading = 0 (for bilinear curve)

Unloading stiffness degradation parameter $\gamma = 0.2$

Unloading control parameter $\theta = 0.2$

3.6.3 Modeling assumptions

The floors are assumed to act rigidly in the horizontal direction (two-dimensional rigid diaphragm). The mass of each floor is lumped at the beam-column joints according to the tributary areas. The frame joints are assumed to be rigid and rigid zones are applied at the ends of each member. The rigid zone is taken as 0.4 the depth of the member in each side of the joint. P-delta effects are included in the analyses. Figure 3.13 shows the idealization of different members of the studied frames assembled in one figure.

3.6.4 Modeling of existing structures and different rehabilitation schemes

3.6.4.1 Modeling of existing beams and columns:

The beams and columns were modeled as linear elastic element with two inelastic single-component flexure rotation spring located at the ends of the member, CANNY deterioration model CP4 (Figure 3.6) was used to model the nonlinear flexure rotation spring.

The lateral force-displacement ductility relationship of the columns and beams of the existing frames was assumed to have limited displacement ductility, μ_Δ , equal to 2, which is followed by a quick reduction in the lateral load resistance. For the model, the unloading stiffness degradation γ was taken 0.1, while the inner loop stiffness reduction ξ was assumed to be 1.0. The force-displacement ductility backbone curve for the existing frame members is shown in Figure 3.14. The properties of the backbone curve for the existing beams and columns are obtained using sectional analysis and they are shown in Table 3.2.

3.6.4.2 Modeling of rehabilitated columns and beams with FRP-confinements:

In this study the columns were rehabilitated by wrapping them laterally with FRP composites, while the beams were rehabilitated using FRP U-wraps near their ends. The rehabilitated columns and beams were modeled with the same model CP4 as the existing members. The FRP content used in the rehabilitation of the structural elements was assumed to increase their energy dissipation capacities and displacement ductility, μ_Δ, to be equal to 6.0 (compared to 2 in case of existing members). The force-displacement ductility backbone curve for the rehabilitated frame members using FRP confinements is shown in Figure 3.14. The properties of the backbone curve for the FRP-confined beams and columns are shown in Table 3.3.

The element's force-displacement ductility relationship is a combination of flexure and shear resistance. Ignoring the representation of the strength degradation in the overall response of the element once its shear capacity is reached would lead to erroneous response predictions. On the other hand, modeling the structural element using two

independent non-linear springs representing flexure and shear hysteretic responses would result in an uncontrolled displacement ductility capacities of the element, which is a major parameter in the performance-based seismic design approach. Added to that is the difficulty in defining the hysteretic properties of the independent shear subhinge, and ignoring the flexure-shear interaction.

In this model, strength degradation was considered in the element's lateral force-displacement ductility backbone curve in order to represent strength degradation due to the shear failure. The post-peak degradation in strength occurs through a displacement equivalent to one and two times the yield displacement up to a residual force of 0.3 and 0.5 of the ultimate load capacity for the existing and the ductile structure, respectively, as shown in Figure 3.14. The moment-curvature relationship was drawn for every element in the existing structure and consequently the input curves for the FRP-rehabilitated frames were estimated as a multiplier of the existing structure curve as shown in the figure.

3.6.4.3 Modeling of FRP bracings:

Özcebe, *et al.* (2003) proposed an analytical representation to predict the behaviour of masonry-infilled frames when rehabilitated with FRP bracings. The analytical model was correlated to experimental tests carried out at Middle East Technical University (METU) on a number of two-storey masonry-infilled frame specimens rehabilitated with different patterns of FRP, and subjected to cyclic displacement excitations at the storey levels. Similar uniaxial models for the masonry infill and FRP bracings were used in the current study. Figure 3.15 shows the axial stress- axial strain relationship for the tension strut of FRP bracings. The FRP bracings were modeled as

uniaxial tension strut with maximum axial strain of 0.003 and maximum axial stress of 190 MPa, these values takes into account the characteristics of CFRP, infill, and the anchor dowels.

3.6.4.4 Modeling of masonry infill:

The unrehabilitated infill panels were modeled as compression struts, the properties of the compression strut was chosen based on Özcebe, *et al.* (2003), and it was scaled to match the panel dimensions of the studied frames. The tensile resistance of the masonry infill was neglected in the analyses. Figure 3.16 shows the axial stress- axial strain relationship for the compression strut of the infill. In this study, two different masonry infill types with different stiffness were considered, representing soft and stiff infill, in order to investigate the effect of infill stiffness on the response of structures.

3.6.4.5 Modeling of RC structural wall:

The RC wall was modeled using CANNY wall element as shown in Figure 3.13. The wall element has four nodes at the corners in addition to an optional node can be located at the mid points of the top and bottom boundaries. The adjacent panels have compatible deformations at their common three nodes that are connecting them. Multi-Axial spring model is used to represent the flexural and axial tension/compression interaction of the wall elements. The shear deformations can be idealized using a shear spring. Multi-linear curves are used to represent the force-deformation relationship for concrete and steel springs as shown in Figures 3.10 and 3.11, respectively. In the current analyses, the shear deformations were assumed to be linear. A similar representation of

RC walls was used in the analysis of lightly reinforced concrete walls subjected to near-fault and far-field ground motions (Galal 2007).

3.6.4.6 Modeling of steel bracings:

The steel braces were modeled as axial tension/compression struts. CANNY buckling element STB was used to represent the hysteretic behaviour of the bracing member. The model STB is able to represent the reduction in the maximum compressive strength with increasing the number of load cycles as was observed by Jain *et al.* (1980) in their experimental tests (Figure 2.13). The main input data for the model is the maximum tensile force resisted by the member and the effective slenderness ratio which control the value of maximum compressive strength. The hysteretic behaviour of CANNY buckling model STB is shown in Figure 3.17.

3.7. VERIFICATION OF THE ANALYTICAL MODEL USING EXPERIMENTAL RESULTS.

The models used for the masonry infill and FRP bracing were verified using the results of the experimental tests carried out in METU (Özcebe *et al.* 2003). The experimental results of the static pushover analysis are compared with the analytical results carried out using CANNY and the analytical model proposed in the current study, for both unrehabilitated masonry-infilled frame and the rehabilitated frame using FRP bracing. Figure 3.18 shows the comparison of the analytical and experimental results for (a) the unrehabilitated frame and (b) the rehabilitated frame using FRP bracing. From the figures, it can be seen that the analytical model is able to represent the real behaviour of the specimen, and that ensure the validity of using this model in the current study.

3.8. DETAILED STUDY ON REHABILITATION USING FRP-CONFINEMENT.

In this study, the performance of the three existing frames is evaluated when rehabilitated using different configurations of FRP-confinements. Two FRP contents and four different rehabilitation patterns were investigated. The studied patterns include rehabilitation of both columns and beams (1) along the full height and (2) in the lower half of the structure height; and rehabilitation of columns only (3) along the full height and (4) in the lower half. The two FRP contents used in the rehabilitation of the structural elements will increase their energy dissipation capacities and displacement ductility to be moderately and highly ductile with μ=4 and μ=6, respectively (compared to μ=2 for the existing structure). The actual amount of glass or carbon FRP sheets needed to reach the targeted displacement ductility level (i.e. $\mu_\Delta = 4$ or $\mu_\Delta = 6$) can be easily calculated using models available in the literature (e.g. Galal 2007 or Sheikh and Li 2007). The force-displacement ductility backbone curves for the existing, moderately ductile and highly ductile frames are shown in Figure 3.19. Table 3.4 shows the relative properties of the structural element's force-displacement backbone curves for the two rehabilitation schemes considered in the analysis (moderately and highly ductile) as related to the existing structure properties. In Figure 3.19, it can be noticed that the case of no shear degradation was also considered, in order to investigate the importance of accounting for the post-peak degradation in the analyses.

Table 3.1. Properties of the selected ground motions. (PEER 2006 and Tso *et al.* 1992)

No.	Earthquake	Site	Date	A (g)	V (m/s)	A/V		Duration (s)	Soil condition
						(g. s/m)	Level		
1	Lower California	El Centro	Dec. 30, 1934	0.160	0.209	0.766	Low	90.36	Stiff soil
2	San Fernando, Cal.	2500 Wilshire Blvd., LA	Feb. 9, 1971	0.101	0.193	0.518		25.32	Stiff soil
3	Long beach, Cal.	LA Subway Terminal	Mar. 10, 1933	0.097	0.237	0.409		99.00	Rock
4	San Fernando, Cal.	234 Figueroa St., LA	Feb. 9, 1971	0.200	0.167	1.198	Med.	47.10	Stiff soil
5	Kern County, Cal.	Taft Lincoln School Tunnel	July 21, 1952	0.179	0.177	1.011		54.42	Rock
6	Imperial Valley	El Centro	May 18, 1940	0.348	0.334	1.042		53.76	Stiff soil
7	Lytle Creek, Cal.	6074 Park Dr., Wrightwood	Sep. 12, 1970	0.198	0.096	2.063	High	16.74	Rock
8	Parkfield, Cal.	Cholame, Shandon	June 27, 1966	0.434	0.255	1.702		44.04	Rock
9	San Francisco	Golden Gate Park	Mar. 22, 1957	0.105	0.046	2.283		39.88	Rock

Table 3.2. Properties of the backbone curves for the existing columns and beams.

Section	P_c (kN)	P_y (kN)	Δ_{cr} (mm)	Δ_y (mm)	μ_Δ	K_o (kN)	K (kN)	α	β
C1	28.29	98.21	1.014	15.668	2	437.11	74.77	0.0084	-0.1749
C2	29.88	141.66	1.014	15.492	2	456.45	119.61	0.0063	-0.2375
C3	14.97	46.00	1.531	18.132	2	177.26	33.89	0.0040	-0.1976
C4	16.16	70.14	1.531	18.132	2	191.32	58.96	0.0146	-0.2859
C5	97.16	355.07	0.845	15.492	2	1781.21	272.80	0.0040	-0.1525
C6	101.16	437.53	0.845	15.492	2	1854.54	355.79	0.0050	-0.1807
C7	43.25	137.85	1.074	16.548	2	666.46	101.16	0.0063	-0.1598
C8	46.44	215.20	1.074	18.220	2	787.91	179.33	0.0080	-0.2108
C9	179.40	587.08	0.704	14.083	2	3588.06	429.13	0.0052	-0.1266
C10	186.30	769.23	0.704	15.844	2	4191.78	610.04	0.0016	-0.1388
B1	18.75	73.33	2.940	32.400	2	206.63	60.03	0.0234	-0.2837
B2 +ve	21.17	133.33	3.456	37.800	2	231.55	123.45	0.0096	-0.4391
B2 -ve	-19.61	-73.33	-3.198	-32.400	2	-198.64	-59.61	0.0233	-0.2944

To be read with Figures 3.1 and 3.14

Table 3.3. Properties of the backbone curves for the FRP-confined columns and beams

Section	P_c (kN)	P_y (kN)	Δ_{cr} (mm)	Δ_y (mm)	μ_Δ	K_o (kN)	K (kN)	α	β
C1	28.29	112.95	1.014	15.668	6	437.11	90.52	0.0084	-0.0564
C2	29.88	162.91	1.014	15.492	6	456.45	142.35	0.0063	-0.0729
C3	14.97	52.92	1.532	18.132	6	177.26	41.45	0.0040	-0.0598
C4	16.16	80.67	1.532	18.132	6	191.32	70.46	0.0145	-0.0926
C5	97.16	408.34	0.845	15.492	6	1781.21	329.13	0.0040	-0.0467
C6	101.16	503.17	0.845	15.492	6	1854.54	425.21	0.0049	-0.0555
C7	43.25	158.52	1.074	16.548	6	666.46	123.27	0.0063	-0.0505
C8	46.44	247.48	1.074	18.220	6	787.90	213.64	0.0079	-0.0663
C9	179.40	675.14	0.704	14.083	6	3588.06	521.83	0.0052	-0.0401
C10	186.30	884.62	0.704	15.844	6	4191.78	730.79	0.0016	-0.0411
B1	18.75	84.33	2.940	32.400	6	206.63	72.13	0.0234	-0.0985
B2 +ve	21.17	153.33	3.456	37.800	6	231.55	145.46	0.0096	-0.1332
B2 -ve	-19.61	-84.33	-3.198	-32.400	6	-198.64	-71.82	0.0234	-0.1015

To be read with Figures 3.1 and 3.14

Table 3.4. Properties of the FRP-rehabilitated structural elements as compared to those of the existing structure.

Model properties	Existing structure	Moderately ductile	Highly ductile
Initial stiffness	K	1.1 K	1.15 K
Yield Capacity	F_y	1.1 F_y	1.15 F_y
Displ. Ductility Capacity	2.0	4.0	6.0

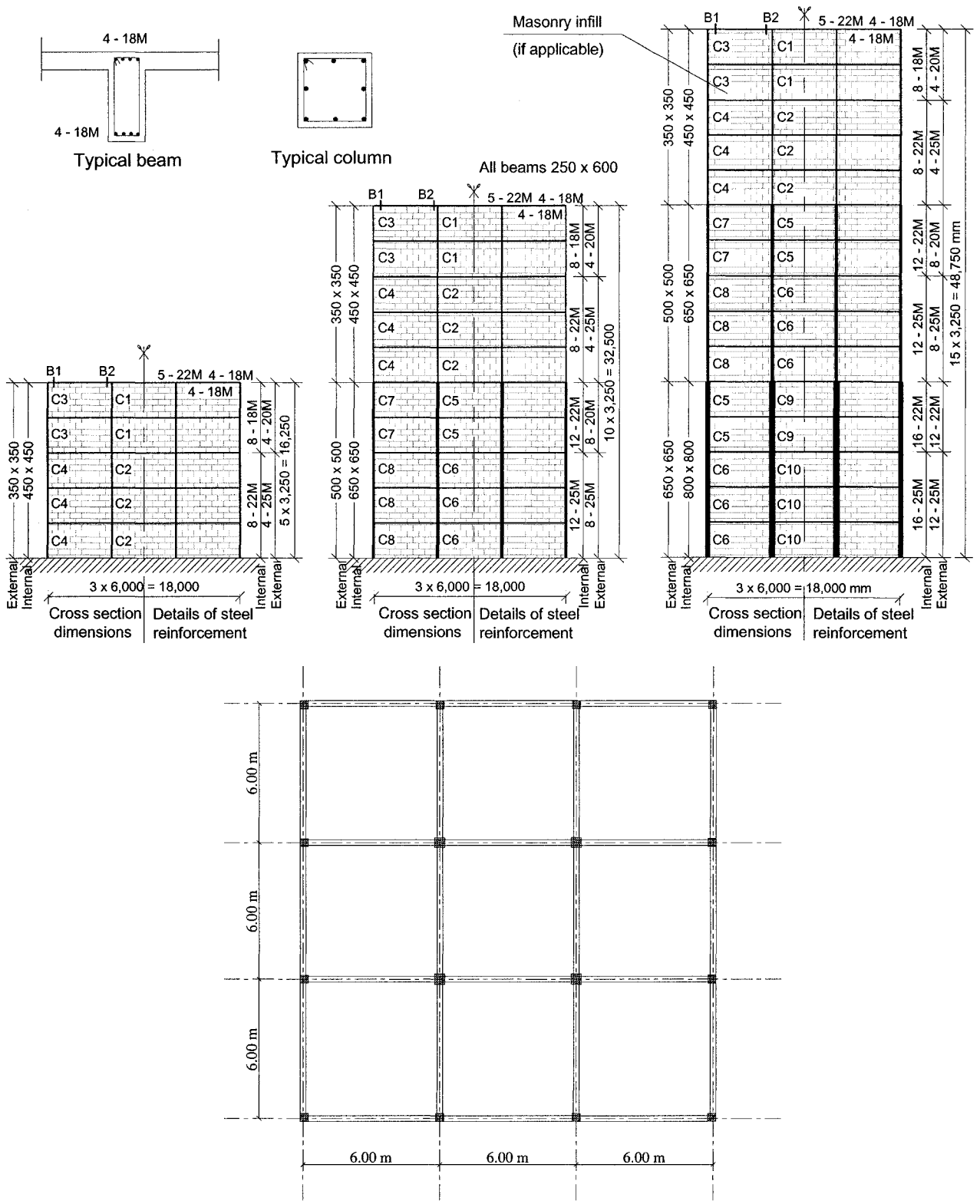

Fig. 3.1. Elevations and plan of the studied 5, 10 and 15 storey frames.

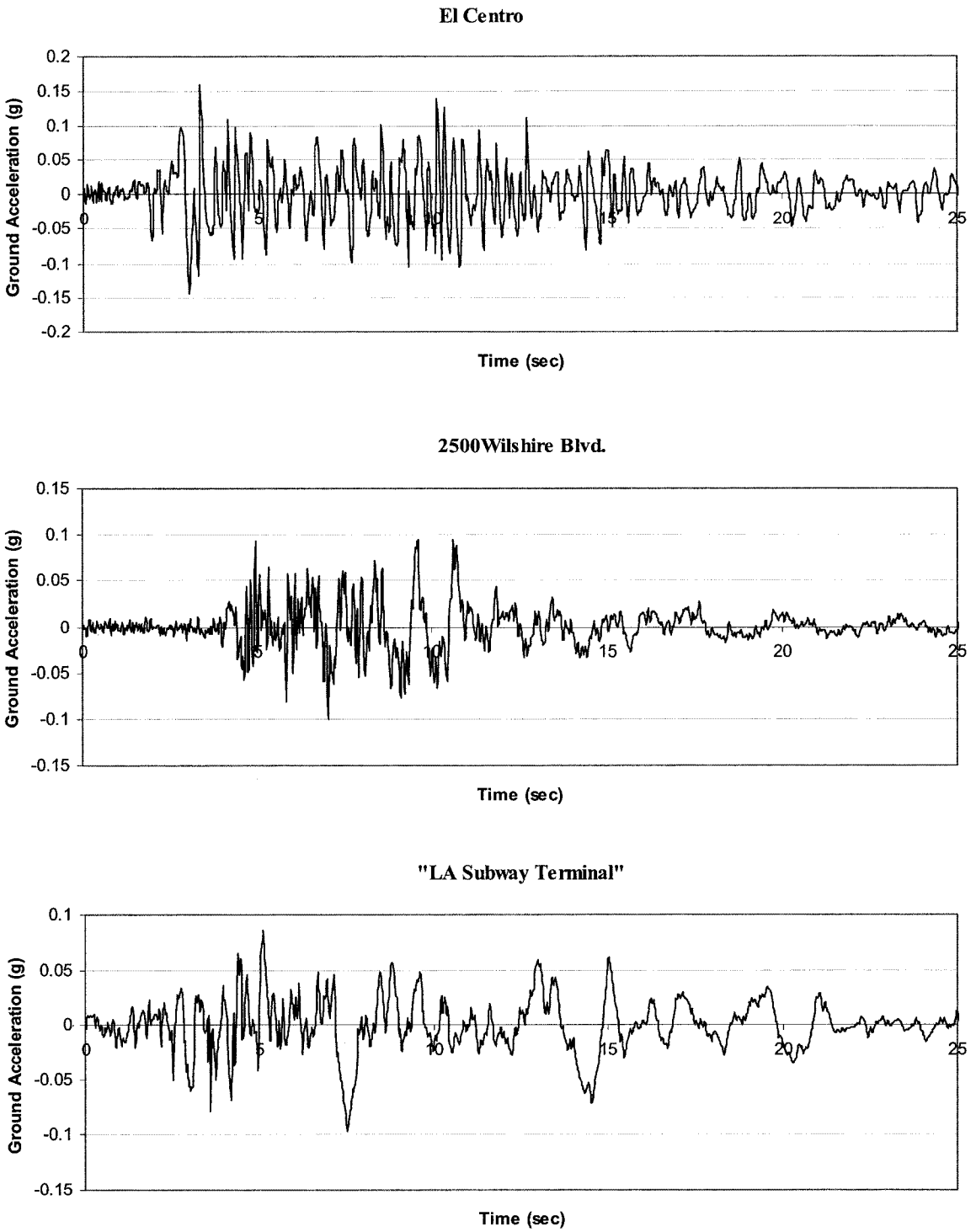

Fig. 3.2(a). Acceleration time histories of the low A/V ratio ground motion records.

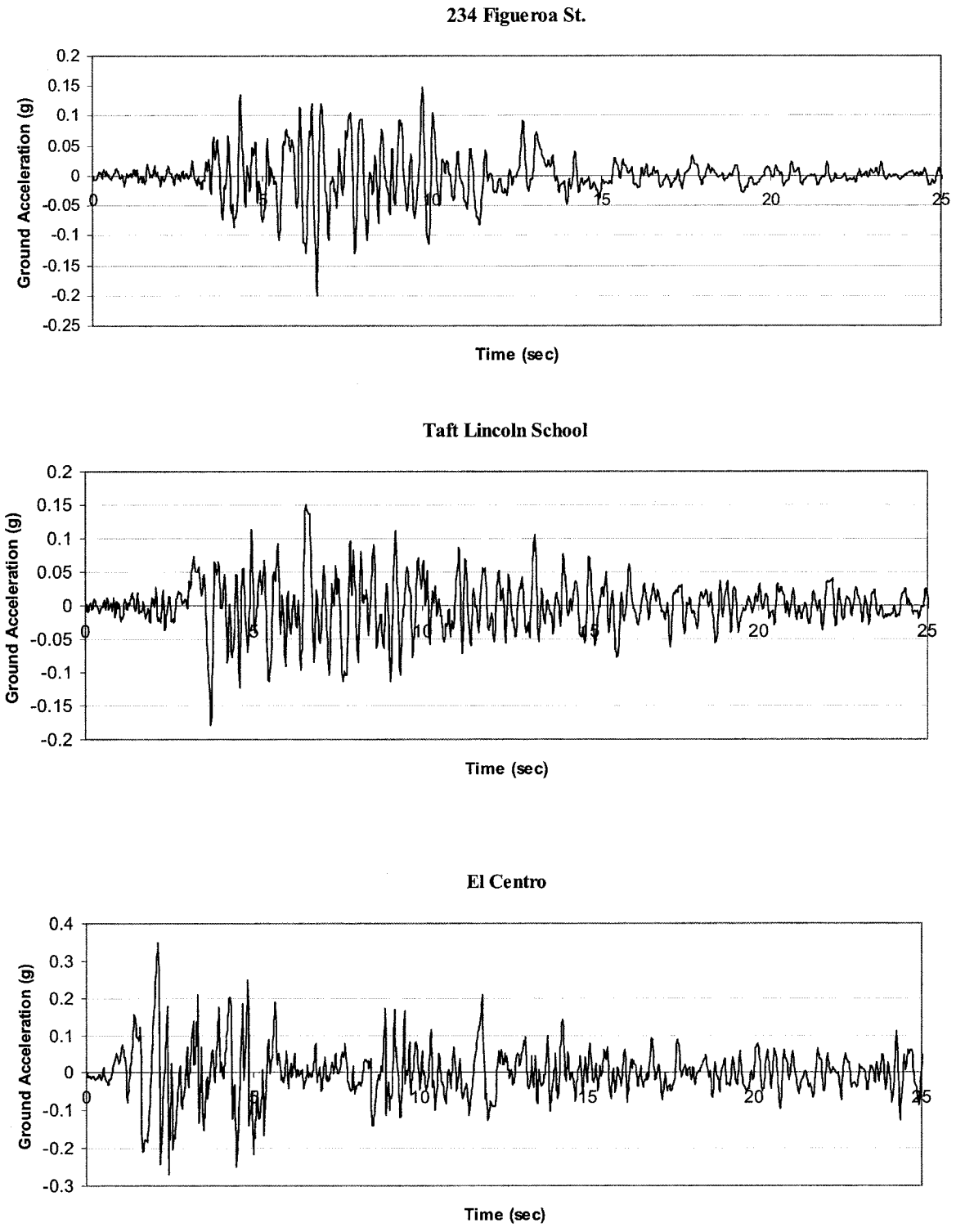

Fig. 3.2(b). Acceleration time histories of the medium A/V ratio ground motion records.

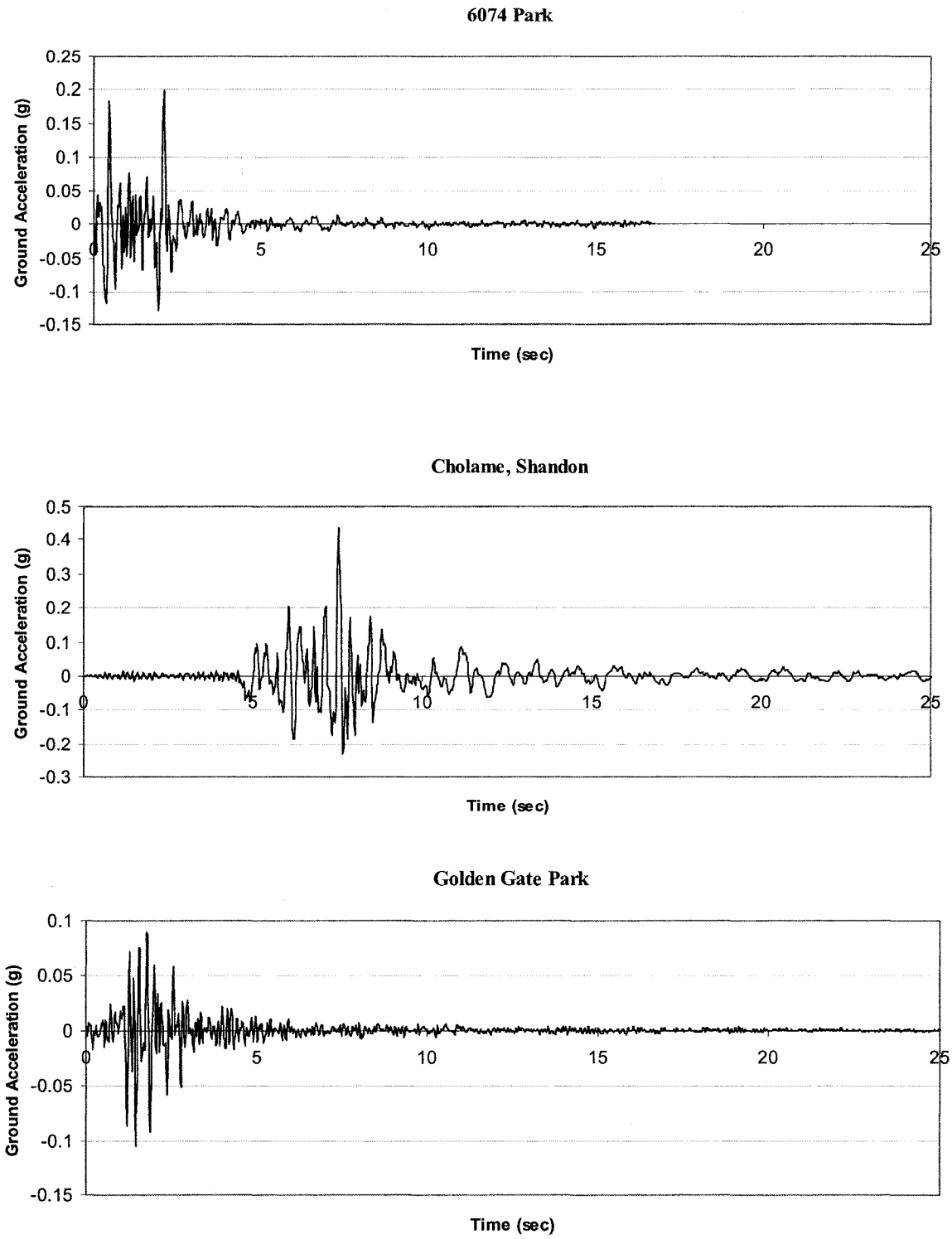

Fig. 3.2(c). Acceleration time histories of the high A/V ratio ground motion records.

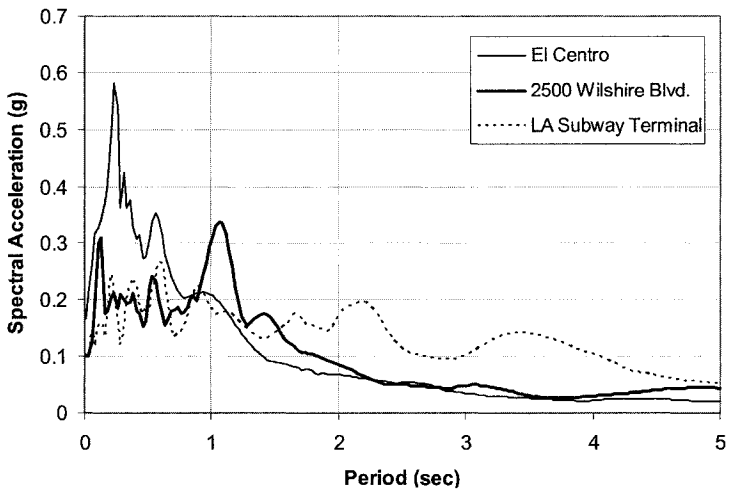

Fig. 3.3(a). The 5% damped elastic acceleration response spectra for low A/V ratio ground motion records.

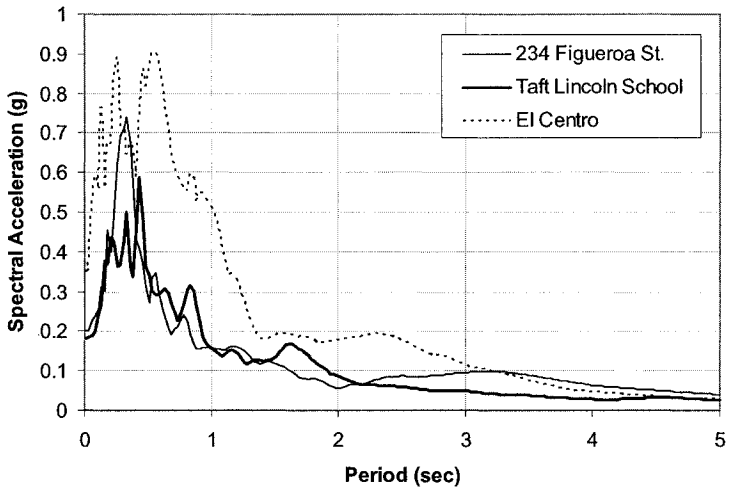

Fig. 3.3(b). The 5% damped elastic acceleration response spectra for medium A/V ratio ground motion records.

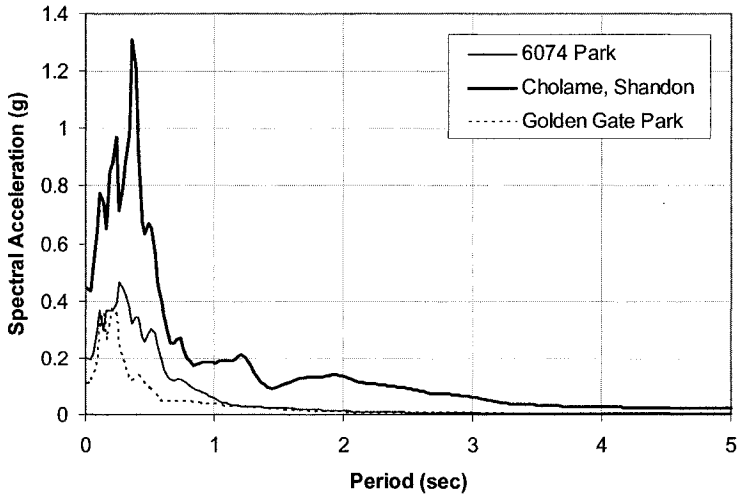

Fig. 3.3(c). The 5% damped elastic acceleration response spectra for high A/V ratio ground motion records.

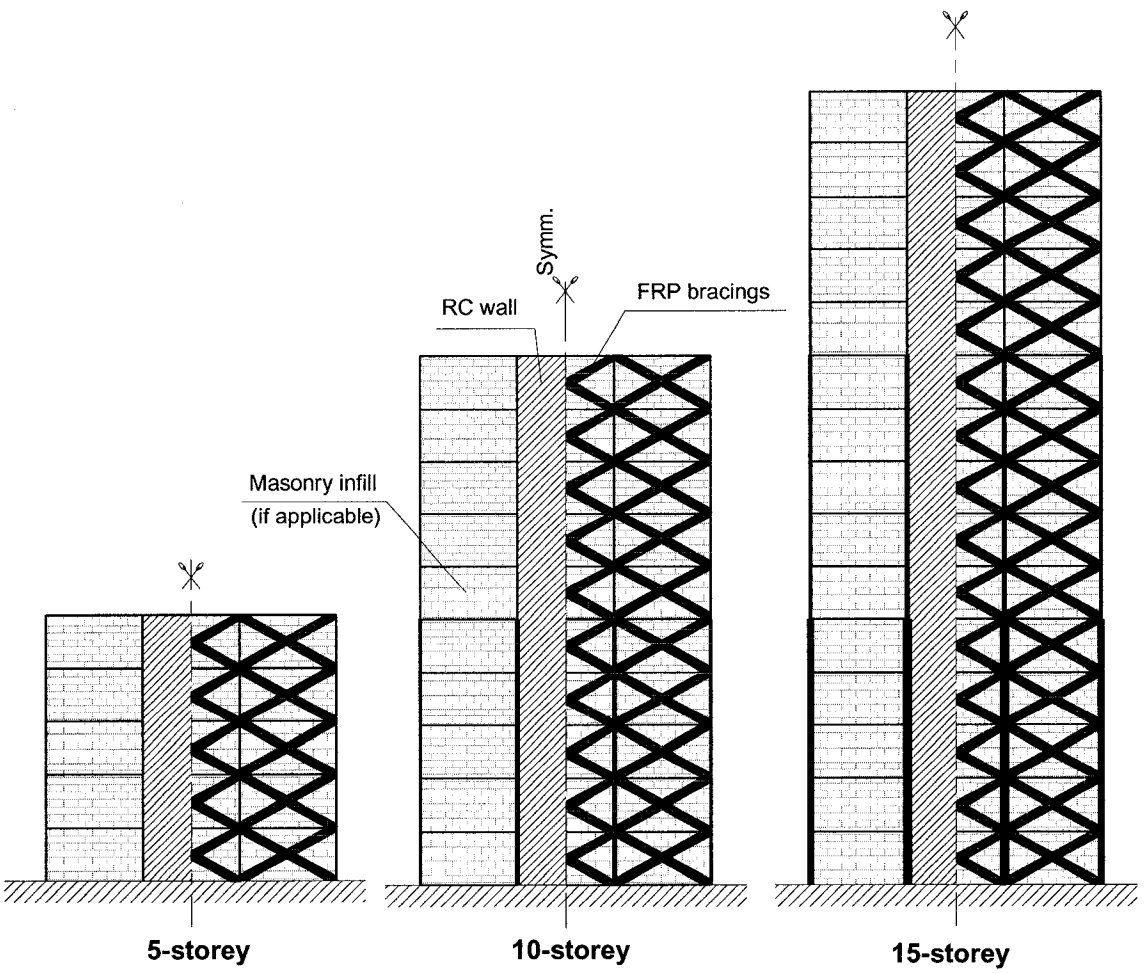

Fig. 3.4. The rehabilitation schemes using FRP bracing and the introduction of RC wall.

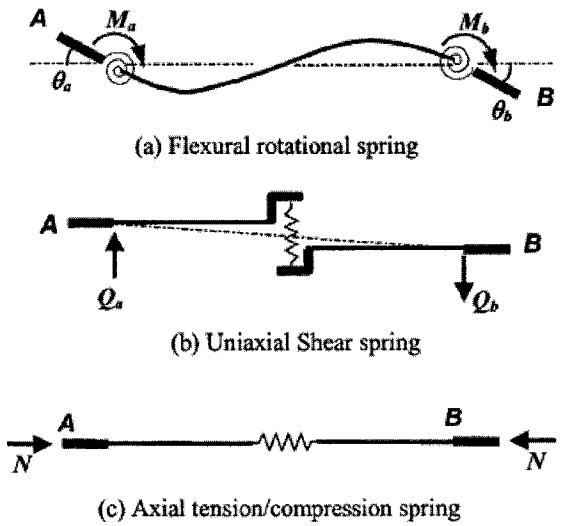

Fig. 3.5. Section models for line element. (Li 2006)

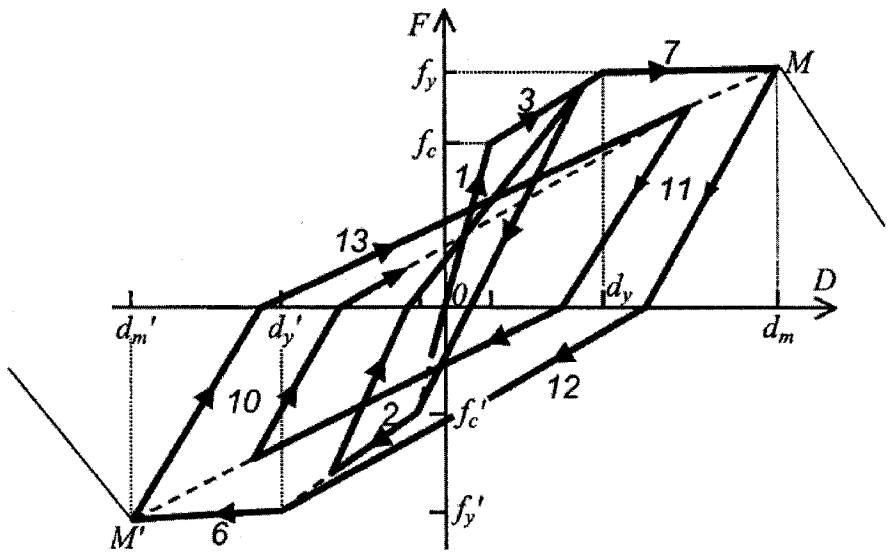

Fig. 3.6. Hysteretic behaviour of the model CP4. (Li 2006)

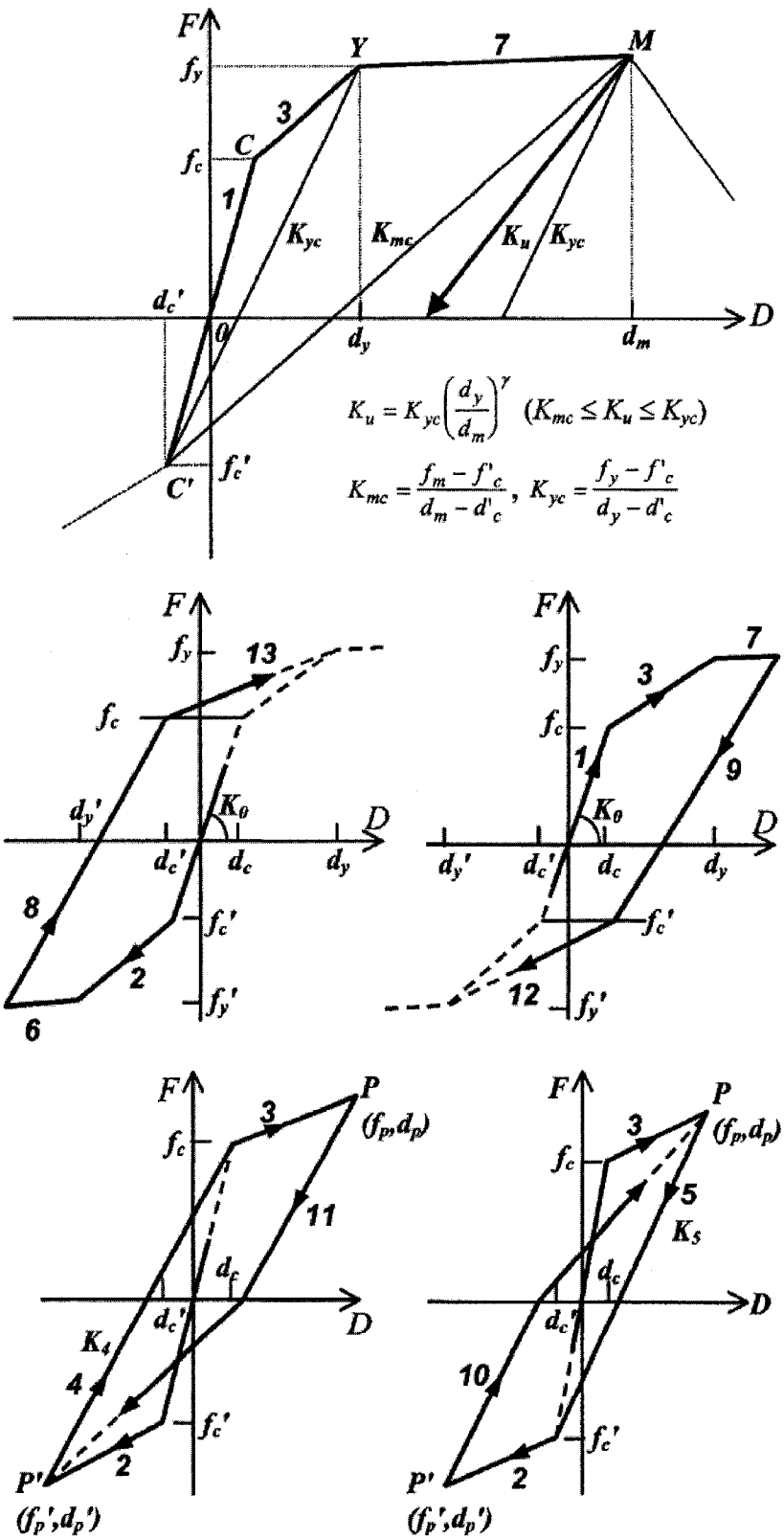

Fig. 3.7. Unloading rules for model CP4. (Li 2006)

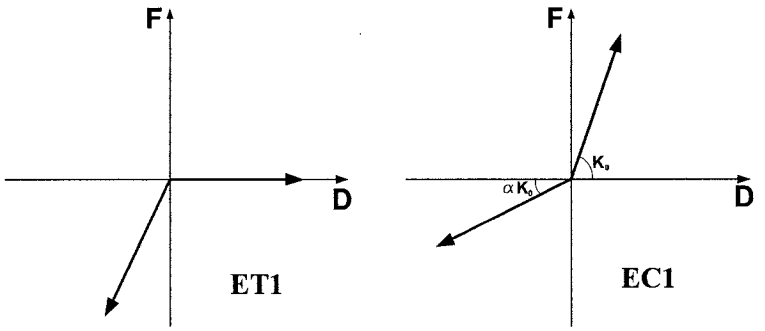

(a) Tension only elastic model

(b) A symmetrical model ($\alpha = 0$: compression only)

Fig. 3.8. Linear elastic models ET1 and EC1. (Li 2006)

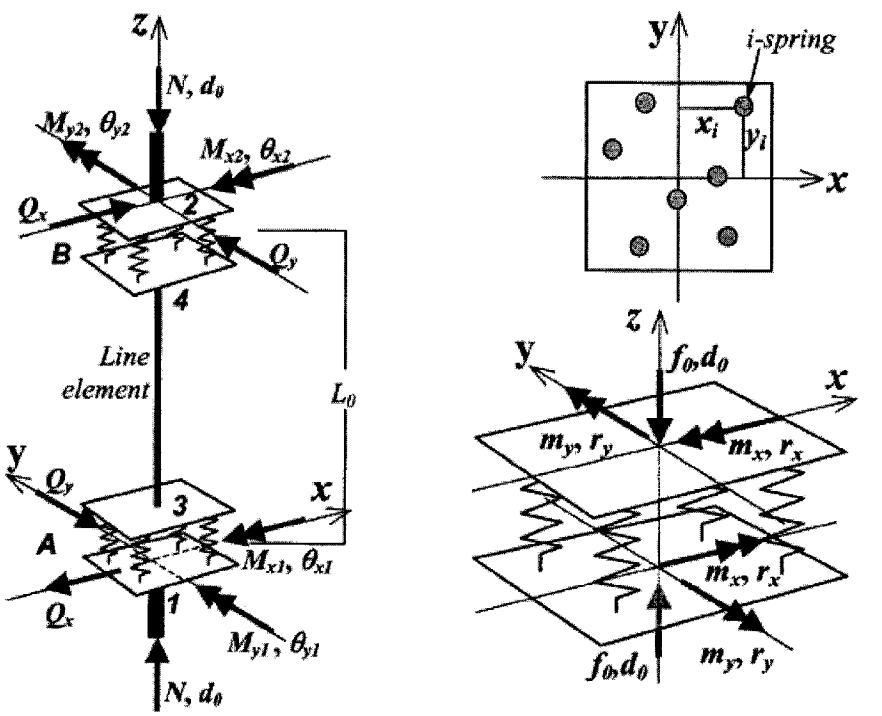

a) Columns with MS element

b) MS element and the forces and displacements (positive)

Fig. 3.9. Columns idealized by MS model

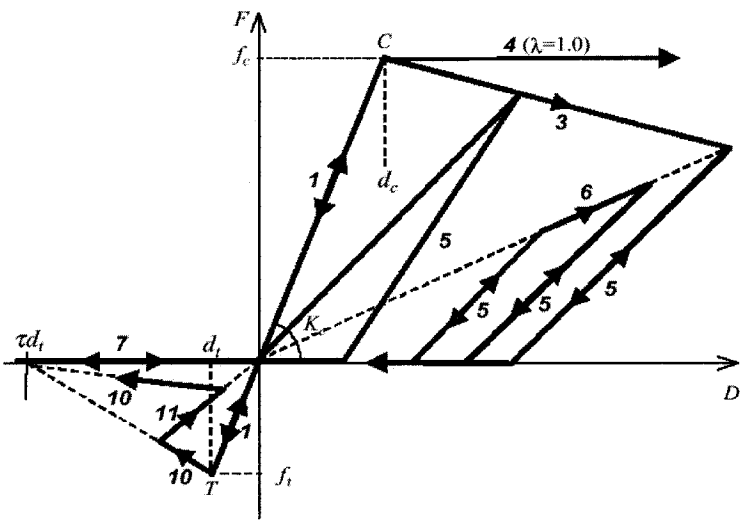

Fig. 3.10. Bilinear model CS2 used to represent the concrete material. (Li 2006)

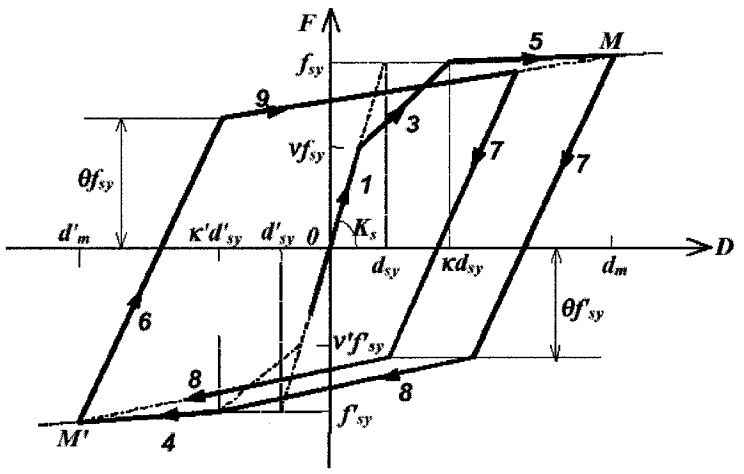

Fig. 3.11. Trilinear / bilinear model SS3 used to represent the steel material. (Li 2006)

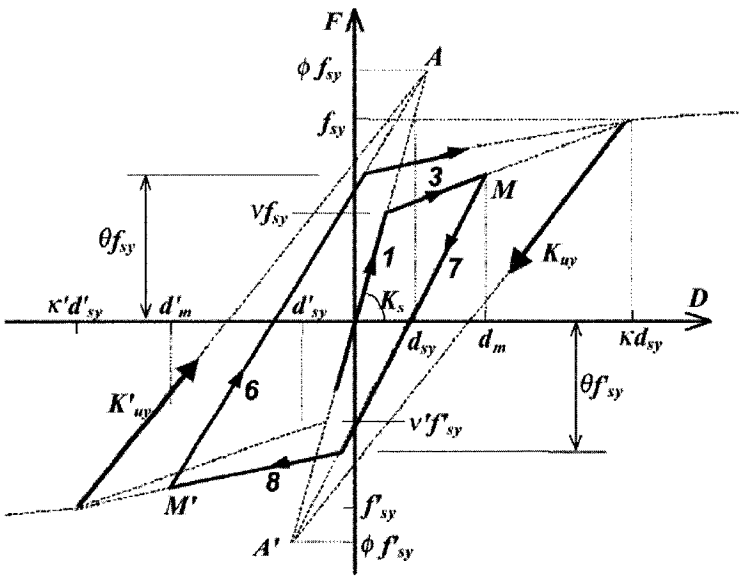

Fig. 3.12. Unloading before yielding for steel model. (Li 2006)

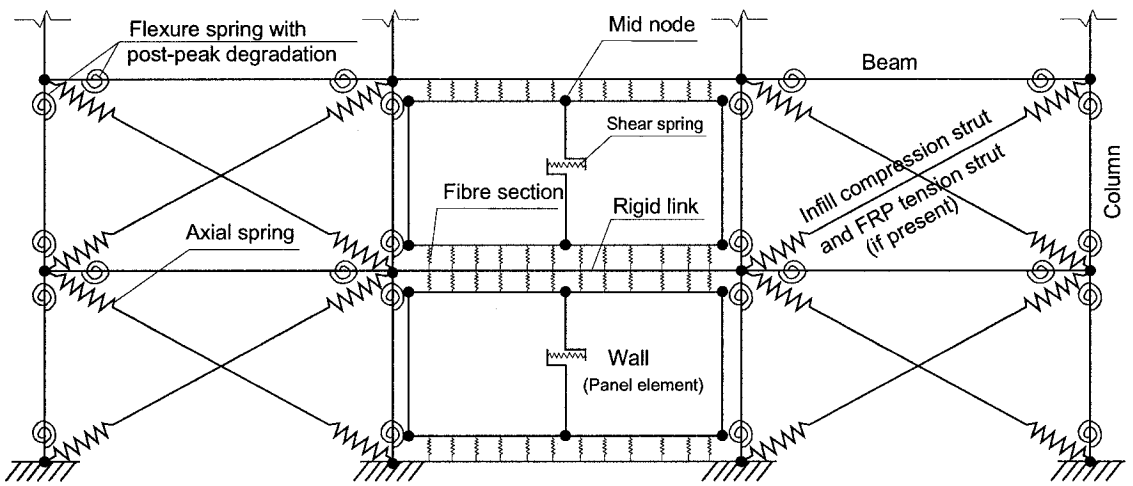

Fig. 3.13. Idealization of different members of the studied frames (generic).

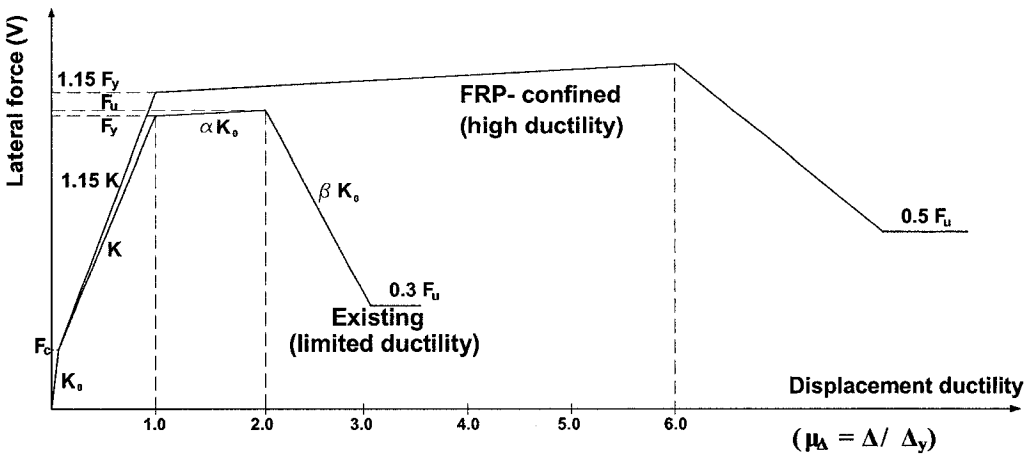

Fig. 3.14. The force-displacement ductility relationships of the existing and FRP-confined columns or beams.

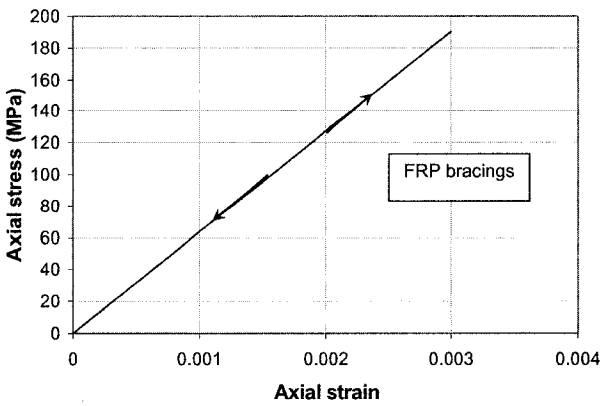

Fig. 3.15. Axial stress-axial strain relationship for the tension strut of FRP bracing.

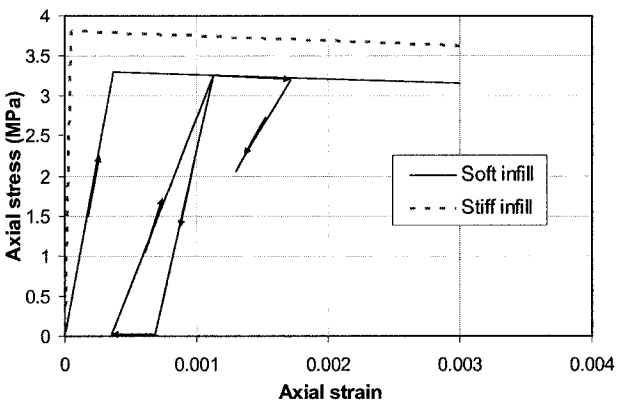

Fig. 3.16. Axial stress-axial strain relationship for the compression strut of the infill.

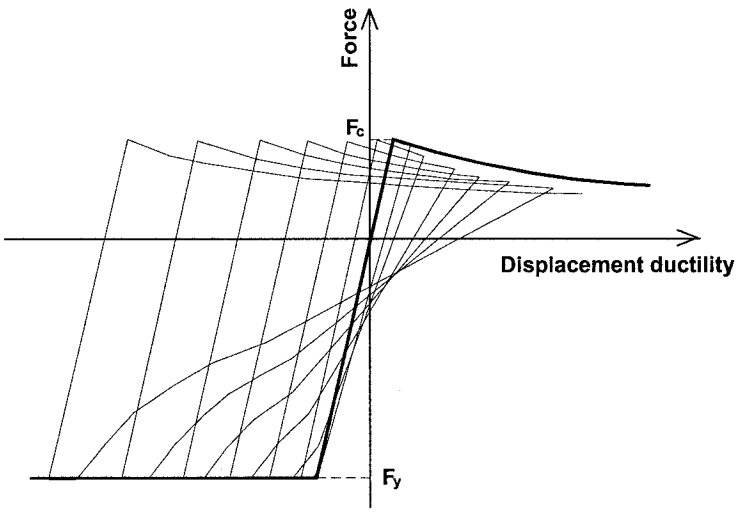

Fig. 3.17. Hysteretic behaviour of the CANNY buckling model STB. (Li, 2006)

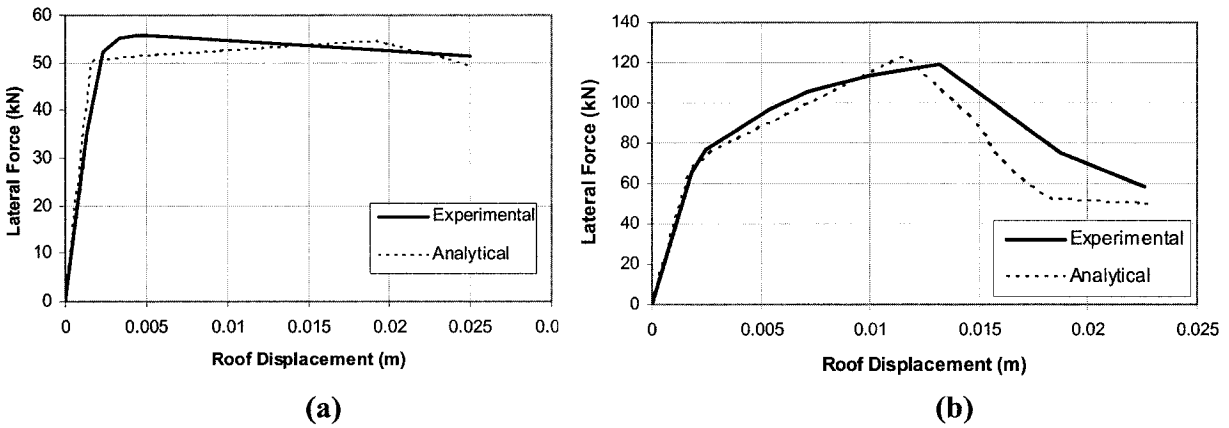

Fig. 3.18. Comparison of the experimental results (Özcebe, *et al.* 2003) and analytical results of the pushover analyses for (a) the unrehabilitated and (b) rehabilitated specimens

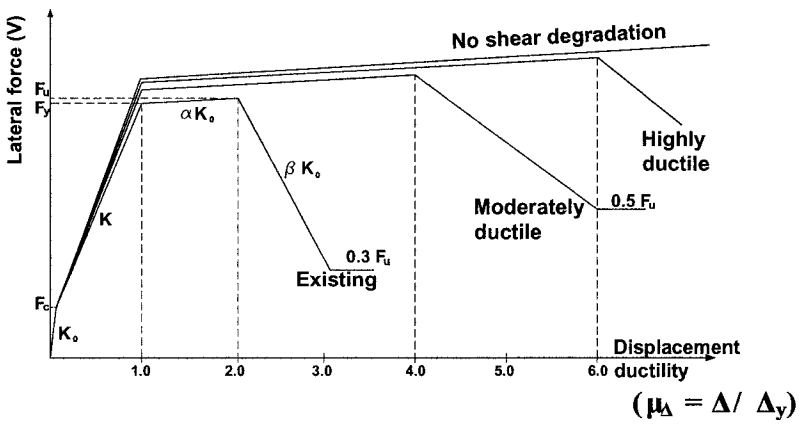

Fig. 3.19. Lateral force-displacement ductility relationships of the existing, moderately ductile and highly ductile models.

CHAPTER 4

ANALYSIS RESULTS

4.1 INTRODUCTION

This chapter introduces the results of the nonlinear static and dynamic analyses for the existing and rehabilitated frames. The importance of accounting for the masonry infill in the analysis is also discussed. In this chapter, a comparative study was done on the performance of structures rehabilitated using different techniques, namely; (1) introducing a RC structural wall, (2) rehabilitating using X-steel bracings, (3) rehabilitating using FRP bracings, and (4) rehabilitating using FRP-confinements. The importance of accounting for the shear degradation in the model of columns and beams is also investigated. The analysis results are drawn in terms of maximum PGA or PGV resisted by the frames, maximum I.D. ratio capacity, maximum storey shear / weight ratio, and maximum energy dissipated by the frames.

4.2 ANALYSIS RESULTS

4.2.1 Dynamic properties of the structures

Modal analysis is conducted for the 5, 10 and 15 storey frames for the existing structures and the ones rehabilitated using different rehabilitation schemes. A 5% damping ratio was considered. Table 4.1 shows the modal analysis results for the studied cases. It should be noted that the existing structures and the rehabilitated ones using the FRP confinement have almost the same natural period. This is due to the fact that the FRP-confinement increases the ductility of the rehabilitated elements with a negligible influence on their stiffnesses. On the other hand, introducing of RC wall or steel bracings

reduced the natural period of the frames due to their contribution to the structure's stiffness.

4.2.2 Maximum applied PGA

9 earthquake records were applied on the studied frames. The ground motion records represent a sample of earthquakes with low, medium and high frequency contents. In the analyses, the maximum earthquake intensities that can be resisted by the 5, 10 and 15 storey frames were evaluated for different rehabilitation schemes and earthquake records. Figures 4.1 (a), (b) and (c) show the maximum PGA resisted by different rehabilitation patterns and different infill stiffnesses for 5, 10 and 15 storey frames, respectively. The figures show the average value for the PGA capacity for earthquakes with low, medium and high frequency contents (A/V ratio). This is useful to evaluate the effect of earthquake frequency content on the seismic behaviour of the studied frames. The figures also show the average PGA capacity value for all earthquakes. From the figures, it can be seen that the use of FRP bracings increases the maximum PGA resisted by the studied frame, while rehabilitating the frames using RC wall or steel bracing has resulted in a higher PGA capacity compared to FRP bracings. The figures also show that rehabilitating the columns and beams using FRP-confinement is an efficient technique in increasing the PGA capacity of the frames, especially for medium- and high-rise buildings.

4.2.3 Maximum PGV capacity versus maximum PGA capacity

Table 4.2 shows the maximum PGV that can be resisted by the low, medium and high-rise frames. From the table, it can be noticed that the values of PGV capacity of the

frames that has natural periods higher than 0.6 sec are close for earthquakes with low and medium A/V ratio, while for high A/V earthquake records, a higher PGV can be resisted by the frames, which indicates a better seismic capacity for earthquakes with high frequency content.

From Figures 4.1 (a), (b) and (c), it can be seen that the maximum PGA resisted by the studied frames increased with the increase of A/V ratio of the selected ground motions. This trend is different than the trend of PGV capacity shown in Table 4.2. It should be noted that both trends (of PGA and PGV capacities) correlate well with the mean acceleration response spectra for the three A/V ratio groups studied by Tso *et al.* (1992) and shown in Figure 4.2. This figure shows the mean 5% damped elastic acceleration response spectra for low, medium, high A/V ratio and the whole ensemble of records scaled to (a) a common peak acceleration of 1g, and (b) when scaled to a common peak velocity of 1 m/s. From Figure 4.2 (a), it can be seen that the mean spectral acceleration decreases with the increase of A/V ratio for periods longer than 0.5 sec, which implies that the maximum PGA resisted by the frames increases with the higher frequency content of the ground motion. This correlates well with the results for the maximum PGA capacity of the rehabilitated frames shown in Figures 4.1. On the other hand, Figure 4.2 (b) shows that for periods longer than 1 sec, the mean spectral acceleration for low and medium A/V ratio are similar and higher than that of high A/V ratio. This correlates as well with the results for the maximum PGV capacity shown in Table 4.2.

4.2.4 Maximum inter-storey drift

Figures 4.3 (a), (b) and (c) show the maximum inter-storey drift (I.D.) ratio capacity for the 5, 10 and 15 storey frames for different rehabilitation schemes and different infill stiffnesses, respectively. From the figures, it is noticed that FRP bracings has negligible effect on the maximum I.D. ratio capacity, which matches the experimental test results carried out in METU (Özcebe *et al.* 2003). On the other hand, rehabilitating the frames using a RC wall or steel bracing resulted in a reduced maximum I.D. capacity. This can be attributed to the fact that adding the RC wall or steel bracings increased the stiffness of the structure. It should be noted that for the three above mentioned rehabilitation schemes, the failure occurred in the non-ductile columns and beams of the existing structure. Also it can be seen that the maximum I.D. ratio capacity is high for the rehabilitated frames using FRP confinement (FRP wrapped columns and beams) for low, medium and high-rise frames, which leads to a more ductile structure with a higher I.D. ratio capacity.

From the figures, it can be noticed that for a certain building (i.e. low, medium or high-rise), and certain dynamic and hysteretic properties of the building, the maximum I.D. capacity slightly changed with respect to the change in the earthquake properties (A/V ratio). This was not the case for the maximum PGA or PGV capacities of the structures which were affected by the frequency content of the ground motion record as shown in Figures 4.1 (a), (b), (c) and Table 4.2. This justifies the validity of using the maximum inter-storey drift as a uniform and reliable damage parameter that can be used to judge the performance of rehabilitated structures. The figures also show the

performance levels that represent the damage degree of structure in terms of inter-storey drifts as recommended by Vision 2000 (1995) and FEMA 273/274 (1997).

Figure 4.4 shows the PGA–I.D.$_{max}$ capacity curves of the existing 5, 10 and 15 storey frames with soft infill when rehabilitated using different rehabilitation patterns. From the figure, it can be seen that rehabilitating the frame with FRP bracings resulted in a decrease in the maximum I.D. ratio for a certain PGA level when compared to the existing frame. While for the same PGA level, rehabilitating the frames using a RC wall or steel bracing decreased the value of maximum I.D. compared to the use of FRP bracings. It is worth noting that the rehabilitation scheme using steel X-bracing resulted in a significant increase of axial force on the existing columns at the lower stories, which indicates the importance of strengthening the existing columns (e.g. by jacketing them) to increase their axial capacity in order to be able to tolerate the axial force accompanied by the lateral loads due to the introduction of steel braces, also retrofitting of foundation maybe needed. The figure also shows that rehabilitating the frames using FRP confinement didn't decrease the value of maximum I.D. ratio at the same PGA level but it increased the maximum PGA and maximum I.D. ratio capacities for the structure significantly.

Fig. 4.5 shows the distribution of inter-storey drift ratio along the height of low- and high-rise frames with soft infill when subjected to the scaled El Centro earthquake record. The figure shows the effectiveness of each rehabilitation scheme in reducing the value of the maximum I.D. ratio. The figure also shows the change occurred in the I.D. profile and location of max. I.D. for the cases of RC wall and steel bracings.

4.2.5 Maximum storey shear

Figures 4.6 (a), (b) and (c) show the maximum storey shear-to-the total structure weight ratio obtained for 5, 10 and 15 storey frames for different rehabilitation schemes and two infill stiffnesses, respectively. It can be seen that rehabilitating the frames using a RC wall or steel bracing attracts higher forces due to the increase of stiffness, which results in a reduction in the natural period of the structure. The figures show also that the presence of masonry infill leads to a stiffer structure and hence increasing the demand, thus highlighting the importance of inclusion of infill models in the analysis of masonry-infilled structures. It can be also seen that the rehabilitation using FRP-confinements didn't increase the storey shear demand significantly. This can be attributed to the fact that FRP-confinements do not contribute to the structure stiffness, but they increase the ductility capacity of the structural elements of the building without altering their stiffness.

4.2.6 Energy dissipation capacity

Energy dissipation capacity is an important indicator of the structure's ability to withstand severe ground motions. It can be determined from the area enclosed by the hysteretic loops of the load deformation relationship. Figures 4.7 (a), (b) and (c) show the maximum energy dissipated by the 5, 10 and 15 storey frames for different rehabilitation patterns and two infill stiffnesses, respectively. It can be seen that for low-rise building, rehabilitation using a RC wall or steel bracing dissipated higher energy than the case of FRP bracings or FRP confinement, which indicates that the introduction of RC wall will be more efficient in resisting the lateral loads than the use of FRP bracing or FRP-confinements, yet this solution will be impractical if the building was occupied while rehabilitation. In that case the steel bracing, FRP bracing or FRP confinement could be

alternative solutions. The figure also indicates that for the studied medium- and high-rise frames, wrapping the columns and beams using FRP-confinements will dissipate higher energy than introducing a RC wall, steel bracing or FRP bracings.

4.3 PUSHOVER ANALYSIS

The pushover analysis is a simplified inelastic static procedure that used to evaluate the performance of a structure when subjected to lateral loads due to wind or earthquakes. In pushover analysis, a set of monotonically increasing static forces are applied at the floor levels and the structure is pushed until either a mechanism occurs (i.e. the structure becomes unstable) or until its displacement exceeds a predefined limit. This predefined displacement limit can be maximum allowable I.D. ratio, maximum roof displacement or ductility limits. The choice of the lateral load pattern of the pushover should be based on the dominant mode shape of the building or a combination of the first mode shapes.

The base shear coefficient–roof drift capacity curve is the main output of the pushover analysis, which can be an indicator of the ability of the building to resist earthquake ground motions. In this study, pushover analyses of the existing frames and the rehabilitated ones were performed. An inverted triangular load pattern was selected which represents the first mode of vibration. CANNY (Li 2006) software was used to conduct the pushover analyses for the 5, 10 and 15 storey frames, for the existing and studied rehabilitation schemes and for different infill stiffnesses. Figures 4.8 (a), (b) and (c) show the base shear coefficient versus the roof drift for the 5, 10 and 15 storey frames,

respectively. From the figures, by comparing the relative capacities of the existing structures and different rehabilitation schemes, the same conclusions regarding the maximum PGA capacity obtained from the time history analyses can be noticed. This shows that the pushover analysis can give some indications on the seismic capacity of structures, especially when the time history analysis is too complex or time-consuming. It should be noted that the pushover analysis is not able to capture the behaviour of structures regarding the maximum I.D. ratio and energy dissipation capacities. Moreover, the pushover analysis is not able to capture the effect of the frequency content of the ground motion on the response of the structures.

4.4 IMPORTANCE OF ACCOUNTING FOR THE MASONRY INFILL IN THE ANALYSIS

Masonry infill can significantly improve the seismic response of structures or, in contrary, it can cause unexpected damages. Therefore, the influence of masonry infill on the seismic performance of structures should not be overlooked. In this study, the selected frames were analyzed for cases of neglecting (bare frame) and accounting for the presence of the masonry infill (soft infill and stiff infill), and the response was compared in both cases. Figure 4.9 shows the performance of the 15 storey frame in cases of rehabilitating using FRP bracings or introducing a RC wall. The figure compares the PGA– $I.D._{max}$ curve for the cases of ignoring or accounting for the masonry infill. From the figure, it can be seen that at the same level of PGA, the presence of masonry infill reduces the I.D. ratio which represents a better seismic performance of the structure according to the Vision 2000 (1995) criteria.

Figures 4.1, 4.3, 4.6 and 4.7 show the bare frames response compared to that of the masonry infilled frames. It can be seen that accounting for masonry infill in the analyses has improved the performance of the 5, 10 and 15 storey frames, especially for energy dissipation capacity. On the other hand, it should be noted that the current model is not capable of representing some of the non-ductile failures that can occur due to the presence of infill, such as short column mechanism at the columns' ends.

4.5 EFFECT OF NUMBER OF REHABILITATED BAYS FOR THE CASE OF FRP BRACINGS

For the case of rehabilitation using FRP bracings, the effect of number of rehabilitated bays was investigated. The selected frames were studied in case of rehabilitating the intermediate bay only, compared to rehabilitating the whole structure using FRP bracing. Table 4.3 shows the performance parameters of the 5 and 15-storey frames with different infill stiffnesses, when rehabilitated using one bay or three bays of FRP bracings. It can be seen that rehabilitating the whole frame resulted in better performance than rehabilitating one bay only. It should be noted that a life cycle cost analysis should be considered in order to decide on the most economical choice.

4.6 COMPARISON BETWEEN THE BEHAVIOUR OF THE FRP-CONFINEMENT REHABILITATION SCHEME AND OTHER SCHEMES

The nonlinear dynamic analyses conducted on the selected frames rehabilitated using FRP-confinements showed that this rehabilitation scheme is very efficient in increasing the maximum PGA, I.D. and energy dissipation capacities, especially for

medium- and high-rise frames. From Figure 4.4, we noticed that the FRP-confinement scheme didn't reduce the value of I.D. at the same PGA level but it increased the PGA and I.D. capacities, and this was attributed to the fact that FRP-confinement doesn't contribute to the structure stiffness like other studied rehabilitation schemes do, but it increases the ductility of the rehabilitated structure. This leads to the importance of investigating the behaviour of studied rehabilitation schemes when two frames only of the studied building (e.g. the external frames) were rehabilitated using a particular scheme and the other frames remain without rehabilitation. In this study each 15-storey rehabilitated frame (i.e. frame with RC wall, with steel X-bracing, with X-FRP bracing, and with FRP-confinements) with soft infill was added to the existing frame. The two frames were modeled and connected using rigid links at the floor levels representing the RC slabs. The frames' models were subjected to the 9 ground motion records selected for this study and the average values were calculated for each model.

Table 4.4 shows the results of the nonlinear dynamic analyses for each individual frame and for the combined frames (existing + rehabilitated frame) for the high-rise building with soft infill. From the table, it can be seen that rehabilitating the external frames only using RC walls, steel X-bracing or X-FRP bracing improved the behaviour of the whole structure. On the other hand, rehabilitating the external frames using FRP-confinement didn't result in a significant enhancement in the structure response as it is expected. This can be attributed to the fact that FRP-confinements increase the ductility capacity of the frame members without altering their strength significantly. In that case rehabilitating the external frames only of the structure will not be efficient as the global behaviour of the structure will be controlled by the non-ductile (unrehabilitated) frames,

and the FRP-confined frames will not reach their ultimate ductility capacity (i.e. the maximum I.D. capacity of the existing frame is much smaller than that of the FRP-confined frames). Consequently, in case of FRP-confinement rehabilitation pattern, all the structure's existing frames should be rehabilitated in order to achieve the ductility level required for the seismic enhancement of the structure. On the other hand, rehabilitating the external frames only using RC structural wall, steel X-bracing, or X-FRP bracing was found to be efficient, as the maximum I.D. capacity of the existing frame is higher or equal to that of the rehabilitated frames, and hence the rehabilitated frames were able to reach their maximum capacities when they are connected to the existing frames.

4.7 DIFFERENT ALTERNATIVES FOR REHABILITATION USING FRP-CONFINEMENT

The performance of 5, 10 and 15 storey existing frames was evaluated when rehabilitated using FRP-confinements for the cases of moderate and high load-displacement ductility capacities of rehabilitated columns and beams shown in Figure 3.19. Four different rehabilitation patterns were investigated. The studied patterns include rehabilitation of both columns and beams (1) along the full height and (2) in the lower half of the structure height; and rehabilitation of columns only (3) along the full height and (4) in the lower half.

4.7.1 Maximum applied PGA

9 earthquake records are applied on the three frames with different rehabilitation schemes. Figures 4.10 (a), (b) and (c) show the maximum PGA that can be resisted by 5, 10 and 15 storey frames, respectively. From the figure it can be seen that, for low-rise

building, the difference between rehabilitation scheme of the columns and beams (full height) and rehabilitation of columns only (full height) is not significant, which implies that rehabilitation of columns only will be effective in case of low-rise structure. On the other hand, the figure shows that, for medium- and high-rise buildings, rehabilitation of columns only was not as effective as rehabilitation of both columns and beams for the full height of the structure.

The aforementioned results can be attributed to the mode of failure in the studied low, medium and high-rise frames. For the low-rise building, the failure was observed to occur in the columns, while the failure occurred in the beams for the high-rise building. This observation occurred for both FRP rehabilitation patterns: columns only, and columns and beams. Therefore, it can be stated that the insignificant gain in PGA capacity for nominally ductile low-rise building when rehabilitating the beams (in addition to the columns) is due to the high relative strength of the beams to that of the columns of low-rise building (both designed to carry gravity loads). Consequently, as the relative strength of the beams to that of the columns of medium- and high-rise building reduces, the gain in the PGA capacity of the building increases with the rehabilitation of the beams. Also, it can be seen from the figure that the rehabilitation of the lower half (for the cases of rehabilitating both columns and beams or columns only) is not effective in increasing the PGA capacity for the studied frames. This can be attributed to the sudden change in the ductility capacity of the structural elements at the mid-height of the building.

4.7.2 Maximum inter-storey drift

Figures 4.11 (a), (b) and (c) show the maximum inter-storey drift (I.D.) ratio for the 5, 10 and 15 storey buildings, respectively, for the case of rehabilitating both columns and beams and the case of rehabilitating the columns only (full height or lower half) for the existing structure to be moderately ductile or highly ductile, when subjected to ground motions with different frequency contents (low, medium and high). For the three frames, it can be noticed that the max. I.D. value increases with the increase of FRP content, which leads to a more ductile structure with higher inter-storey drift capacity. The figure shows that for low rise building, the difference in max. I.D. between rehabilitation scheme of the whole structure (columns and beams) and rehabilitation of columns only is not significant. On the other hand, rehabilitation of columns only in case of medium- and high-rise buildings did not result in a significant increase in the max. I.D. capacity compared to the case of rehabilitation of the whole structure. The same response was observed for the maximum PGA capacities, as mentioned earlier. Performance levels that represent the damage degree of structure in terms of inter-storey drifts as recommended by Vision 2000 (1995) and FEMA 273/274 (1997) are depicted in Figures 4.11.

Figure 4.12 shows the I.D. distribution along the height for low- and high-rise frames with different rehabilitation schemes when subjected to the maximum scaled El-Centro earthquake record that the building can resist. The figure shows that the maximum I.D. occurs at the first floor level for the 5 storey frame, indicating that the first mode of vibration governed the response of the low-rise building. On the other hand, for the high-rise building, the maximum I.D. occurred about one-third of the height of the building. This can be attributed to the effects of higher modes.

4.7.3 Maximum storey shear

Figure 4.13 shows the maximum storey shear-to-the total weight of structure ratio (average capacity for the nine earthquakes) for 5, 10 and 15 storey buildings. Figure 4.14 shows the maximum storey shear-to-total weight with the maximum I.D. relationship for low- and high-rise frames. It can be seen that the maximum storey shear demand increased slightly when the structures were rehabilitated using FRP confinement. This can be attributed to the fact that FRP-confinements do not contribute to the structure's stiffness significantly. The effect of FRP rehabilitation in increasing the storey shear capacity is more significant for the high-rise building compared to the low-rise building. The result of the analysis showed that the value of the max. storey shear for the 5 storey building is not influenced by the change of ground motion frequency content. On the other hand, the maximum storey shear values for the 10 and 15 storey buildings are affected by the frequency content of the earthquake record used.

4.7.4 Energy dissipation capacity

Figure 4.15 shows the maximum energy dissipated by the 5, 10 and 15 storey frames. It can be seen that the energy dissipation capacity of the frames increased when they were rehabilitated using FRP confinement. The figure shows that increasing the FRP content will lead to a more ductile structure and hence higher energy dissipation capacity. The figure also shows that rehabilitation of columns only (full height) was effective in case of low-rise structure, while it wasn't as effective as rehabilitation of both columns and beams for the full height of high-rise frames. This was observed previously from the results of maximum PGA capacities of the structures.

4.7.5 Rehabilitation of damaged members only versus the selected rehabilitation schemes

In this study, the efficiency of FRP-confinement rehabilitation of selected damaged members of the structure when subjected to a specific earthquake was examined. The 5- and 15-storey existing frames are subjected to El Centro earthquake ground motion of maximum peak ground acceleration of 0.15 g and 0.3g, respectively.

For the 5-storey frame, four plastic hinges occurred at the base of the first floor columns, while for the 15-storey frame, the plastic hinges occurred at the end of the second span beams at the 3^{rd}, 4^{th}, 5^{th} and 6^{th} floors as shown in Figure 4.16. These locations were selected for rehabilitation with FRP-confinements for both structures. The PGA capacities are calculated for the case where the damaged members only are rehabilitated and are compared to the PGA capacities of the full rehabilitation pattern of beams and columns. Table 4.5 shows the PGA capacities for the three considered cases. From the table, it can be noticed that, the rehabilitation of the damaged members only was not effective in enhancing the seismic performance of the structures significantly. This is due to the fact that the overall capacity of the structure will be dominated by the weakest structural member, which will be transferred from one location (upon its rehabilitation) to another, etc.

4.8 IMPORTANCE OF ACCOUNTING FOR STRENGTH DEGRADATION IN THE NONLINEAR MODEL OF COLUMNS AND BEAMS

The hysteretic response of RC members must experience a post-peak degradation, even when rehabilitated using FRP for a highly ductile targeted performance. This degradation in strength can arise from several mechanisms, such as: reaching the shear capacity, P-Δ effect, crushing of concrete in compression, buckling of compression rebars, or sudden tear of the FRP confinement. Ignoring the strength degradation beyond the peak capacity of the element would lead to erroneous response predictions of the structure performance.

Figure 4.17 shows the effect of inclusion of strength degradation in the analysis. The figure compares the maximum PGA resisted by the highly ductile frames of 5 and 15 storey buildings and the maximum I.D. ratio in two cases; the first case when the element strength degradation is included in the analysis, while the second case does not account for the strength degradation. In the later case, the failure of the structure was assumed to occur when the structure reached a roof displacement equal to 5% of the structure height. The values represent the average response of the frames to the nine ground motion records selected for this study. The figure shows a major difference in the predicted results in both cases, which emphasizes on the significance of accounting for the strength degradation on the predicted performance of structures.

Table 4.1. Natural periods for the studied frames (sec).

No. of Storeys	Bare frame				Soft infill frame					Stiff infill frame				
	Existing	+ RC Wall	+ Steel bracing	+ FRP-confinements	Existing	+ RC Wall	+ Steel bracing	+ FRP bracing	+ FRP-confinements	Existing	+ RC Wall	+ Steel bracing	+ FRP bracing	+ FRP-confinements
5	1.01	0.38	0.59	1.01	0.39	0.28	0.35	0.38	0.39	0.22	0.21	0.21	0.21	0.22
10	1.74	0.88	1.15	1.74	0.85	0.70	0.78	0.83	0.85	0.58	0.55	0.58	0.58	0.58
15	2.49	1.52	1.75	2.49	1.38	1.19	1.28	1.36	1.38	1.04	1.02	1.04	1.04	1.04

Table 4.2. Maximum PGV (in m/s) resisted by low, medium and high-rise buildings.

No. of Storeys	A/V ratio	Bare frame				Soft infill frame					Stiff infill frame				
		Existing	+ RC Wall	+ Steel bracing	+ FRP-confinements	Existing	+ RC Wall	+ Steel bracing	+ FRP bracing	+ FRP-confinements	Existing	+ RC Wall	+ Steel bracing	+ FRP bracing	+ FRP-confinements
5 Storey	Low	0.20	1.18	0.80	0.37	0.47	1.74	1.05	0.64	0.61	0.40	1.58	0.84	0.51	0.48
	Med.	0.20	0.61	0.50	0.36	0.37	0.89	0.68	0.45	0.57	0.31	0.75	0.58	0.37	0.41
	High	0.41	0.55	0.61	0.76	0.54	0.66	0.87	0.64	0.87	0.42	0.61	0.66	0.53	0.60
10 Storey	Low	0.34	0.52	0.46	0.62	0.49	0.87	0.75	0.62	1.06	0.43	0.78	0.64	0.59	0.64
	Med.	0.23	0.50	0.42	0.49	0.48	0.77	0.70	0.57	0.98	0.41	0.68	0.56	0.48	0.59
	High	0.69	0.67	0.58	1.31	0.73	0.98	0.87	0.87	1.72	0.60	0.80	0.74	0.70	1.36
15 Storey	Low	0.35	0.45	0.41	0.93	0.59	0.81	0.78	0.73	1.31	0.44	0.66	0.61	0.58	0.85
	Med.	0.31	0.45	0.40	0.74	0.46	0.78	0.73	0.59	0.97	0.39	0.61	0.57	0.53	0.70
	High	0.88	0.69	0.71	2.02	0.95	1.09	1.07	1.12	2.28	0.72	0.88	0.83	0.93	1.50

Table 4.3. Effect of number of bays rehabilitated with FRP bracing on the seismic performance of the frames

No. of Storeys	Infill type	No. of rehabilitated bays	Max. PGA (g)	Max. I.D. (%)	Storey shear /weight	Max. Energy (kN.m)
5 Storey	Soft	1 bay	0.64	1.09	0.245	361
		3 bays	0.71	1.09	0.333	490
	Stiff	1 bay	0.50	0.79	0.202	684
		3 bays	0.58	0.72	0.251	598
15 Storey	Soft	1 bay	0.98	1.18	0.12	1391
		3 bays	1.14	1.21	0.15	1884
	Stiff	1 bay	0.79	1.14	0.10	964
		3 bays	0.95	1.17	0.13	1323

Table 4.4. Behaviour of the individual and combined 15-storey frames with soft infill.

Analysis results	Individual systems					Combined systems			
	Existing	RC structural Wall	Steel bracing	X-FRP bracing	FRP-Confinement	Existing +RC structural Wall	Existing + Steel bracing	Existing + X-FRP bracing	Existing + FRP-Confinement
PGA (g)	0.94	1.19	1.15	1.14	2.18	1.11	1.25	1.03	0.96
I.D. (%)	1.16	0.99	1.04	1.21	4.42	0.98	1.06	1.18	1.16
Storey shear/weight	0.11	0.40	0.28	0.15	0.15	0.28	0.22	0.13	0.12
Energy dissipated (kN.m)	1180	3170	2670	1880	4350	5020	5010	3000	2520

Table 4.5. Max. PGA capacities for existing and rehabilitated frames

No. of storeys	Existing frame	Rehabilitated frame	
		Damaged members only *	All beams and columns
5	0.17 g	0.23 g	0.42 g
15	0.42 g	0.43 g	1.11 g

* after being subjected to El Centro ground motion with PGA of 0.15g and 0.3g for 5- and 15-storey frame, respectively.

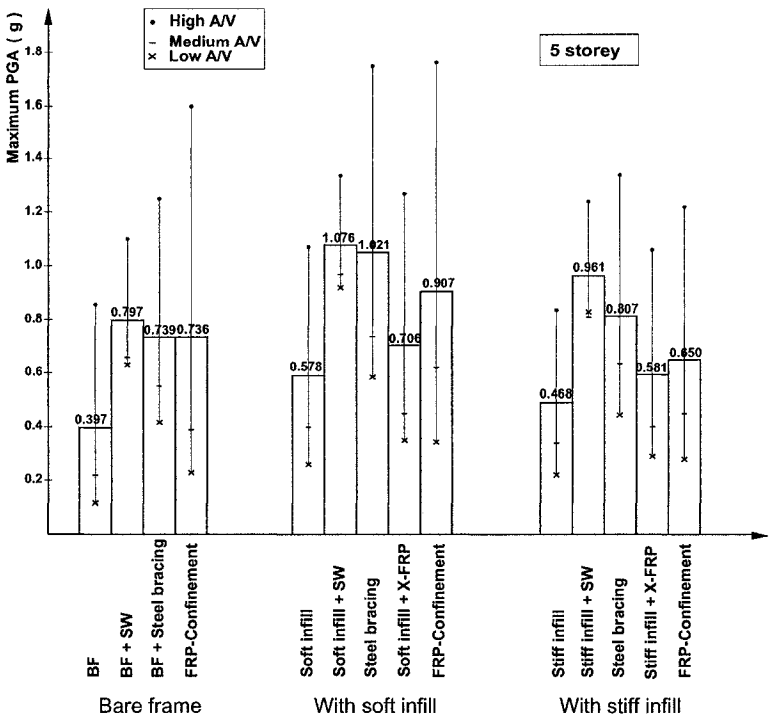

Fig. 4.1 (a) Maximum PGA resisted by the 5-storey frame.

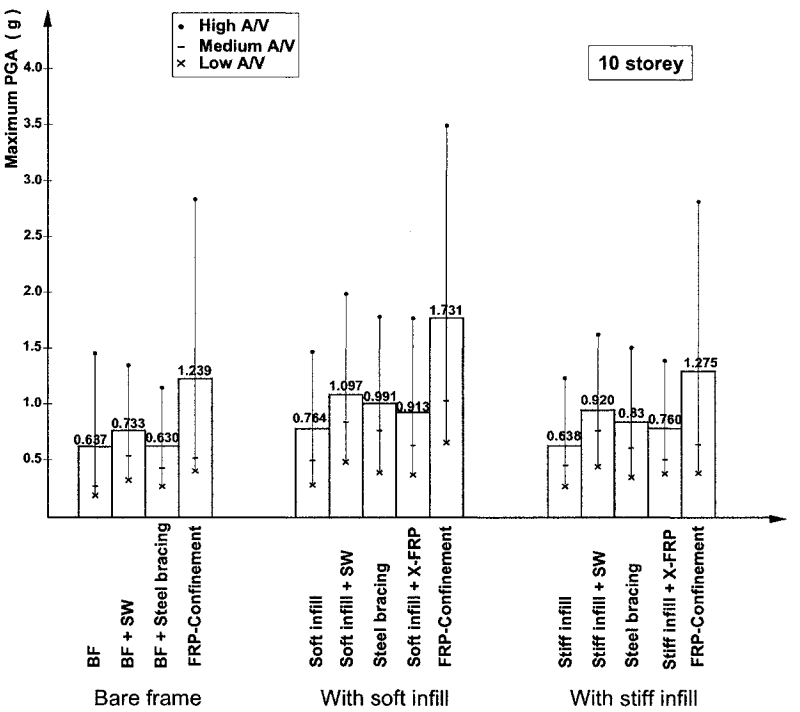

Fig. 4.1 (b) Maximum PGA resisted by the 10-storey frame.

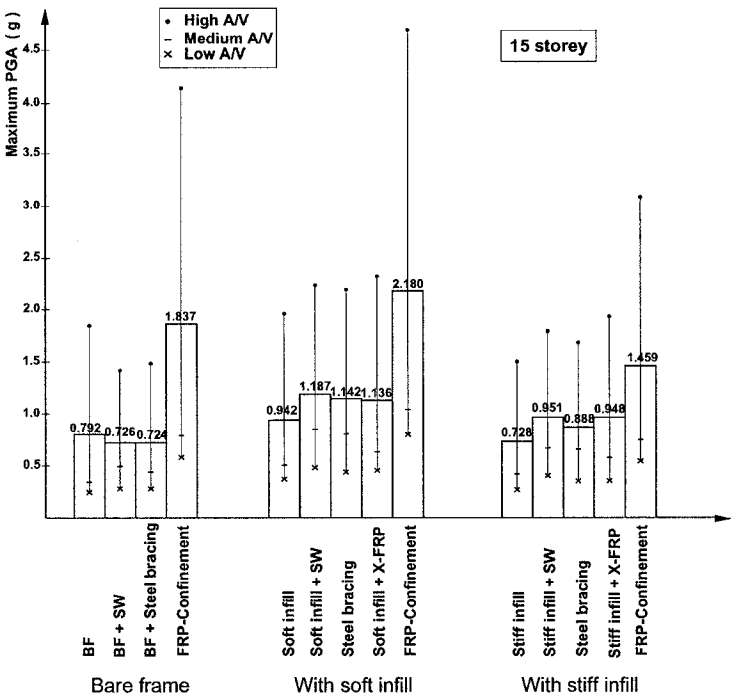

Fig. 4.1 (c) Maximum PGA resisted by the 15-storey frame.

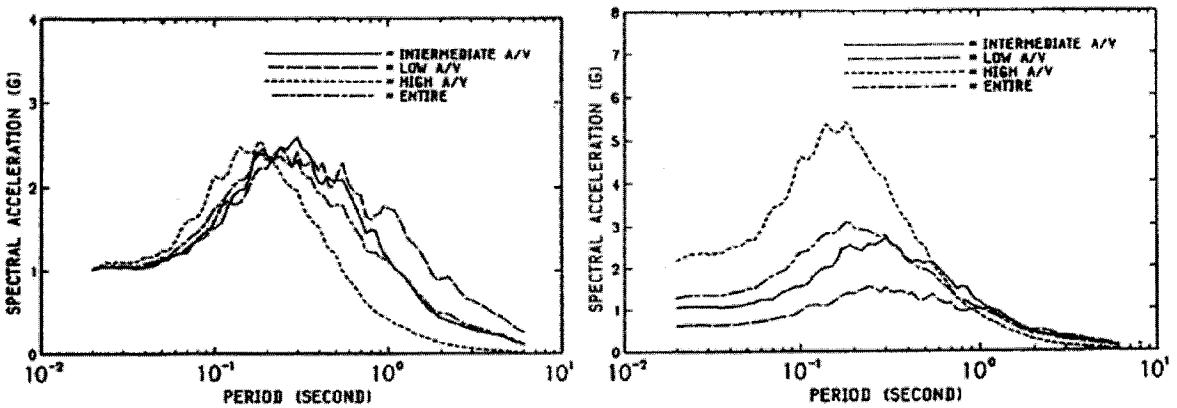

Fig. 4.2. Mean 5% damped elastic acceleration response spectra for records scaled to: (a) a common peak acceleration of 1 g; and (b) a common peak velocity of 1 m/s. (Tso *et al.* 1992)

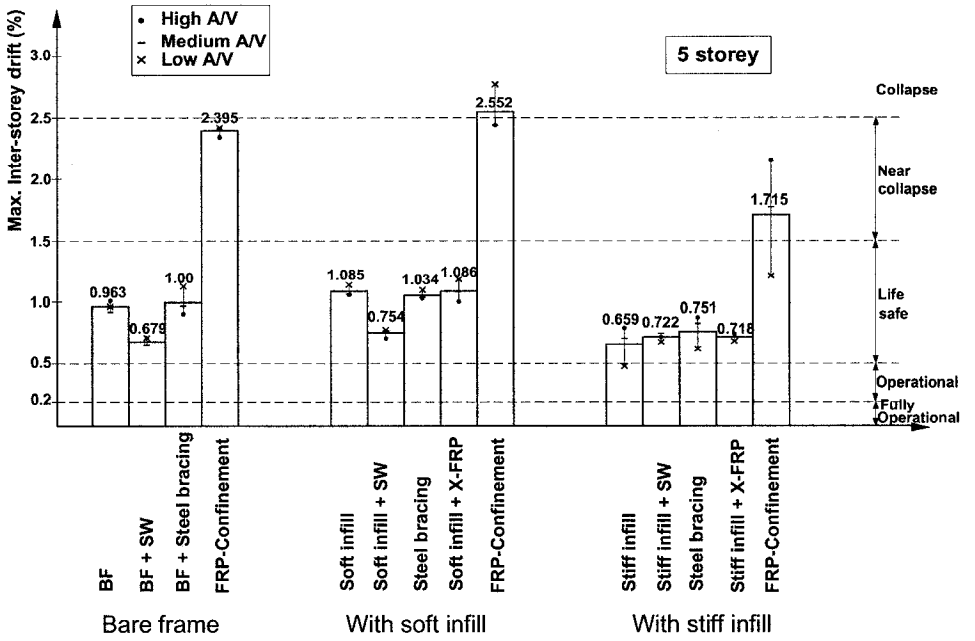

Fig. 4.3 (a) Maximum inter-storey drift ratio capacity for the 5-storey frame.

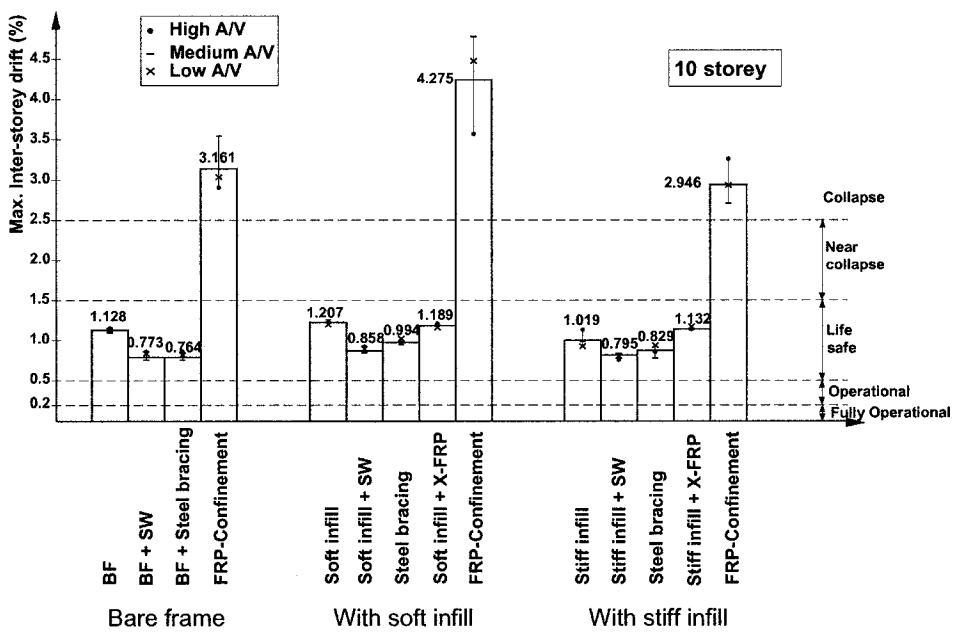

Fig. 4.3 (b) Maximum inter-storey drift ratio capacity for the 10-storey frame.

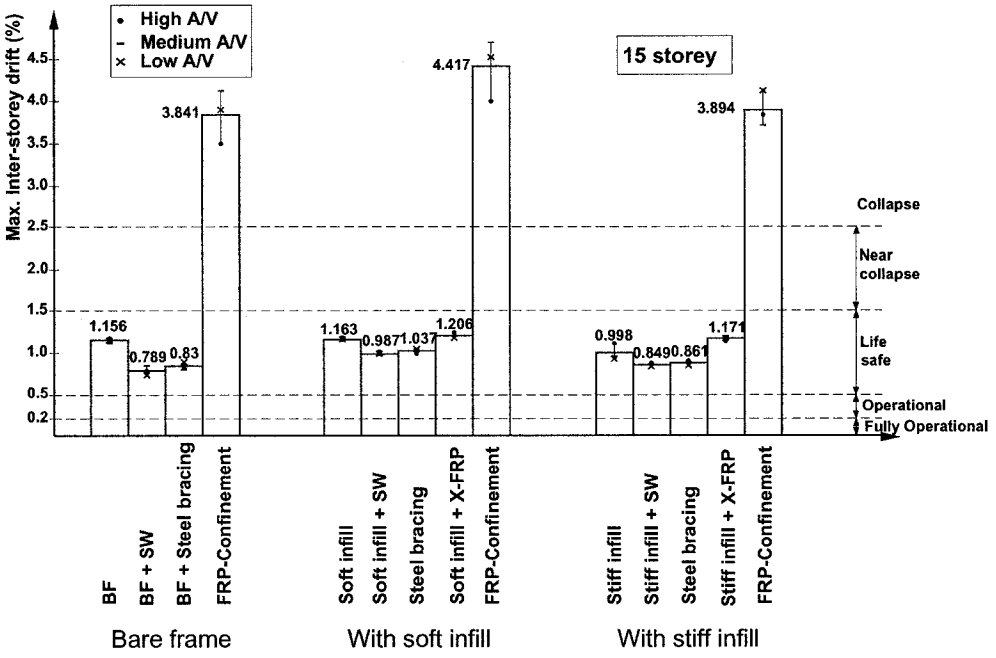

Fig. 4.3 (c) Maximum inter-storey drift ratio capacity for the 15-storey frame.

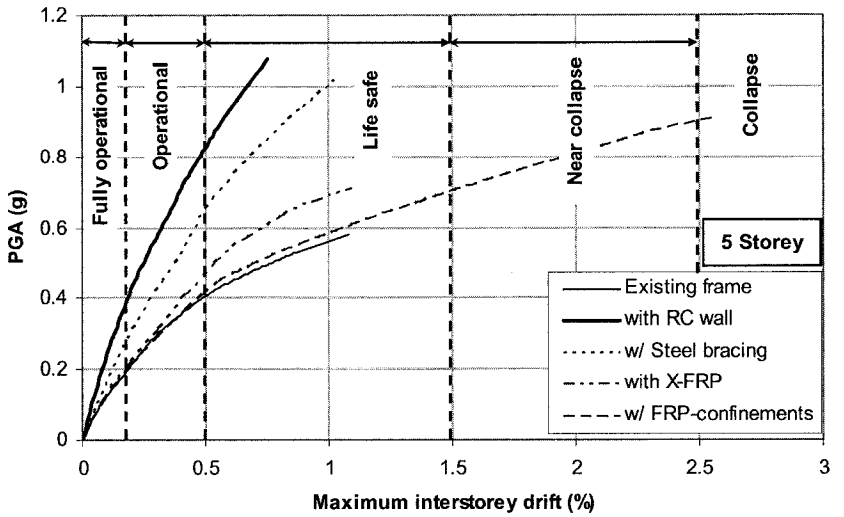

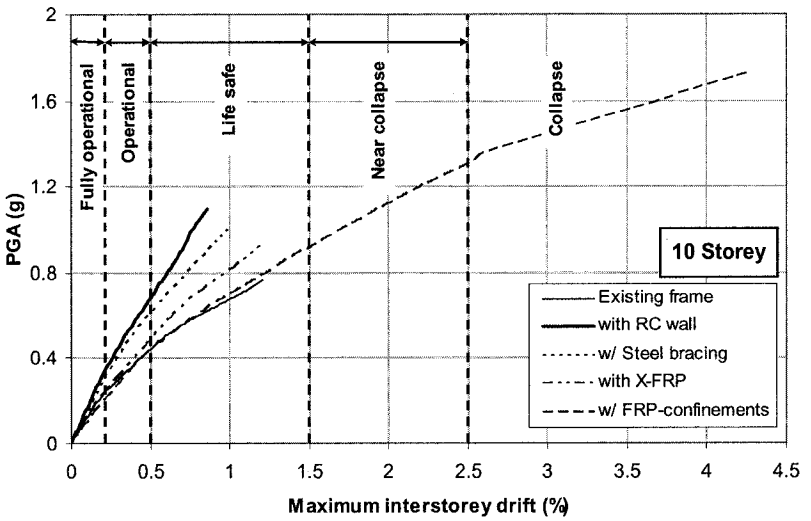

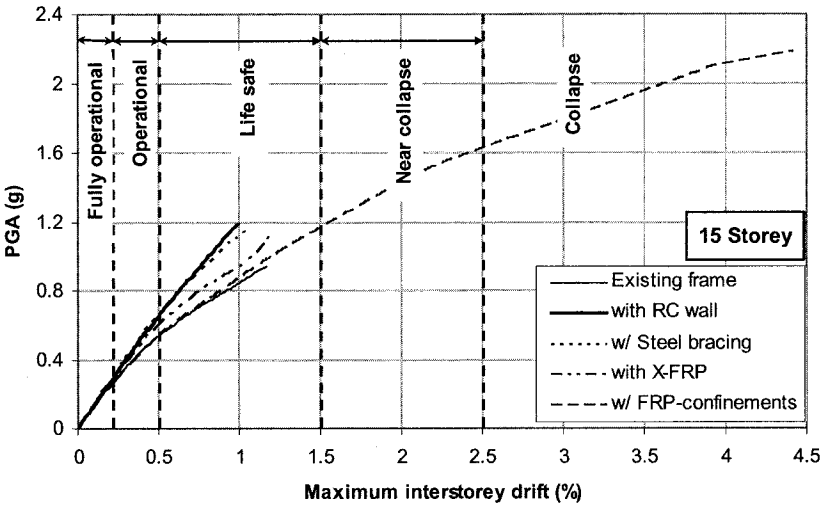

Fig. 4.4. Capacity curves of 5, 10, and 15 storey frames with soft infill.

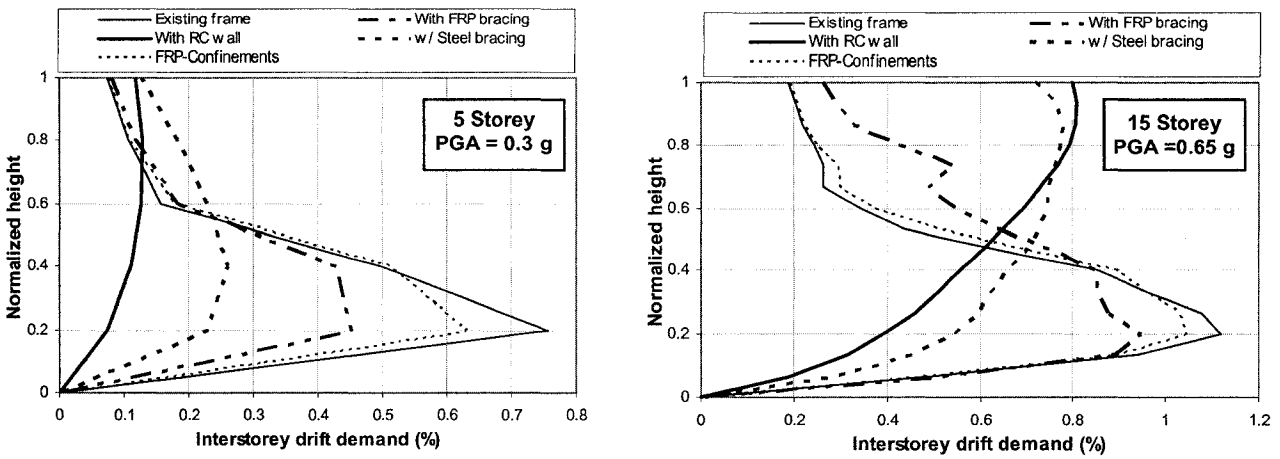

Fig. 4.5 I.D. distribution along the height of low- and high-rise frames with soft infill when subjected to the scaled El Centro earthquake record.

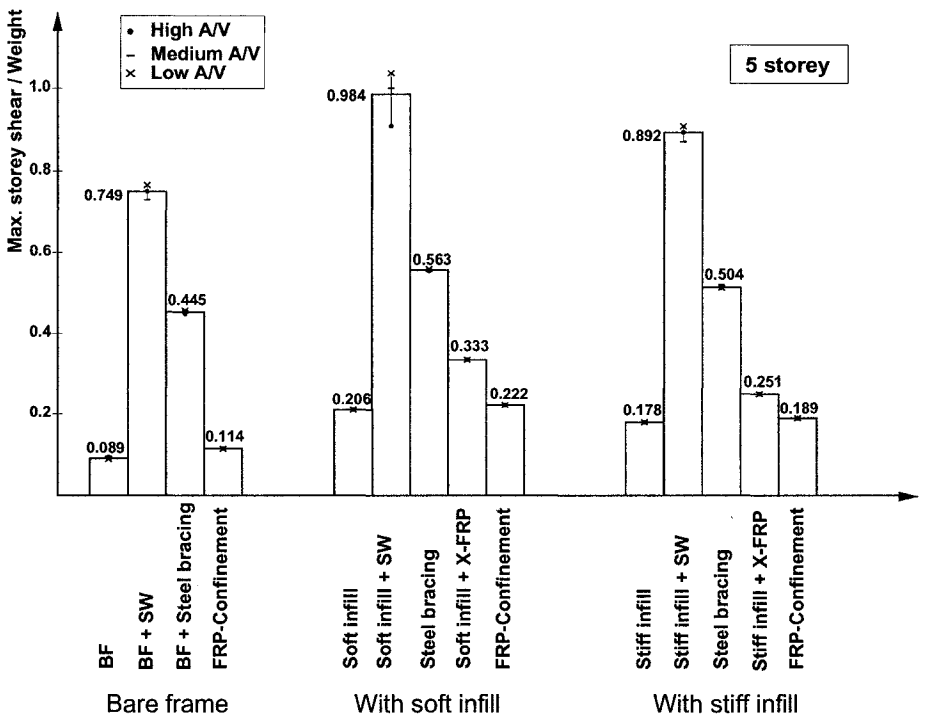

Fig. 4.6 (a) Maximum storey shear / weight for the 5-storey frame.

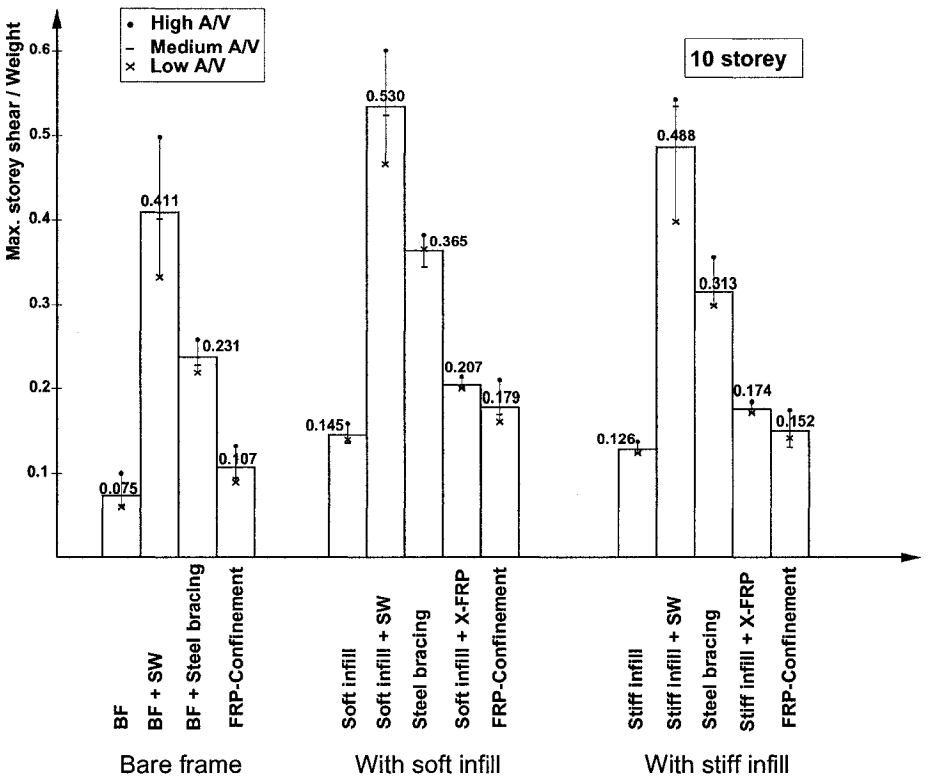

Fig. 4.6 (b) Maximum storey shear / weight for the 10-storey frame.

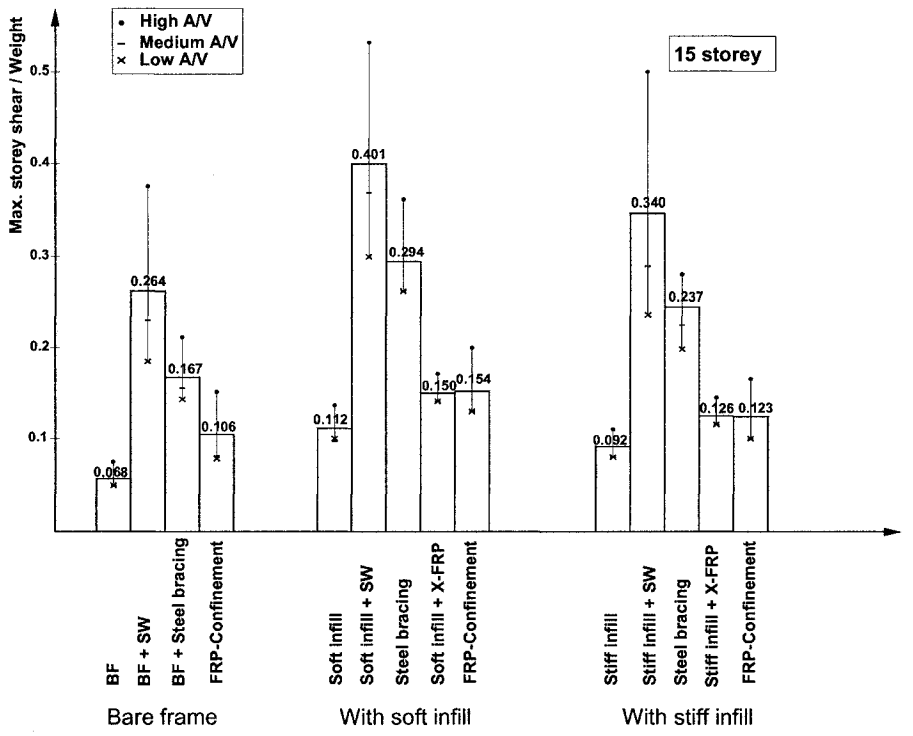

Fig. 4.6 (c) Maximum storey shear / weight for the 15-storey frame.

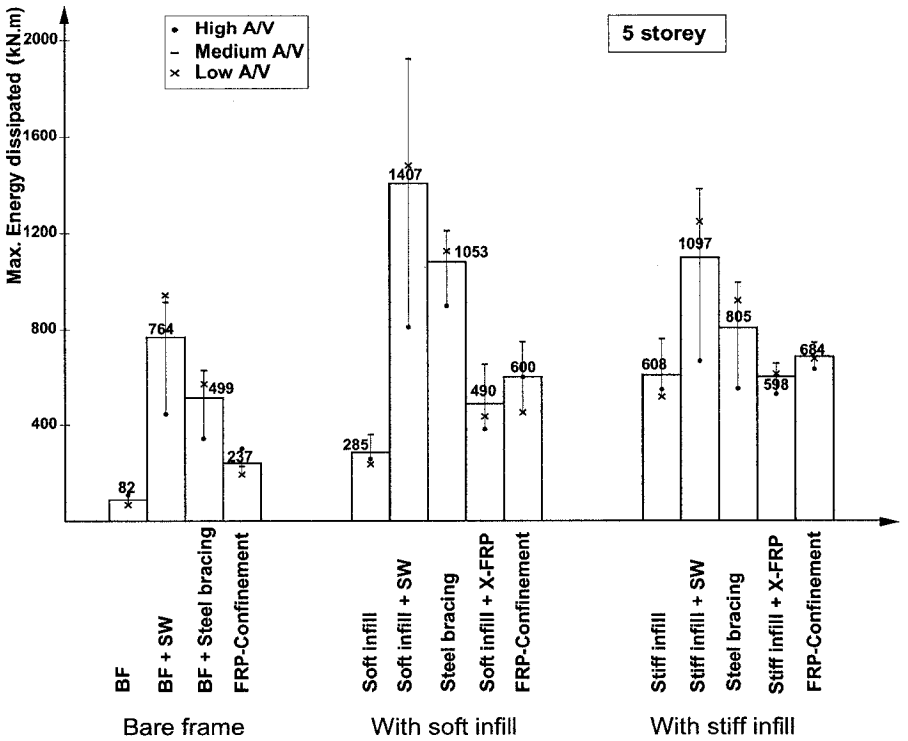

Fig. 4.7 (a) Maximum energy dissipated for the 5-storey frame.

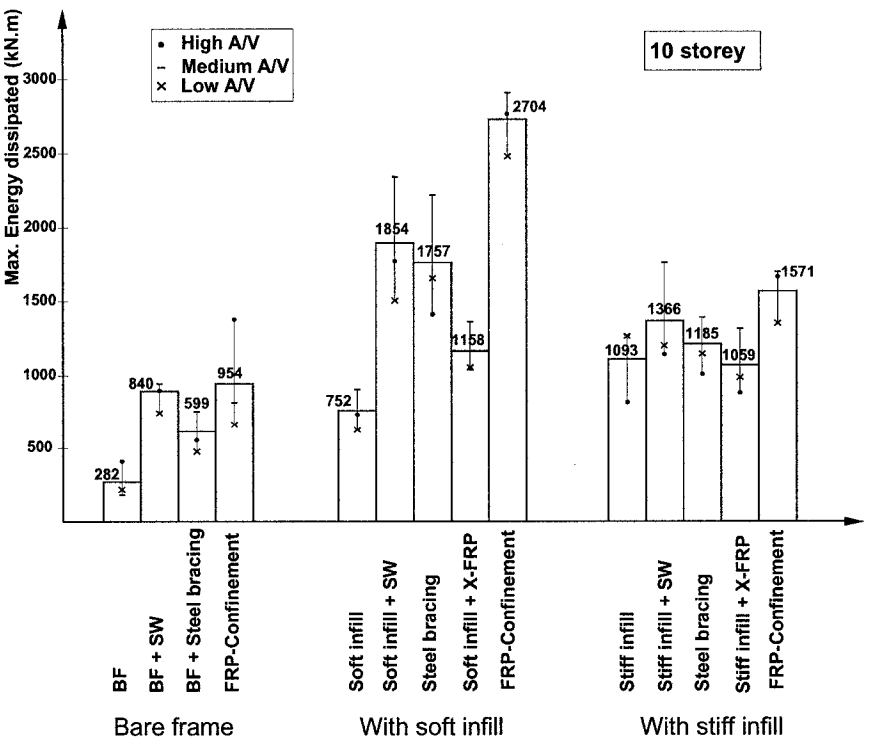

Fig. 4.7 (b) Maximum energy dissipated for the 10-storey frame.

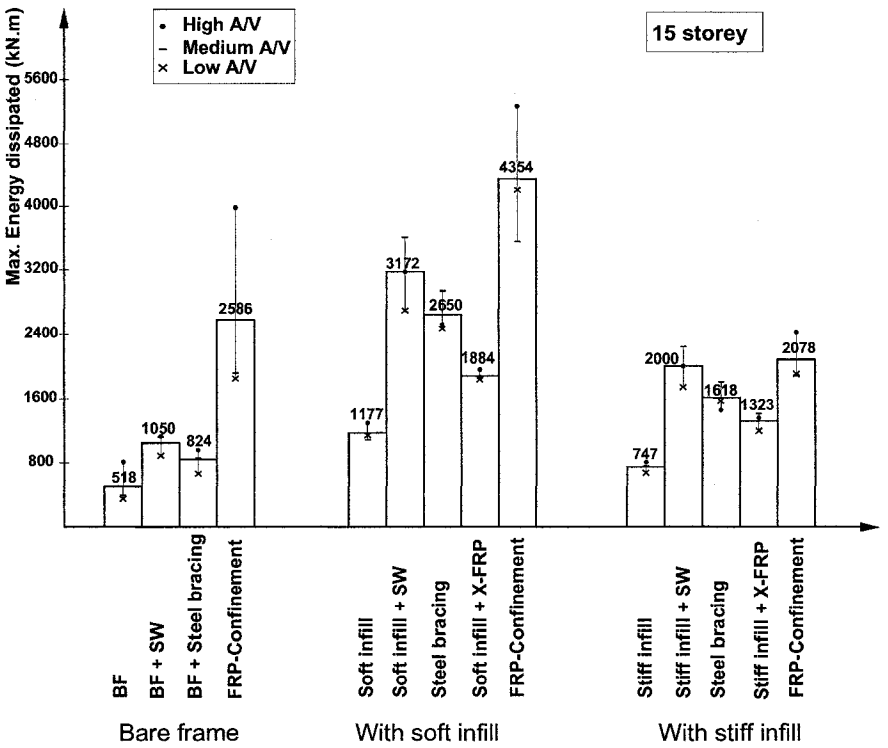

Fig. 4.7 (c) Maximum energy dissipated for the 15-storey frame.

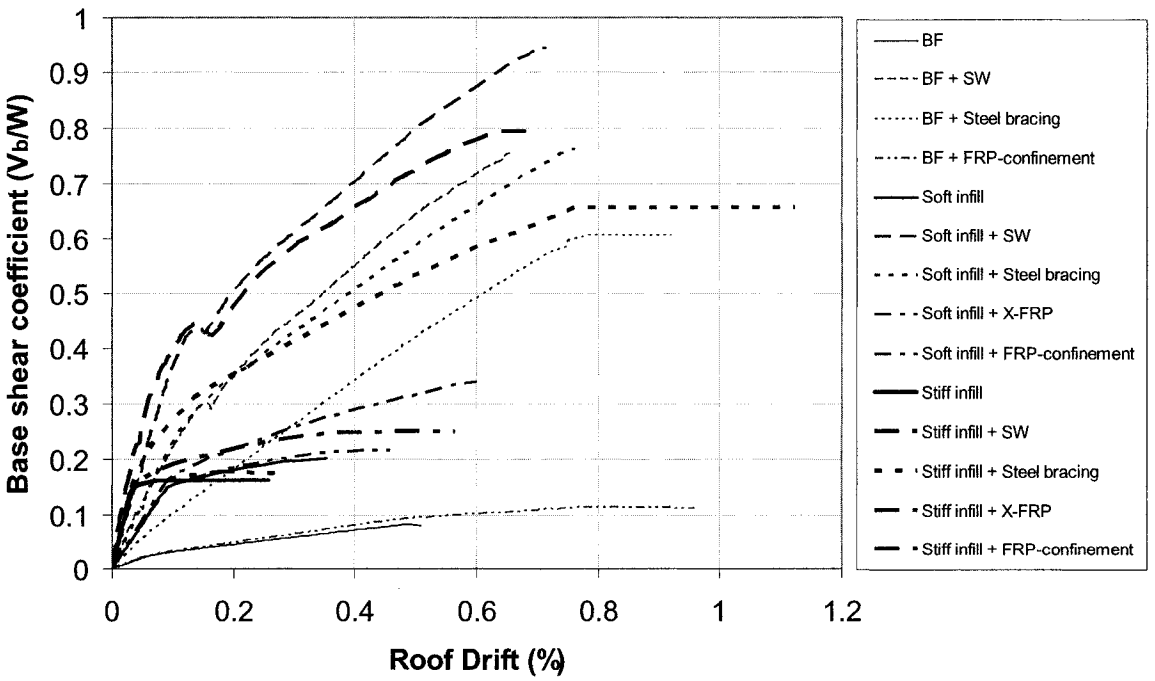

Fig. 4.8 (a) Static pushover analysis for the 5 storey frame.

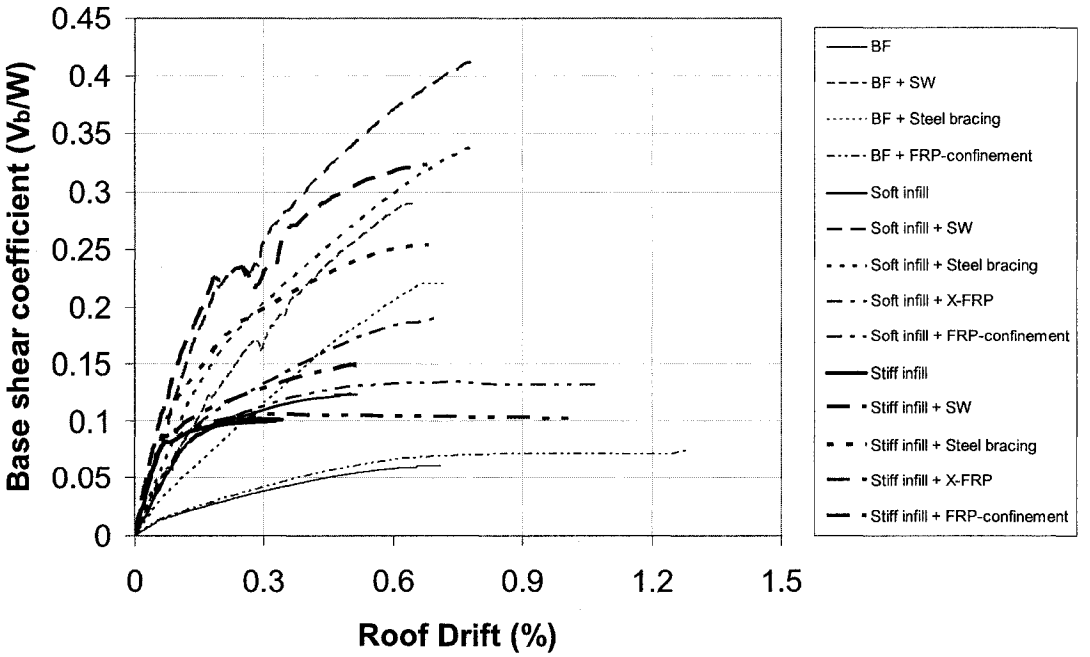

Fig. 4.8 (b) Static pushover analysis for the 10 storey frame.

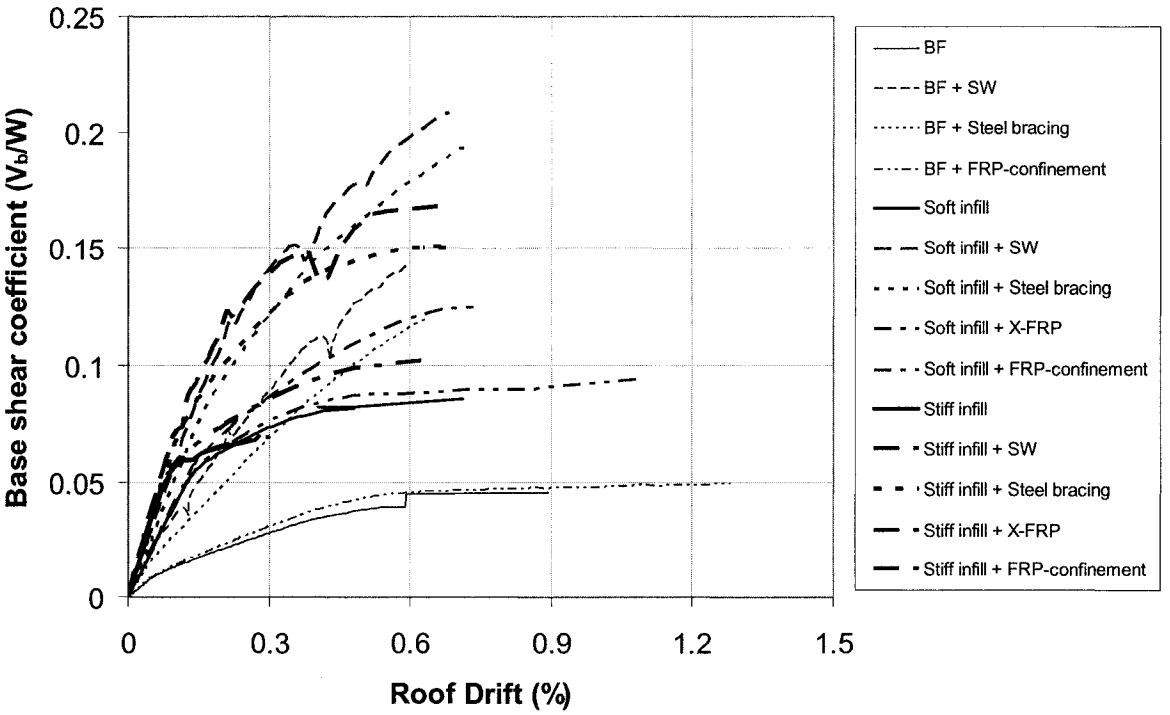

Fig. 4.8 (c) Static pushover analysis for the 15 storey frame.

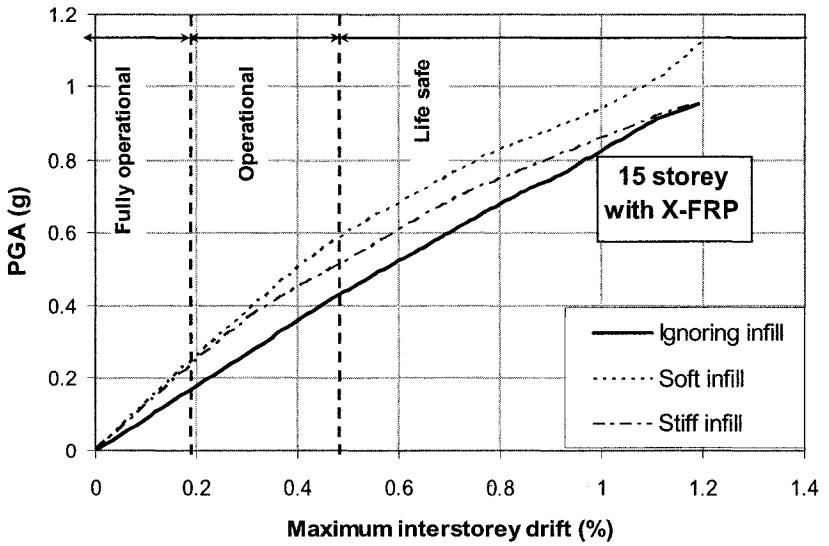

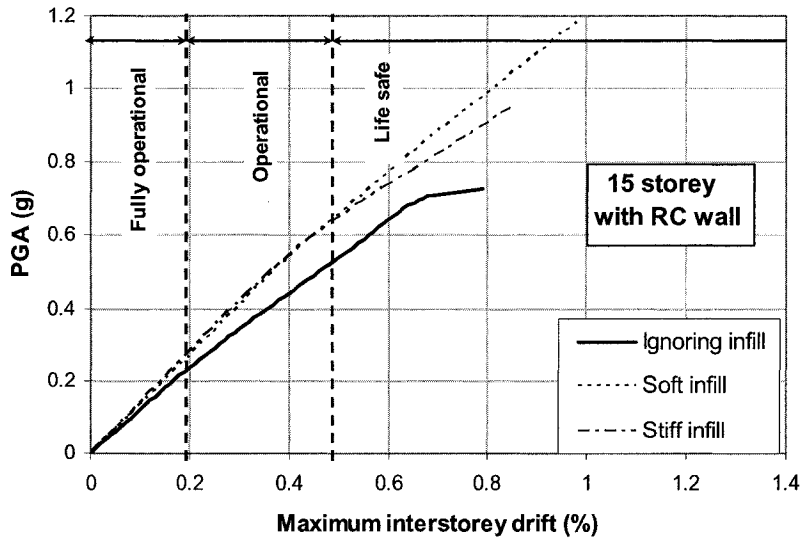

Fig. 4.9. Performance of the 15 storey frame in cases of ignoring or accounting for masonry infill.

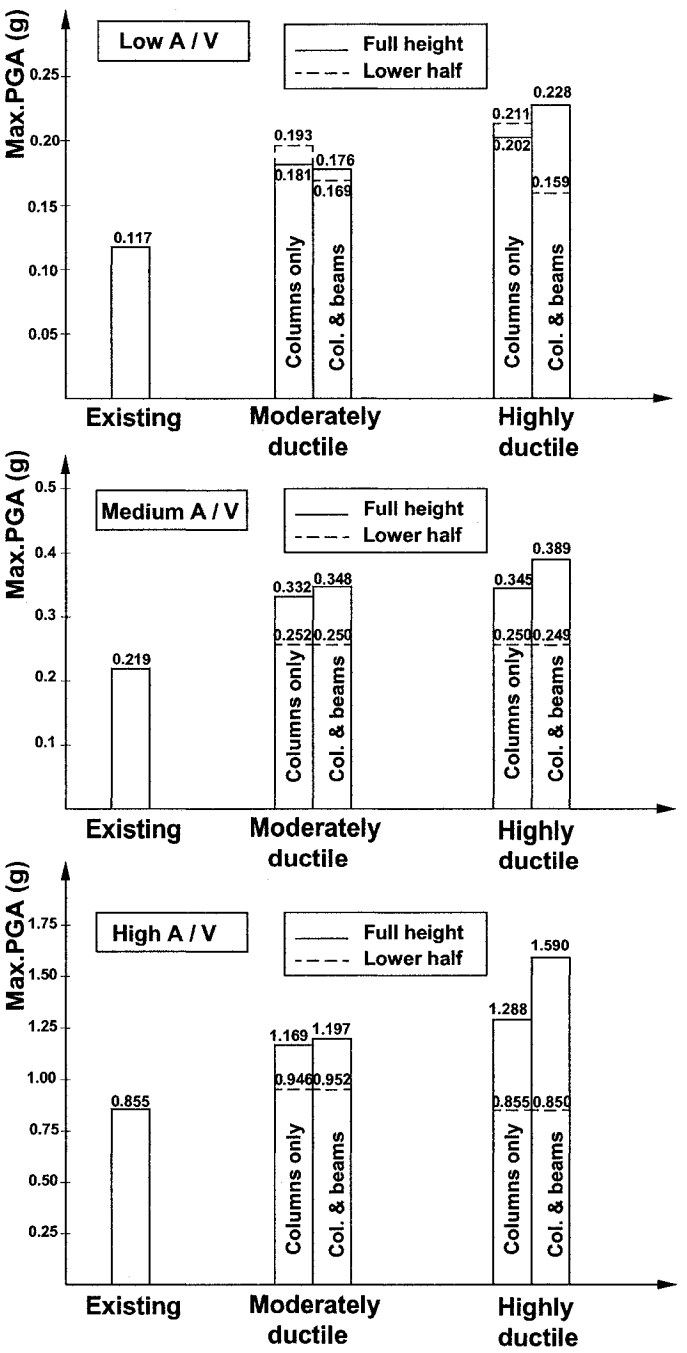

Fig. 4.10 (a) Maximum PGA resisted by 5-storey building (case of FRP-confinement).

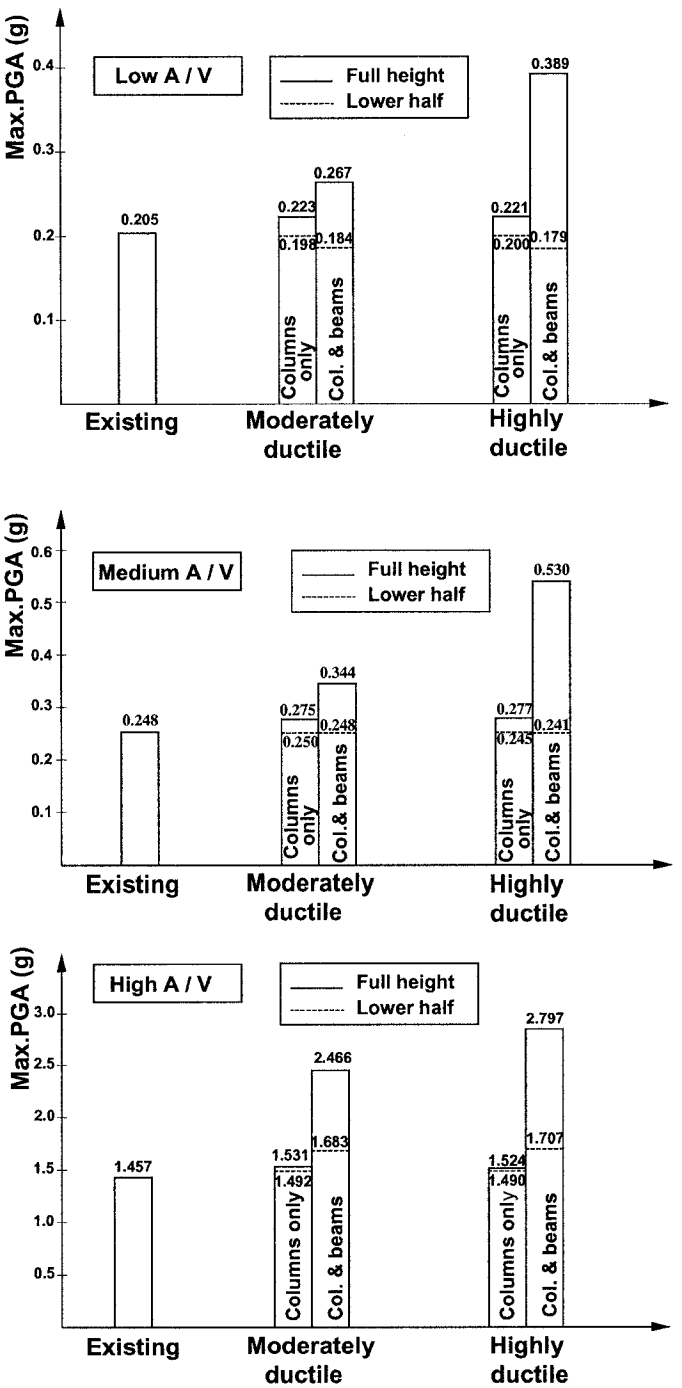

Fig. 4.10 (b) Maximum PGA resisted by 10-storey building (case of FRP-confinement).

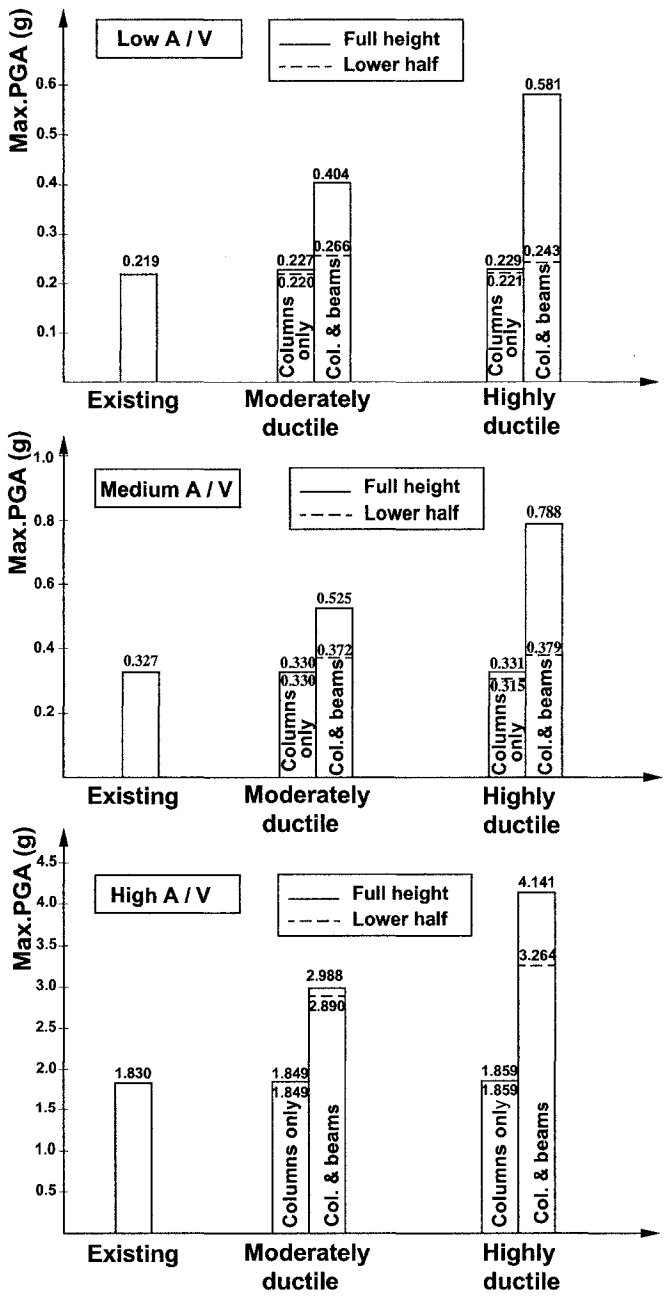

Fig. 4.10 (c) Maximum PGA resisted by 15-storey building (case of FRP-confinement).

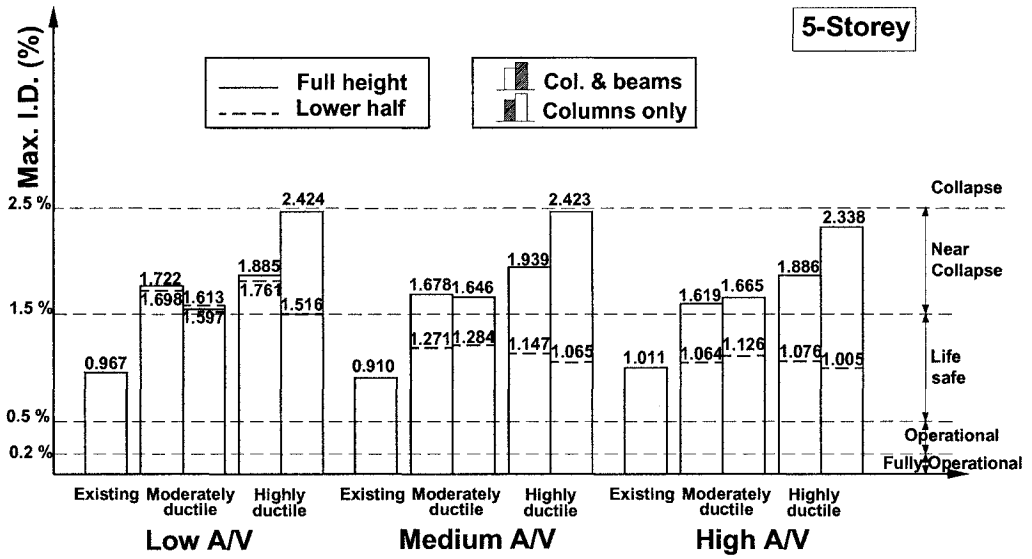

Fig. 4.11 (a) Maximum inter-storey drift ratio capacity for 5-storey building (case of FRP-confinement).

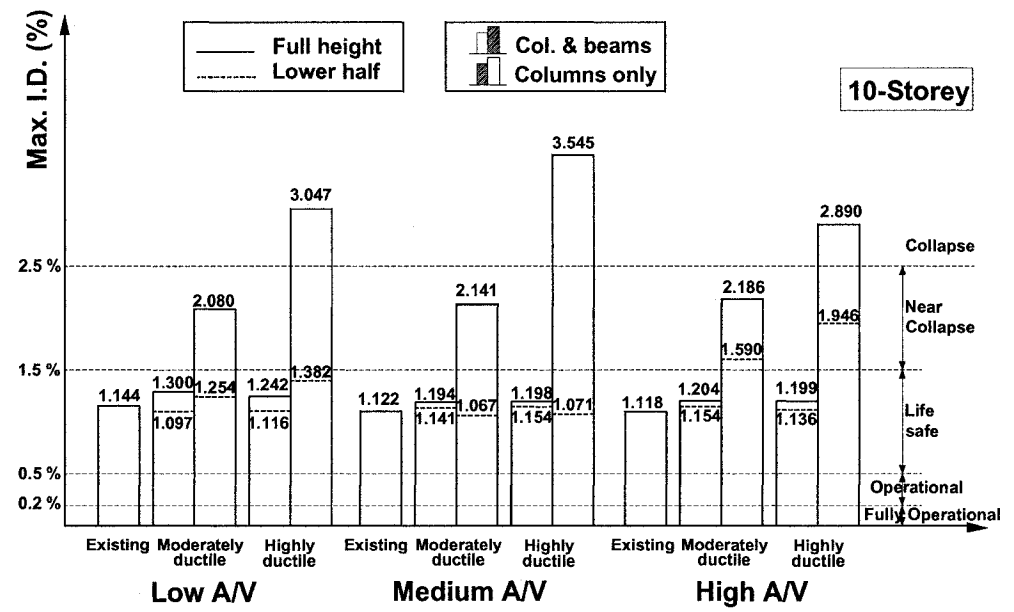

Fig. 4.11 (b) Maximum inter-storey drift ratio capacity for 10-storey building (case of FRP-confinement).

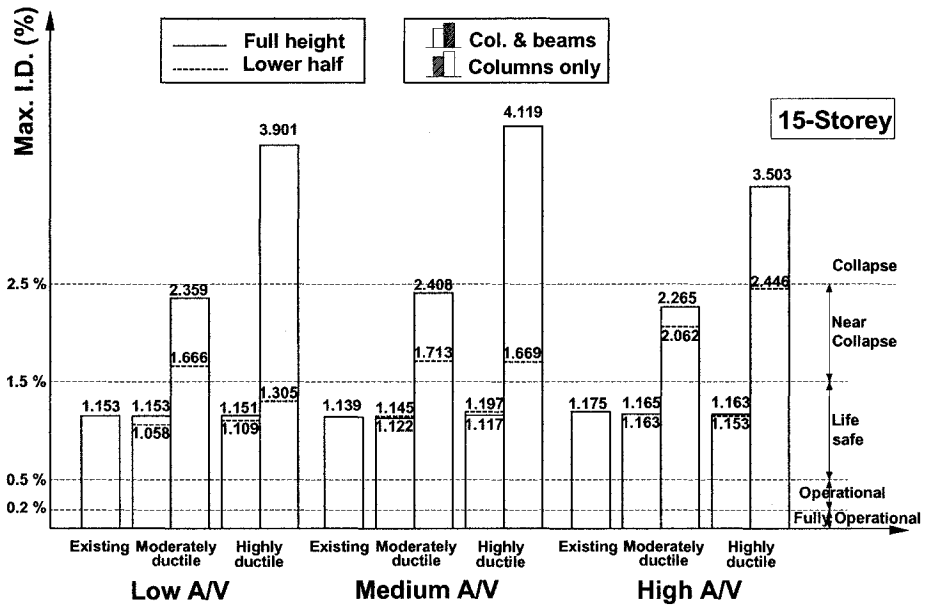

Fig. 4.11 (c) Maximum inter-storey drift ratio capacity for 15-storey building (case of FRP-confinement).

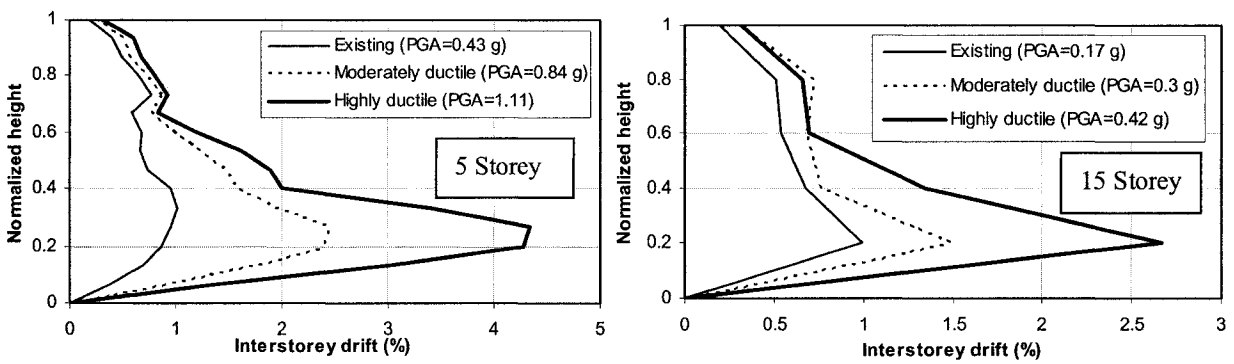

Fig. 4.12. I.D. distribution along the height of low- and high-rise buildings subjected to the maximum scaled El Centro earthquake record that the building can resist (case of FRP-confinement).

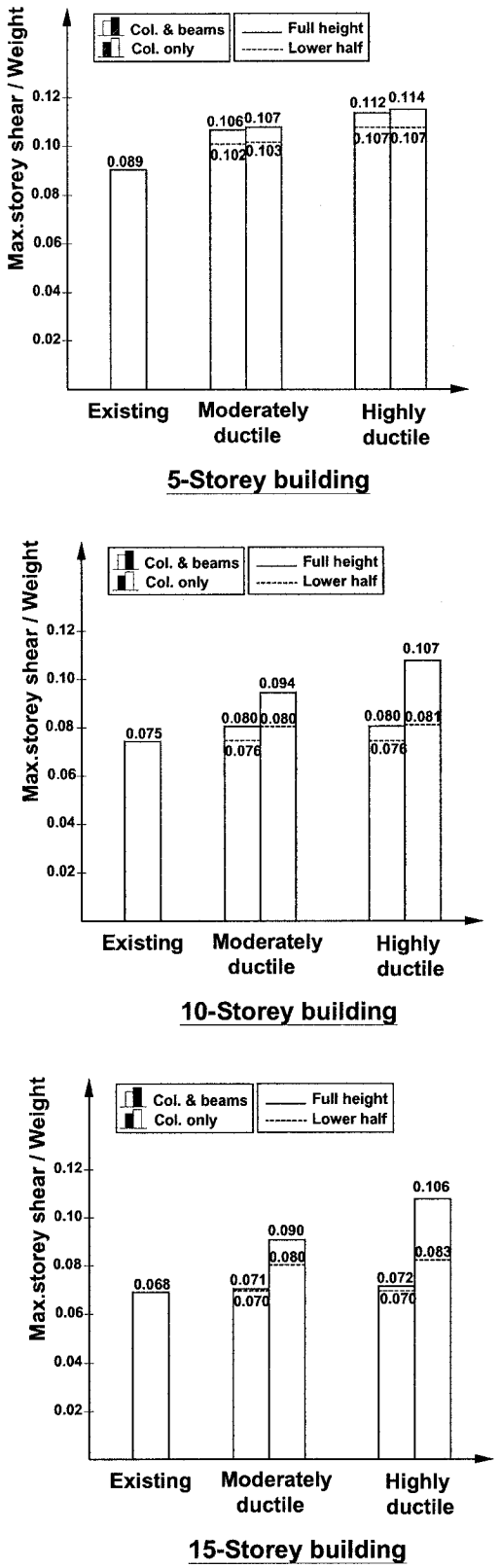

Fig. 4.13. Max. storey shear / weight for 5, 10 and 15 storey frames(case of FRP-confinement).

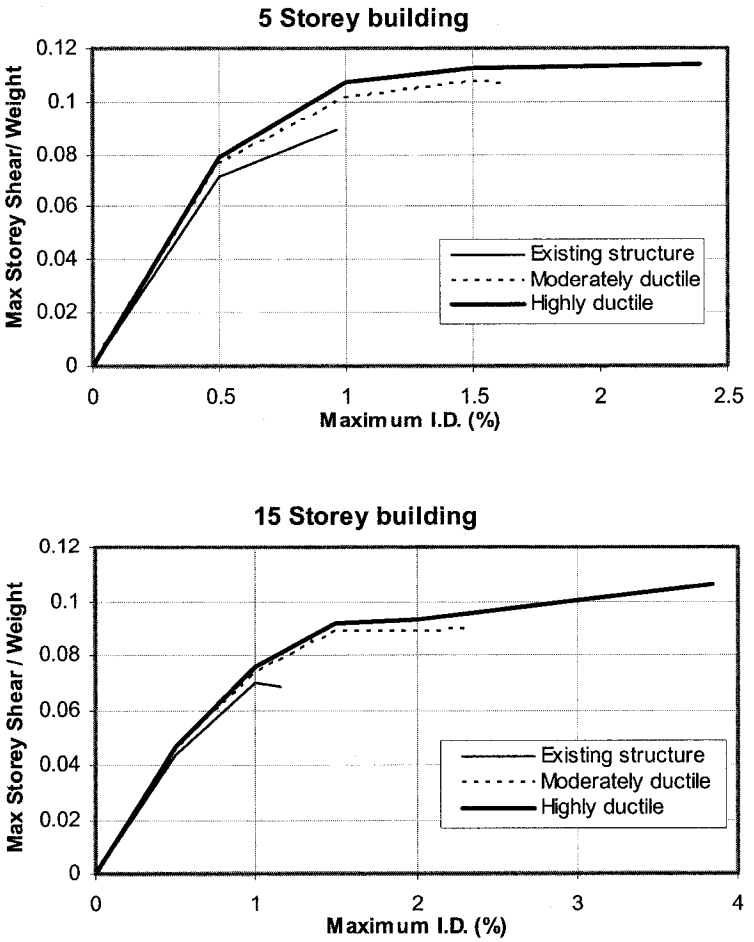

Fig. 4.14 Max. storey shear / weight with max. I.D. for low- and high-rise buildings (case of FRP-confinement).

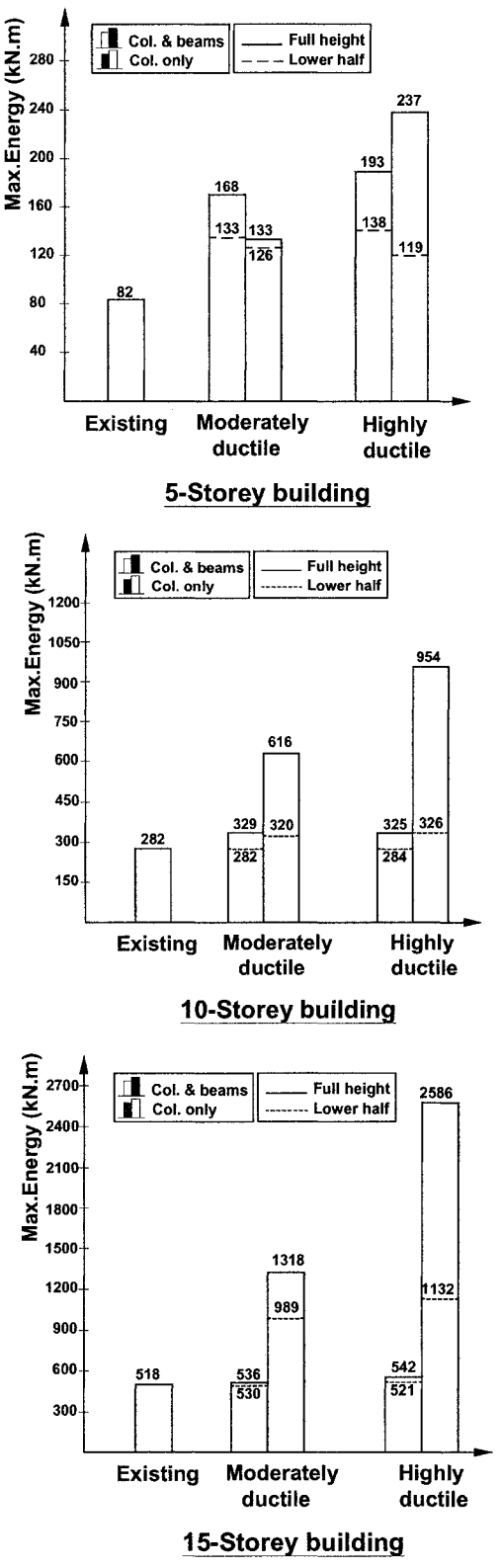

Fig. 4.15. Maximum energy dissipated for 5, 10 and 15 storey frames (case of FRP-confinement).

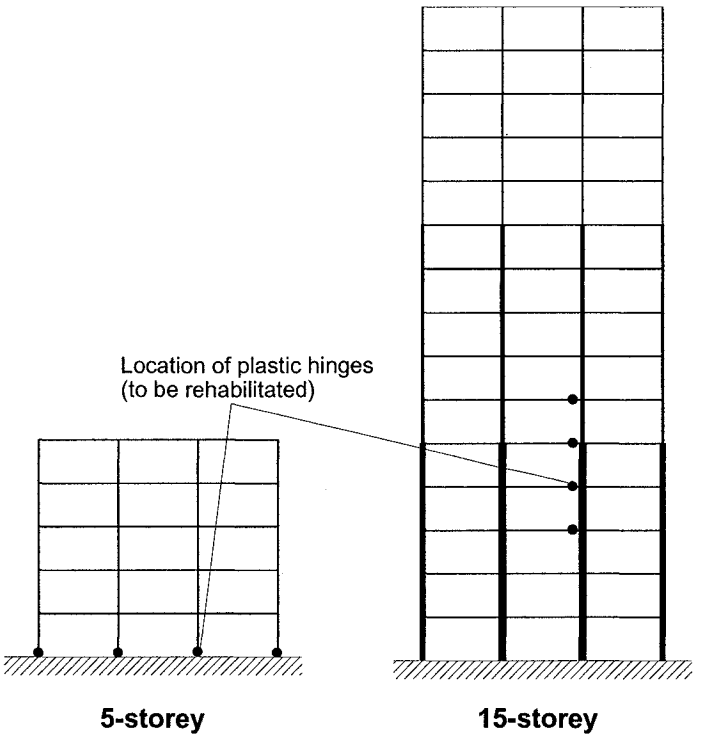

Fig. 4.16. Location of damaged members for the 5 and 15 storey frames when subjected to El Centro earthquake of PGA of 0.15g and 0.3g, respectively.

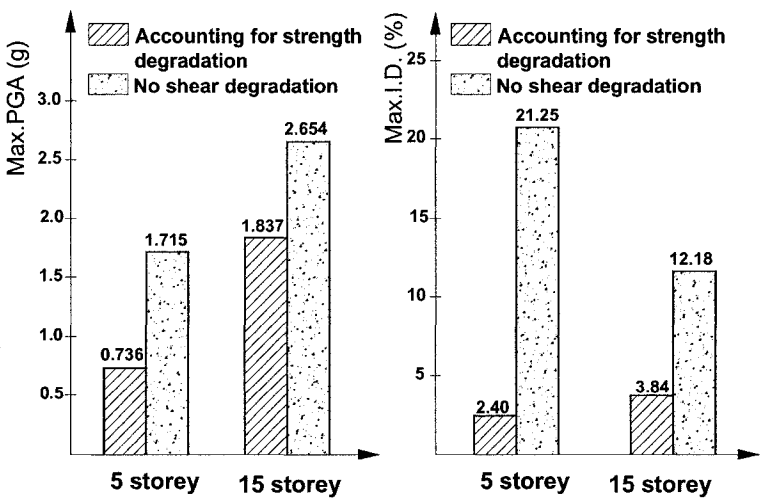

Fig. 4.17. Accounting for strength degradation.

CHAPTER 5

CONCLUSIONS AND RECOMMENDATIONS

5.1 SUMMARY

The effectiveness of different rehabilitation patterns in upgrading the seismic performance of existing non-ductile RC frame structures was evaluated. Three RC frames with different heights were selected for the analyses representing low, medium and high-rise frames. The frames were rehabilitated using four techniques; the first is by introducing a RC wall, the second is by using X-steel bracing, the third is by using X-FRP strips (FRP bracings) in case of masonry-infilled frames, and the fourth technique is by rehabilitating the structural members using FRP confinements. Two different masonry infill types with different stiffness (soft and stiff infill) were considered in the analyses. The bare frames ignoring the effect of masonry infill were also studied. For the case of FRP-confinement, four different rehabilitation patterns were considered in the analysis, the studied patterns include rehabilitation of both columns and beams or columns only along the full height or in the lower half of the structure height. Nonlinear dynamic analyses have been conducted for the existing RC frames and the rehabilitated ones when subjected to three types of ground motion records. The ground motion records were selected to represent earthquakes with low, medium and high frequency contents. The seismic performance enhancement of the analyzed frames was evaluated based on the maximum applied peak ground acceleration or velocity resisted by the frames, maximum inter-storey drift ratio, maximum storey shear to total weight ratio and energy dissipation capacity. The importance of accounting for the masonry infill on the seismic behaviour of structures was also investigated. The effect of accounting for the

post-peak strength degradation in the hysteretic nonlinear model of RC frame members was also investigated.

5.2 CONCLUSIONS

The conducted analyses have resulted in the following conclusions:

1- For the studied low-rise frame, introducing a RC wall increased the PGA, PGV, storey shear, and energy dissipation capacities while rehabilitating the columns and beams of the structure using FRP confinement increased the I.D. ratio capacity.

2- For the studied medium- and high-rise frames, introducing a RC wall increased the storey shear demand, while rehabilitating the columns and beams of the structure using FRP-confinement increased the PGA, PGV, I.D., and energy dissipation capacities.

3- For a certain building height (i.e. low, medium or high-rise) and certain dynamic properties of the building, the maximum inter-storey drift capacity is slightly influenced by the earthquake properties. This justifies the validity of using the maximum inter-storey drift as a uniform and reliable damage parameter that can be used to judge the performance of rehabilitated structures.

4- For the case of FRP-confinement rehabilitation technique, all the structure's existing frames should be rehabilitated in order to achieve the ductility level required for the seismic enhancement of the structure. On the other hand, for the other rehabilitation techniques, rehabilitating a limited number of the structure's

frames was found to be efficient. The number of frames needed to be rehabilitated can be determined according to the seismic enhancement needed for the structure.

5- In case of using FRP confinement, for low-rise RC frame structures, FRP-rehabilitation of the columns only was effective in increasing the structures' PGA and maximum interstorey drift demands. On the other hand, FRP-rehabilitation of all the columns and beams of the structure did not result in a significant increase in the seismic performance of the rehabilitated structure compared to the case of rehabilitating the columns only. This can be interpreted that, for low-rise buildings, the relative strength of the beams to that of the columns is high, which resulted in failure in the columns, so the gain in the PGA capacity of the building with the rehabilitation of the beams (in addition to the columns) is not significant.

6- For medium- and high-rise RC frame structures, the rehabilitation of columns only was not as effective as rehabilitation of both columns and beams for the full height of the structure. This can be interpreted that, for high-rise buildings, the relative strength of the beams to that of the columns is low, which resulted in failure in the beams, so the gain in the PGA capacity of the building increased with the rehabilitation of the beams.

7- Rehabilitation of selected frame members (beams and columns that are expected to have damage for a specified earthquake hazard) was not as effective as rehabilitation of both columns and beams for the whole structure.

8- Ignoring representing the post-peak strength degradation in the hysteretic nonlinear model of FRP-rehabilitated RC columns and beams would lead to over-estimation of the seismic performance of the structure.

9- Accounting for the presence of masonry infill in the analytical model has decreased the maximum I.D. ratio and increased the energy dissipation capacity of the frames. Hence, ignoring the effect of masonry infill would lead to under-estimation of the seismic performance of structures.

5.3 RECOMMENDATION FOR FUTURE RESEARCH

From the above conclusions it can be seen that the choice of the most suitable rehabilitation scheme should consider the properties of the structure, seismic hazard, propertied of the expected ground motion, and the desired performance parameter needed to be enhanced.

It's important to clarify that the drawn results are for the studied cases and the selected earthquakes. More earthquakes should be considered and more analyses including life cycle cost analysis are needed for the conclusions to be generalized.

More experimental studies should be done to evaluate the seismic behaviour of the whole RC frame rehabilitated using FRP-confinements instead of testing the frame members (columns or beams) individually. Other experimental studies should be conducted to evaluate the response of RC structural walls under dynamic excitations.

REFERENCES

1. ABAQUS, 1996. "Users' Manual & Theory Manual" V. 5.5, Hibbitt, Karlsson & Sorensen, Inc., Pawtucket, RI.

2. Abou-Elfath, H. and Ghobarah, A, 2000. "Behaviour of reinforced concrete frames rehabilitated with concentric steel bracing" *Canadian Journal of Civil Engineering*, No. 27, p 433-444.

3. American Concrete Institute (ACI), 1968. "Manual of concrete practice, part 2. Committee 318-1R-68.", Detroit, USA.

4. ANSYS, Inc, 2002, South Pointe, Canonsburg (PA), Release 7.0 UP20021010.

5. Almusallam, T.H. and Al-Salloum, Y, 2007. "Behavior of FRP strengthened infill walls under In-plane seismic loading" *Journal of Composites for Construction*, Vol. 11, No. 3, p 308-318.

6. Bakis C, Bank L, Brown V, Cosenza E; Davalos J, Lesko J; Machida A; Rizkalla S and Triantafillou T., 2002. "Fiber-Reinforced Polymer Composites for Construction—State-of-the-Art Review". *Journal of Composites for Construction, ASCE*; 6(2):73-87.

7. Belmouden, Y. and Lestuzzi, P., 2007. "Analytical model for predicting nonlinear reversed cyclic behaviour of reinforced concrete structural walls" *Journal of Engineering Structures*, No. 29, p 1263-1276.

8. Binici, B., Özcebe, G. and Ozcelik, R., 2007. "Analysis and design of FRP composites for seismic retrofit of infill walls in reinforced concrete frames." *Journal of Composites: Part B*, No. 38, p 575-583.

9. Carr, A.J. 1996. RUAUMOKO the Maori god of volcanoes and earthquakes. Computer Program Library, 27 January 1996 Release, Department of Civil Engineering, University of Canterbury, Christchurch, New Zealand.

10. Chen, P.F. and Powell, G.H., 1982. "Generalized Plastic Hinge Concepts for 3D Beam-Column Elements," EERC Report No. 82-20, Earthquake Engineering Research Center, University of California, Berkeley, California.

11. Combescure, D, 2002. IAEA CRP-NFE Camus Benchmark: experimental results and specifications to the participants. Rapport DM2S. SEMT/EMSI/RT/02-047/A.

12. CSA, 1994. Design of concrete structures for buildings. Standard CAN-A13.3-94, Canadian Standards Association, Rexdale, Ontario.

13. Dolsek, M. and Fajfar, P., 2002. "Mathematical modeling of an infilled RC frame structure based on the results of pseudo-dynamic tests." *Journal of Earthquake Engineering and Structural Dynamics*, No. 31, p 1215-1230.

14. FEMA 273/274, 1997. Commentary on the NEHRP Guidelines for the Seismic Rehabilitation of Buildings.

15. Filiatrault, A., Lachapelle, E. and Lamontagne, P., 1998. "Seismic performance of ductile and nominally ductile reinforced concrete moment resisting frames. I. Experimental study" *Canadian Journal of Civil Engineering*, No. 25, p 331-341.

16. Filiatrault, A., Lachapelle, E. and Lamontagne, P., 1998. "Seismic performance of ductile and nominally ductile reinforced concrete moment resisting frames. II. Analytical study" *Canadian Journal of Civil Engineering*, No. 25, p 342-352.

17. Galal K., 2006. "Modeling of lightly reinforced concrete walls subjected to near-fault and far-field earthquake ground motions" *Journal of the Structural Design of Tall and Special Buildings* (In press).

18. Galal, K., 2007. "Shear capacity of retrofitted rectangular RC short columns" *Journal of Structural Engineering and Mechanics*, V. 25, No. 1: 75–90.

19. Galal, K., Arafa, A., and Ghobarah, A., 2005. "Retrofit of RC square short columns" *Journal of Engineering Structures*, No. 27, 801–813.

20. Galano, L. and Gusella, V., 1998. "Reinforcement of masonry walls subjected to seismic loading using steel X-bracing" *Journal of Structural Engineering*, Vol. 124, No. 8, p 886-895.

21. Ghobarah A, Abou Elfath H., 2001. "Rehabilitation of a reinforced concrete frame using eccentric steel bracing." *Journal of Engineering Structures*; No. 23, p 745–755.

22. Ghobarah, A., Abou Elfath, H., and Biddah, A., 1999. "Response-based damage assessment of structures" *Journal of Earthquake Engineering and Structural Dynamics*, No. 28, p 79-104.

23. Ghobarah, A., El-Attar, M. and Aly, N.M., 2000. "Evaluation of retrofit strategies for reinforced concrete columns: a case study." *Journal of Engineering Structures*, No. 22, p 490-501.

24. Haroun, M., Feng, M., Elsanadedy, H., and Mosallam, A., 2002. "Composite jackets for the seismic retrofit and repair of bridge columns." *Seventh U.S. national conference on Earthquake Engineering*, p.10.

25. Heidebrecht, A.C. and Naumoski, N., 1999. "Seismic performance of ductile medium height reinforced concrete frame buildings designed in accordance with the

provisions of the 1995 National Building Code of Canada" *Canadian Journal of Civil Engineering*, No. 26, p 606-617.

26. Humar, J. and Bagchi, A., 2004. "Seismic performance of concrete frame buildings designed according to NBCC 2005." *13th World Conference on Earthquake Engineering Conference Proceedings.*

27. Jain, A., Goel, S., and Hanson, R., 1980. "Hysteretic cycles of axially loaded steel members" *Journal of the Structural Division*, Vol. 106, No. ST8, p 1777-1795.

28. Jiang, Y., and Saiidi, M., 1990. "Four-Spring Element for Cyclic Response of R/C Columns," *Journal of Structural Engineering*, ASCE, Vol. 116, No. 4, pp. 1018-1029

29. Kazak, I., Yakut, A., Gülkan, P., 2006. "Numerical simulation of dynamic shear wall tests: A benchmark study" *Journal of Computers and Structures*, No. 84, p 549-562.

30. Kim, T. and Foutch, D.A., 2007. "Application of FEMA methodology to RC shear wall buildings governed by flexure" *Journal of Engineering Structures* (In press).

31. Kunnath, S.K., Reinhorn, A.M., and Lobo, R.F., 1992. IDARC Version 3.0: a program for inelastic damage analysis of reinforced concrete structures. Report NCEER-92-0022, National Center for Earthquake Engineering Research, Buffalo, N.Y.

32. Lai, S.S., Will, G.T., and Otani, S., 1984. "Model for Inelastic Biaxial Bending of Concrete Members," *Journal of Structural Engineering, ASCE*, Vol. 110, No. 11, pp. 2563-2584.

33. Li, K, 2006 (CANNY). Three dimensional nonlinear static and dynamic structural analysis.

34. Linde, P., 1998. "Evaluation of structural walls designed according to Eurocode 8 and SIA 160" *Journal of Earthquake Engineering and Structural Dynamics*, No. 27, p 793-809.

35. Lu, Y., 2002. "Comparative study of seismic behaviour of multistory reinforced concrete framed structures." *Journal of Structural Engineering*, 2002, Vol. 128, No. 2, p 169-178.

36. Madan, A., Reinhorn, A.M., Mander, J.B., Valles, R.E., 1997 "Modeling of masonry infill panels for structural analysis. *Journal of Structural Engineering*, V. 123, No. 10, p 1295-1302.

37. Mander, J.B., Nair, B., Wojtkowski, K. and Ma, J., 1993. "Experimental study on the seismic performance of brick-infilled steel frames with and without retrofit" Tech.

Rep. NCEER-93-0001, Nat. Ctr. For Earthquake Engrg. Res., State Univ. of New York, Buffalo, N.Y.

38. Marini, A. and Spacone, E., 2006 "Analysis of reinforced concrete elements including shear effects" *American Concrete Institution (ACI) Structural Journal*, V. 103, No. 5, p 645-655.

39. Mo, Y.L., 1994. "Dynamic behavior of concrete structures", *Journal of Developments in Civil Engineering* Vol. 44, Elsevier, Amsterdam and New York, 409 pages.

40. NBCC. 1995. National building code of Canada. Associate Committee on the National Building Code, National Research Council of Canada, Ottawa, Ont.

41. NBCC. 2005. National building code of Canada. Associate Committee on the National Building Code, National Research Council of Canada, Ottawa, Ont.

42. Ngo, D., and Scordelis, A.C., 1967. "Finite Element Analysis of Reinforced Concrete Beams," *ACI Structural Journal*, Vol. 64, No.3.

43. Özcebe G., Keskin U. and Tankut T., 2003. "Strengthening of brick-infilled RC frames with CFRP" Tech. Rep. Structural Engineering Research Unit, Middle East Technical University (METU).

44. Panneton, M., Léger, P and Tremblay, R., 2006. " Inelastic analysis of a reinforced concrete shear wall building according to the National Building Code of Canada 2005" *Canadian Journal of Civil Engineering*, No. 33, p 854-871.

45. PEER Strong Motion Database, 2006. Available from the Pacific Earthquake Engineering Research Center and the University of California. Website: http://peer.berkeley.edu/smcat/.

46. Petrangeli, M., 1999. "Fiber Element for Cyclic Bending and Shear of RC structures. II: Verification," *Journal of Engineering Mechanics*, Vol. 125, No. 9, pp. 1002-1009.

47. Powell, G.H., and Campbell, S., 1994. "DRIAN-3DX: Element Description and User Guide," SEMM Report No. 94/08. Department of Civil Engineering, University of California, Berkeley, California.

48. Prakash, V., Powell, G.H. and Campbell, S., 1993. DRAIN 2DX, Department of Civil Engineering, University of California at Berkeley.

49. Said, A.M. and Nehdi, M.L., 2004. "Use of FRP for RC frames in seismic zones: Part I. Evaluation of FRP beam-column joint rehabilitation techniques." *Journal of Applied Composite Materials*, No. 11, p 205-226.

50. Saiidi, M., Lawver, R., and Hart, J., 1986, "User's Manual for ISADAB and SIBA, Computer Programs for Nonlinear Transverse Analysis of Highway Bridges Subjected to Static and Dynamic Lateral Loads," CCEER Report No 86-2, University of Nevada-Reno, Center for Civil Engineering Earthquake Research, Reno, Nevada, 74 pages.

51. Seible, F., Priestley, M.J., Hegemier, G.A. and Innamorato, D., 1997. "Seismic retrofit of RC columns with continuous Carbon Fiber Jackets" *Journal of Composites for Construction*, Vol. 1, No. 2, p 52-62.

52. Sheikh, S.A., 2002. "Performance of concrete structures retrofitted with fibre reinforced polymers." *Journal of Engineering Structures*, No. 24, p 869-879.

53. Sheikh, S.A. and Li, Y., 2007 "Design of FRP confinement for square concrete columns." *Journal of Engineering Structures*, No. 29, p 1074-1083.

54. Stafford-Smith, B., 1966. "Behavior of square infilled frames," *Journal of Structural Division*, ASCE, 1, 381-403.

55. Tremblay, R., Léger, P. and Tu, J., 2001. "Inelastic seismic response of concrete shear walls considering P-delta effects" *Canadian Journal of Civil Engineering*, No. 28, p 640-655.

56. Tso, W., Zhu, T., and Heidebrecht, A., 1992. "Engineering implication of ground motion A/V ratio." *Journal of Soil Dynamics and Earthquake Engineering*, No. 11, p 133–144.

57. Vision 2000 Committee, 1995. Structural Engineers Association of California (SEAOC).

58. Xiao, Y., Priestley, N., and Seible, F., 1993. "Steel Jacket Retrofit for Enhancing Shear Strength of Short Rectangular Reinforced Concrete Columns," Report No. SSRP-92/07, Structural Systems Research Project, University of California-San Diego, San Diego, Calif.